Linked Rising Trends of Cannabis Use and Autism Incidence Demonstrated by Close Three Level Geospatiotemporal Relationships, USA, 1990-2011.

Short Title:
Cannabis Drives USA Autism at Three Levels

Albert Stuart Reece, MBBS(Hons.), FRCS(Ed.), FRCS(Glas.), FRACGP, MD (UNSW) [1,2]

Gary Kenneth Hulse, BBSc.(Hons.), MBSc., PhD. [1,2]

Affiliations:

1 - Division of Psychiatry,

University of Western Australia,

Crawley, Western Australia 6009, Australia.

2 – School of Medical and Health Sciences,

Edith Cowan University,

Joondalup, Western Australia, 6027, Australia.

*** Address Correspondence to**:

Albert Stuart Reece

39 Gladstone Rd.,

Highgate Hill,

Brisbane, Queensland, Australia.

Ph: (617) 3844-4000

FAX: (617) 3844-4015

Email: stuart.reece@bigpond.com

Keywords: Depression, serious mental illness, geospatial analysis, spatiotemporal analysis, suicidality, substate areas

Word count: 5,948

Abstract

Introduction

The US epidemic of autism has previously been noted to be growing in an exponential manner or faster. Although some causes of autism and disordered brain development have been elucidated the underlying causes of this striking phenomenon remain obscure. Routine linear regression techniques were recently used to suggest that the renaissance of the nation's cannabis use may be a primary driver of this mega-trend. The present study brings to bear the power of geospatiotemporal analysis on this question to test the detailed geospatial and temporal associations previously described at the macro-level.

Methods

The Individuals with Disabilities in Education Act (IDEA) dataset was interrogated along with data from the National Survey of Drug Use and Health (NSDUH) conducted by the Substance Abuse and Mental Health Services Administration (SAMHSA) and Drug Enforcement Agency data. Geotemporo-spatial modelling techniques were employed using the R package splm to investigate the national, regional and state level geospatial relationships of cannabis and other drug use with US autism rates. Bonferroni adjustment of the level of statistical significance to $q<0.0013$ was performed to accommodate multiple testing.

Results.

At the national level daily cannabis use in the 18-25 years age group was associated with the autism rate as a main effect from $P=4.69\times10^{-14}$. At the regional level in a full two-step generalized SEM2SRRE+SAR spreml model with 6 years spatial lag cannabis use was again significant as a main effect from $P<2.2\times10^{-16}$. At the state level cannabis was significant as a main effect in an spgm spatial error model from P=0.00016. On t-testing in the whole dataset the autism rate in Decriminalised states was 52.16 ± 3.69 v 31.69 ± 1.04 in Illegal States ($P=2.5958\times10^{-7}$). In a spatial SARAR model decriminalization of cannabis laws was significant from $P=9.96\times10^{-11}$ and medical cannabis laws was significant from $P=8.56\times10^{-13}$.

Conclusions

These data confirm the geospatial and temporal associations of cannabis with the US autism epidemic and demonstrate that cannabis is independently associated with autism at three geospatial levels thereby extending previous investigations. Certain statistical modelling features (high adjusted R-squared, very low P-values, two-step instrumental modelling, uniformity of geospatial scale-invariant results), a plethora of biological mechanistic links between prenatal cannabis exposure and deranged brain development, and robust fulfillment of Hill's causality criteria indicate not only causality, but confirm that indeed increased cannabis use is likely to be a primary driver of the modern US autism epidemic presently in hyper-exponential growth phase. Community-based reports suggest that these quantifiable data may be but the tip of a much larger paediatric neurological epidemiological "iceberg". Important public health messages for the global medical and public health communities clearly follow directly countermanding the current trend for widespread cannabis legalization.

Introduction

The rate of autistic spectrum disorder appears to be undergoing a rapid rise across almost every jurisdiction in USA according to the most recent data. Although a number of causes of autism have been well described and are widely accepted the basic cause of this modern epidemiological tsunami appears to be not at all well understood. It has previously been shown that in fact this acceleration of autism is actually following an exponential growth pattern and is growing at a statistically significantly higher rate in states where cannabis is legal [1]. Concerningly it has recently been shown that at current rates of growth of the epidemic by 2030 the rates in states with legal policies are estimated to be 60% higher than in those which do not [2].

Technically however these studies were methodologically limited fundamentally to ordinary least squares analysis and routine methods of statistical analysis as might be applied to most datasets where variables are distributed independently and identically distributed – so-called "iid" variables. The first law of geography enunciated in 1970 by Waldo Tobler states that things close together affect things more than things further away [3]. In 2017 he modified this law to state that things geographically and temporally close together affect things nearby more, thereby including the temporal dimension in geotemporospatial analysis. Moreover spatially distributed variables can show serial or sequential autocorrelation amongst the variables, or there can be correlation between the error terms and the variables – so-called "endogeneity".

Furthermore the fundamental analytical issue remains that even though trends are well established at the national level this might not apply at higher levels of spatial resolution. Since the autism data exists at state, regional and US national level this dataset lends itself to the novel application of such newly described powerful geospatial analytical tools at multiple spatial scales.

Since the following analysis strongly confirms the original hypothesis at all geospatial levels this greatly strengthens our earlier conclusions and provides added confidence to policy makers that the major conclusion that cannabis is a major factor driving the currently otherwise unexplained epidemic of autism rests on a firm and robust evidence base.

Methodological Comment

The main dataset which will be relied upon is a secondary analysis of anonymous data collected in the US Department of Education Individuals with Disabilities Act (IDEA) dataset [4]. On occasion the dataset from the Autism Developmental Disabilities Monitoring (ADDM) dataset is also used as indicated [4]. Data on cannabinoid exposure in each state over time is computed by multiplying the last month cannabis use rate in that state by the mean concentration of the various cannabinoids found in Federal seizures at that time point [5,6].

Established geospatial analytical tools such as the plm, splm, spdep and spatialreg packages in R-Studio Version 1.2.1335 based on "R" version 3.6.1 from CRAN and GeoDa

downloaded from the University of Chicago along with other programs have been employed as described throughout.

Since 36 final models are presented herein following Bonferroni it is fair to adjust the usual level of statistical significance from $P < 0.05$ to $q < 0.0013$. it is worth bearing these significance thresholds in mind as we present the following analyses.

In each case full initial models are reduced by the classical method of the sequential elimination of least significant variables to arrive at the final reduced model containing only significant variables which is presented.

This study has been authorized by the Human Research Ethics Committee of the University of Western Australia.

Data is presented at the national, regional and state level seriatim.

Results

National Level data.

Figure 1 presents the national rate of autism derived from the IDEA dataset and the state populations taken from the US national Census 2010. It is clear that the autism rate is rising steeply and has now reached 1% nationally. One notes in passing that the diagnosis of autism is not usually finalized till children are eight years of age so this factor inevitably introduces lengthy delays into tracking this epidemic at every geographical level.

Since most of the cases survive it is possible to take a cumulative count of the cases since the commencement of national records. This graph is presented in Figure 2, since each year's cohort survives along with preceding and subsequent cohorts. This figure appears to be rising exponentially. This exponential geometric pattern is confirmed in our earlier reports [1,2] and also in the results presented below.

Figure 3 presents the national pattern of drug use by drug type as quantified annually by the National Survey of Drug Use and Health (NSDUH) published each year from the Substance Abuse and Mental Health Services Administration (SAMHSA).

Panel regression, or cross-sectional time-series analysis, is a well established and standardized way to look at the relationship amongst variables which are measured in repeated locations as a series over time. The plm (panel linear model) package in R also allows the use of two step regression including instrumental variables which allows a more refined examination of putatively causal mechanisms to be considered, and also allows the ready application of time lagged models to look for delayed effects.

Table 1 presents a series of four models which uses two stage generalized least squares panel regression models lagged four and six years. The first model is an interactive model regressing the log autism rate against the five drugs measured consecutively by NSDUH with monthly cannabis use. Models 2 to 4 use measures of daily cannabis use in 18-25 and 26-34 year olds as the measure for cannabis use as DCan1825 and DCan2634 respectively. Model 3 has a cannabis: tobacco interaction and finds the most significant differences with single terms involving the cannabis use variables and interactive terms including daily cannabis use are significant from $P = 4.69 \times 10^{-14}$. The fourth model has the most instrumental variables being six in number. One notes in this series of models the remarkably high values of the R-squared coefficients of all the models which range from 0.956 to 0.992. In each case the model P-vales are very highly significant since they are all $P < 2.2 \times 10^{-16}$. These results demonstrate unusually high levels of statistical relationships between the measured drugs, and particularly daily cannabis use and the reported rates of autism, at a level well beyond a $q < 0.0013$ adjusted for multiple testing.

Whilst it is theoretically possible that some uncontrolled confounding and unidentified covariate is the true underlying covariate responsible for these remarkable statistical findings, the extremely high R-squared values, the vanishingly low P-values, the unanimity of findings across all lagged panel models and the use of the two-step instrumental variable methodology all argue strongly for a causal relationship. This would be consistent with the known neurotoxic mechanisms involved in the activity of numerous cannabinoids on the developing brain further described below.

Regional Level.

USA is divided into four regions for administrative and census purposes as shown in Figure 4. This series of maps is drawn with the R package sf (simple features). These maps show the progress of the autism rate by region across USA and re-sets the scale adjustment with each year with the lightest colours indicating the highest rates. It is clear in these maps that the northeast region of USA is usually the highest region for autism.

Figure 5 performs the same task with the R package ggplot2 and holds the colour scale constant across all years. This figure clearly shows the growth and development of the autism epidemic across USA by regions and again clearly features its concentration in the northeast region.

Figure 6 shows the rate of autism across USA over time by region. The northeast clearly has the highest rates above those of other regions.

Spatial regression can be performed using a spatial lag model on these regional data using the South region as the control region. As shown in Table 2 the other regions have significantly higher rates of autism than the south, an effect most marked for the northeast. Indeed one notes that the $\beta = 0.4350$ with an applicable $P = 6.28 \times 10^{-16}$. The model coefficient phi is one of the error terms and the coefficient lambda is a metric of the autocorrelation spatial lag in the error term of the model.

Table 3 shows the results of spatial regression with full Spatially Autocorrelated with Autocorrelation in the error terms (SARAR) models of the log autism rate against the various drugs. Both models shown are interactive models. The first model shows the results of regressions with and interaction between cigarettes (mcigmon), cannabis (mmrjmon), and abuse or dependence on alcohol (mAbdAlc). The second model shows the interaction between cigarettes, cannabis and opioid analgesics (manlyr). In each case highly significant terms involving cannabis are found. In the first model cannabis is significant as a main effect.

This analysis has been further refined by the use of the spreml function (spatial panel random error maximum likelihood) in the R package splm which allows detailed specification of the error and covariance structures as described by Giovanni Millo [7]. When two stage full spatial and temporal autoregressive error models and random effects including Kapoor, Kelejian and Prucha-type errors and serially correlated remainder errors (SAR+SEM2SRRE models) specified at 2, 4 and 6 lags are employed the results are as shown in Table 4. Again cannabis is shown to be very highly significant in many interactive terms. Cannabis is also significant alone as a main effect in the 2- and 4- lagged models.

State Level data

Figure 7 shows the autism rate by state for the 20 year period 1992-2011 and tracks the emergence and development of the epidemic across the country. Figure 8 plays a similar role drawn in R's ggplot2. The pattern is strongly 'trimodal" with hotspots shown in black in the northeast, the Pacific northwest and centrally in Minnesota.

Figures 7 and 8 also show evidence of missing data in several states. Six data points are absent in the time period 1994 – 2011 which preclude the use of spatial modelling techniques which require completed datasets known as 'balanced panels." For this reason these missing data points were replaced by the established technique of temporal kriging which uses the simple mean of the values at time points on either side for that region to complete the data series. In this way missing values for New Hampshire in 1994, Montana in 2006, Washington DC in 2007, Vermont in 2007 and 2008 and Wyoming in 2010 were replaced with the values 1, 28.5, 69.5, 57.13, 77.87 and 77 respectively.

With these adjustments to the data series the bivariate plots shown in Figure 9 were prepared. The pink and purple areas show areas where both cannabis use and autism are high. This autism-cannabis map is compared with a similarly prepared autism-tobacco map in Figure 10 which appears to be getting progressively more 'blue' as tobacco use rates fall across the country. The two sets of maps look markedly different.

Figure 11 is a cluster analysis prepared in GeoDa by asking the program to pick out 4, 7, 12 and 20 clusters respectively. Interestingly the program effortlessly picks out first the four regions and then apparently clusters reminiscent of those seen on the previous map-graphs.

Figure 12A shows a hinge map which works by analogy to the commonly used box and whisker plot in general statistics. The upper outliers appear in red and the lower outliers appear in blue. Figure 12B is a natural breaks map where the natural breaks in the data are used by the software to pick out the best places to make the categories of the autism rates. Again prominent states are discerned.

Figure 13 is a Dorlings cartogram of autism across USA at the state level where the autism rate is proportional to the redness and size of the circle representing that state.

Figure 14 compares Dorlings cartograms of monthly cannabis use, tobacco use, autism and cannabidiol exposure.

Figure 15 is a bivariate scatterplot matrix of four variables against each other, namely autism, monthly cigarette use, abuse or dependence on alcohol and annual cocaine use. Prominent on this graph is the mostly negative slopes of the regression lines with each of the comparator covariates.

Figure 15 is contrasted with Figure 16 which compares autism to rates of Δ9-THC, cannabidiol and cannabinol. For the autism-Δ9THC and autism-cannabinol regression lines the slopes are obviously strongly positive. For cannabidiol this is not true, but as the cannabidiol exposure over this period underwent a complex inverted U-shaped distribution this line is probably uninterpretable in this context. This finding has previously been deconvoluted and explored in detail [1].

LISA is a powerful spatial statistics technique which stands for 'Local Indicators of Spatial Autocorrelation' and has been very elegantly and directly operationalized in GeoDa.

Figure 17 presents a Lisa plot cluster analysis which identifies the high-high, high-low, low-low and low-high adjoining clusters for autism. Panel B shows the bivariate relationships between cannabis use and autism. The plot indicates that the Global Moran's I, a classical index of spatial autocorrelation, is 0.127 which is a value in the intermediate range. The significance of these changes is indicated in the Lisa significance map below in panel C.

Figure 18 shows a bivariate Lisa plot of autism and Δ9-THC exposure together. This plot highlights the discordances in the distribution of the two variables.

Figure 19 shows two views of a 3-dimensional plot of the three way relationship between time, cannabis use and the autism rate showing the regression surface. It has been drawn with NCSS software.

In Figure 20 this exercise is repeated showing a smoothed surface of best fit. Again two views are shown.

Figure 21 shows a similar exercise plotting a different regression surface for each state. Again there appears to be a general relationship between time, increasing cannabis exposure

and increasing autism rate in most states to the extent that this is discernible from this presentation.

Figure 22 shows a similar three-way time-cannabis autism plot prepared with OriginLab software.

Table 5 presents the results of ordinary least squares (OLS) analysis and mixed effects models of the relationships of drugs and cannabis with the autism rate. In the mixed effects models state is treated as a random factor. In each case the first model presented combined all the other drugs using principal components analysis which is a standard statistical technique for reducing the complexity of models and reducing their dimensionality. In each case last month cannabis use is significant at high level and the β-estimates are large. In the case of the direct linear models the R-squared values are also moderately elevated.

A variogram shows the way a parameter varies with geographical distance. They help to advise what kind of spatial model is best with which to conduct a spatial analysis.

Figure 23 presents a variogram prepared in GeoDa for the autism rate. The variogram cloud is shown in the bottom right. The small nugget is shown in the x-y line plot in the centre of the graphs. The nugget is the distance from the origin of the x-y plot to the commencement of the line on the y-ordinate. The size of the nugget indicates the degree of spatial lag which should be required by a good model which adequately accounts for the data.

Figure 24 presents a variogram for monthly cannabis use. A minimal nugget is noted.

Figure 25 presents a variogram for Δ9-THC exposure. Again a small nugget is noted.

LaGrange Multiplier (LM) tests are used in spatial statistics to determine the most appropriate kind of statistical model to employ to investigate the data. That is to say they help to select the optimal model specification. Table 6 presents a table of Lagrange Multiplier tests prepared in GeoDa. This table shows that a spatial error model is the most appropriate model with which to model the data.

Table 7 presents four simple additive models in parallel where autism is regressed on the first principal component of other drug use and monthly cannabis use. The first is the ordinary least squares (OLS) model presented above. The second model is a spatially lagged model. The third is the spatial error model. And the fourth model combines the spatial lag and spatial error models and is known as a SARMA (Spatial Autoregressive Moving Average) model. As noted above the spatial error model is most appropriate and p is significant in this model, although multiplicity adjusted q is not.

Table 8 presents results of a model regressing autism on all the drugs separately in linear and in various spatial models performed using the splm package in R. The results of the OLS model are presented first. SPGM (spatial general method of moments) from R package splm has been used to conduct the initial regressions. Δ9-THC and cannabichromene exposure are used as instrumental variables for monthly cannabis use in this two-step regression. A

SARAR model is presented next. Next follows a SARAR Model with five instrumental variables; then the spatial error model; followed by a two-step spatial error model with all five cannabinoids (Δ9-THC, cannabidiol, cannabichromene, cannabinol and cannabidiol) as instrumental variables. Multiple models of increasing complexity are presented to show that the highly significant findings relating to cannabis are almost independent of model design or specification and to illustrate the way in which significance changes with increasing model complexity.

Table 9 presents simple additive final regression models performed with spml in the splm package for spatial lag, spatial error and SARMA models. Only in the first model does a significant term for cannabis remain in the final model.

When the same exercise is performed with spml and spgm in various interactive temporospatial models the results shown in Table 10 are derived. As shown there highly significant main and interactive effects for cannabis are shown in each model nearly all of which are significant at the multiplicity testing adjusted threshold of q=0.0013.

Although it is not strictly necessary it was considered of interest to examine the changes over the period of this lengthy dataset. Figure 26 charts these changes across time and has been prepared in R using the sf package for the four time differences indicated. The map-graphs show that Minnesota and some of the northeastern states- Maine, Pennsylvania, Massachusetts and others experienced the most marked changes.

Figure 27 shows that changes in the period 2002-2011 which is the primary period of analysis, being the period for which the SAMHSA NSDUH dataset is complete.

Figure 28 presents map-graphically the relevant changes in all of the variables considered for this period. Interestingly one notes on this graph that Minnesota is only high on the autism and analgesic scales whilst Maine is high on the analgesic, annual cannabis, tobacco and cocaine scales.

Table 11 presents the results of final general method of moments spatial error autocorrelated and spatial error with spatially autocorrelated errors models. In this case the changes in autism have been regressed on the changes in the various drugs. The “d” prefix in front of all the drug terms relates to delta, standing for change in the drug of interest. Again interactive terms containing cannabis are significant beyond the multiplicity threshold.

Impact of Cannabis Legal Status on Autism Rates

Figure 29 shows that in both the IDEA and ADDM datasets [4] states with legal cannabis had higher rates of autism than states which did not. Finding the same result in two datasets is very highly significant indeed. We have previously published these findings [1,2].

Figure 30 presents boxplots of the autism rate by various legal status parameters for the period 1995-2011. One reads the boxplot by noting where the notches do not overlap which

indicates statistical significance. The first panel shows the autism rates applying under each legal paradigm. The progressive rise from Illegal to Medical to Decriminalized status is noted and also that the notches for the Decriminalized states do not overlap those for the Illegal states. The second panel dichotomizes the legal status and compares the illegal status with other states which are essentially legal or *de facto* legal paradigms. Again one notices that the notches for the two groups do not overlap. The third panel compares the autism rates in jurisdictions which changed the legal status of cannabis for more liberal paradigms with those which did not. In each case clear indications of significant differences in terms of non-overlapping notches are noted.

It is possible to quantitate these time-based graphically-indicated changes using t-tests. The following t-statistics can be calculated from the 1995-2011 change dataset, n=51. For the status of illegal v. decriminalized the two rates are 75.51 $\pm$ 5.07 v 114.20 $\pm$ 12.69 (mean $\pm$ standard error of the mean), t = 2.8295, df = 12.00, P = 0.01518. For the dichotomous illegal v non-illegal comparison the two rates are 75.51$\pm$5.07 v 100.54$\pm$7.98, t = -2.6476, df = 36.89, P = 0.01185. For the illegal paradigm v changed paradigm the two rates are respectively 81.36$\pm$5.72 and 100.77$\pm$7.35, t = 2.0819, df = 27.64, P = 0.04673.

When one looks at the whole IDEA dataset for the dichotomous comparison Illegal v Decriminalized, n=961, the values are 31.6871$\pm$1.0391 v 52.1626$\pm$3.6899, t=5.3412, df=191.938 and P = 2.5958 x10^{-7}.

Table 12 presents the results of increasingly complex OLS models of legal status. In each case highly significant results are found well below the multiplicity-adjusted threshold. Importantly the adjusted R-squared in each case is remarkably high for such simple models; indeed in the most sophisticated final model adjusted $R^2 = 0.8215$. One note that the model quadratic in time is superior to the simple model linear in time with Anova: F = 197.09, df=1, P < 2.2 x 10^{-16}, so that the final model is the most preferred. In this model decriminalized status is significant P = 1.49 x 10^{-11}.

Table 13 presents the results of LM tests for model structure from GeoDa. These results unequivocally indicate that the spatial error model is the preferred model.

Table 14 presents the results of investigating this issue using the highly sophisticated spatial spreml regression routines from R's splm package. In each case at 2-, 4- and 6- lags the impacts of cannabis decriminalization on the autism rate is significant below the multiplicity threshold limit.

Table 15 presents the results of investigating the issue of the time dependent changes in autism rate 1994-2011 with spatial regression from R's splm package. In each case of the SARAR and error spml and spgm models the impacts of cannabis decriminalization on the autism rate is highly significant well beyond the threshold limit of multiplicity testing.

Discussion

The above considerations establish beyond reasonable doubt that increasing rates of cannabis use are so closely associated with the exponentially increasing rates of autism as to raise serious concerns as to the likelihood of a causal relationship.

One notes that all of the criteria of causality defined by Austin Bradford Hill in 1965 are met by the described cannabis – autism link. The data obviously demonstrate major strengths of association, consistency across various levels of geospatial resolution, specificity for cannabis and not other drugs of addiction, appropriate temporality, and, based on the regression results presented above, a dose response relationship. Quite apart from the data being described at three geospatial levels within USA, the data is also consistent other data observed elsewhere and similar findings have also been reported in clinics seeing high numbers of such children in Australia [1,2].

Mechanistic Considerations

However cellular and molecular mechanistic considerations under Hill's biological plausibility and experimental verification criteria are central to any discussion of potential causality. It is considered that it is worth enumerating just a select few of the mechanisms by which several cannabinoids have been shown to interfere with brain formation and brain function as it seems that such data [8-35] are in fact not widely known amongst the medical or related health professions.

1) Epigenetic pathways. Cannabis and several cannabinoids have been shown to leave a heavy footprint on both neural genes and immune genes. Whilst neural genes are obviously involved in neuronal patterning and brain formation it is often not well appreciated that the immune system is a major sculptor and formative agent in the brain reaching its final form [36,37]
2) Expression of autism genes is disrupted [38-42]
3) Epigenetic effects in sperm [43-47]
4) CNS synapses actually harbour transsynaptic receptor-ligand pairs which form the protosynapse before it becomes electrically active and play central roles in forming arranging and later scaffolding the synaptic machinery. One such key receptor-ligand pair is neurexin – neuroligin which plays a central role in synapse formation and has also been heavily implicated in the development of diseases such as schizophrenia and autism [48-53].
5) Cannabis interferes with cell division of the neuroblasts which are required to actively form the brain [21,54-58]
6) Cannabis interferes with radial glial cell function from which the neuronal precursors form and which also form the 'rails' along which the new neuroblasts move into their cortical and subcortical locations
7) Cannabinoids adversely affect the development of the prefrontal and other cortices which play a vital role in higher cortical and executive functioning [59-70]
8) Δ9-THC has been shown to interfere with axonal pathfinding ability by perturbing the axonal growth cone which steers axonal development by interfering with stathmin

[71,72]. Hence major axonal pathfinding errors implies that cannabinoid exposure will lead to a miswiring of the brain.

9) Stathmin also controls hippocampal cortical neurogenesis and spinogenesis so that these processes are also expected to be perturbed by cannabinoids
10) Prenatal cannabinoid exposure has also been shown to interfere with long range axonal pathfinding from telencephalic corticospinal neurons of both the glutamatergic and GABAergic types via CB1R mediation [12]
11) Prenatal cannabis administration has also been shown to lower the seizure threshold [12]
12) Cannabinoids have been shown to affect numerous genes whose expression has been shown to impact the development of autism [73-82]
13) Cannabis use has been shown to disconnect white matter from grey matter [8,19,65,83-89]
14) Cannabinoids have an adverse effect on the health and function of both oligodendrocytes and oligodendroglial progenitor cells [90-95]
15) Cannabinoids interfere with slit-robo signalling which controls the elaboration of the massive cerebral cortex in humans [10,96-101]
16) Cannabinoids adversely affect the cell fate specification of dividing neuroblasts and tilt the differentiation ratio against neuronal precursor cells towards astrocytic cell lineages [102]
17) In utero proinflammatory signaling is known to be linked with the development of schizophrenia and autism in later adult life. Radial glial cells form the framework upon which the developing cortex and subcortical structures are built [103,104], and these cells carry receptors for inflammatory cytokines and chemokines [105-107]. Several cannabinoids acting through CB1R's are known to exert proinflammatory actions on brain and other tissues [108,109].
18) This finding is in accord with two CDC reports of a near-doubling of the rate of anencephaly in children exposed prenatally to cannabis [110,111]
19) At the time of writing cannabinoid receptors have not been described on radial glial cells, although indirect evidence makes their presence not unlikely
20) Cannabinoids interfere with notch signaling [99,100,112-117] which is a major morphogen for brain [118-129], heart [130-137], and blood vessel [138-144] development and has also been implicated in many cancers [73-82]
21) Several cannabinoids have been shown to interact at multiple levels with Wnt signalling [145-154]. Wnt is a major body morphogen at all stages of body patterning and organ development and particularly involved in brain and heart formation and cancer development [144]. For example it was recently shown that rostral-caudal non-canonical (via Ryk rather than β-catenin) Wnt signalling gradients control the emergence of two major populations of parvalbumin- and somatostatin- expressing GABA interneurons in the cerebral cortex [155]. These interneurons control such fundamental functions as regulating attention states, signal timing and cortical rhythmicity. And it has further been shown that the principal neurons of the telencephalic midbrain, the medium spiny neurons which carry dopamine and cannabinoid receptors, dopamine-and cyclic AMP-regulated phosphoprotein (DARPP32) and GABA Receptors, in the human midbrain hedonic circuit develop under a Wnt gradient in human embryonic brain organoids [147].
22) The hippocampus is a major site of memory formation and is engaged when exploring new and novel environments. Hippocampal neurogenesis continues in adulthood

from the basal layer of the granule layer. It was recently shown that neurovascular coupling was mediated by nitric oxide released from parvalbumin-positive basal GABAergic interneurons' perivascular endfeet which induced the release of vascular IGF1 which in turn controlled the survival of newborn neuroblasts which is the main determinant of net neurogenic activity in the subgranular zone [156]. Neuronal nitric oxide synthase is known to be impacted by both opioids [157-167] and cannabinoids [35,168-182].

23) This implies that hippocampal volume shrinkage which has consistently been identified in long term and heavy users of cannabis [183-192] may be induced by several mechanistic routes, viz. cannabinoid-mediated neurovascular coupling and perturbation of Wnt signalling and inhibition of cell divisions amongst others.
24) Such observations in adult subjects have obvious parallels during key neurodevelopmental periods.
25) Prenatal cannabis exposure has also been linked with a 40% elevation of the risk of the subsequent development of schizophrenia in a major US national survey [14].
26) Cannabinoids are potent suppressors of mitochondrial respiration in general [193-198] and in the brain in particular [199-205]. Indeed CB1R's have been described on the inner membrane of brain mitochondria, along with the complete downstream signal transduction machinery just as exists at the plasmalemma [206-212].
27) This has profound knock-on effects on many aspects of brain function [213] and
28) Since DNA maintenance reactions are largely endothermic and energy requiring [213] inevitably impact and impair genome stability and particularly energy intensive processes such as
29) Mitotic and meiotic cell division [213].

What must be strongly underscored in considering this list of major perturbations of pathways to brain formation is that brains which are perturbed in this way cannot 'become normal - because such brain never were. Brain formation is a delicately balanced sequential finely orchestrated sequence of processes and interference with key steps can readily lead to knock-on downstream effects from which recovery onto a normal brain developmental trajectory can be impossible.

To reiterate: brains which have been developmentally disturbed in this and other ways many times are unable to recover back to normal – as they never were.

Hence this brief review confirms that there are multiple known links between cannabis and disordered brain development which are known to be impactful and are likely to be implicated.

Hence it may rightly be said that indeed the cannabis-autism link thoroughly fulfils all of the Hill criteria for causal relationship.

Several other points to emerge from this analysis are noteworthy. The regression tables shown above show clear and unequivocal evidence of spatial lag and spatial error effects.

This is consistent with the impacts of carefully orchestrated and non-random publicity and popularization campaigns being waged sequentially across USA as is known to have occurred. In this manner this marketing campaign would appear to have left its "footprint" in the data.

This analysis clearly implicates other cannabinoids beyond simply Δ9-THC. In addition to Δ9-THC cannabigerol and cannabichromene are also noted to have risen most sharply in the decades under review and are implicated by the two-step instrumental variable regressions presented. This implies therefore that that cannabinoid preparations which claim to have reduced the Δ9-THC content below some mythical threshold are essentially failing completely to come to grips with the likely heritable neurotoxicity of several cannabinoids at once.

Indeed in view of the toxicity of cannabinoid oils to other plants including the leaves of cannabis sativa plants [214,215], it has been claimed that cannabinoids are in fact natural plant *poisons* designed to impair the reproductive fitness of animals which might graze upon them.

Given the spatial and temporal lags demonstrated herein, concerns relating to the delayed effects of the insertion of cannabinoids into the food chain can hardly be overstated. Being lipid soluble appreciable amounts of cannabinoids can be absorbed by the oral route and indeed cases of per oral poisoning of children and young adults are now well described, especially in Colorado. Indeed reports from birth defects registries exist from areas in France where cannabis in the food chain of Europe is fed to animals and the cattle are born without legs [216-218]. Humans eat such cannabinoid-fed animals and the rate of phocomelia (no arms) is said to have risen some 58-times – which is within the margin of error reported by an impressive Hawaiian study of an odds ratio of 21.9 times with 95%C.I. 4.45-65.63 [219]. And now similar observations are beginning to be made in Germany where three such children have been born in the same medium sized hospital in just three months! [220] Clearly there is no particular reason that such disabilities should be limited to the extremities and comparable findings are to be expected in that most delicate of all organs, the human brain.

It is also important to note that in fact the literature on prenatal cannabis exposure in fact describes a spectrum of disorders from autism to impaired cortical development to smaller heads [221] to microcephalus [219] to complete lack of the forebrain known as anencephalus [110,111] to foetal death. It therefore seems apparent that what we observe as autistic spectrum disorder in fact exists on a clinical spectrum of which autism is but one part.

A further extension of this line of thinking is that more subtle perturbations are also possible – and indeed are virtually a clinical certainty. The very clear clinical and educational reality playing out every day across medical consulting offices and classrooms from Colorado to Australia where caseloads from high cannabis using communities are common is that only the best such patients can even be allowed at school or in clinics. Severe behavioural problems, major attacks on teaching personnel, parents, grandparents and caregivers alike by patients who shortly after are unable to remember any of these attacks have become commonplace in children exposed prenatally to cannabis. As most of the above data have been collected through schools, patients who are not able to be accommodated in the

educational or special educational system “fly under the radar”. On account of these episodes numerous teachers are retiring and being forced out of their profession in both Queensland and Colorado. This implies that notwithstanding the above described robust and objective analytical findings it is our belief therefore that everything we have written about in the above data analysis is the good news for cannabis rather than the bad.

Conclusion

The results of this spatiotemporal investigation confirm, extend and strengthen our earlier reports that cannabinoid exposure is causally associated with US national autism rates, by demonstrating and confirming these relationships at very high levels of statistical significance using advanced spatiotemporal regression techniques with high levels of R-squared in two step models from $P = 0.00016$. At the national level this relationship was significant at $P = 4.69 \times 10^{-14}$. We have also shown that cannabis legal paradigms which weaken the illegal status of cannabis are associated with increased rates of autism from $P = 0.00000339$, that is with very high levels of statistical certainty. Moreover by establishing these results at three spatial levels, the national, regional and state level, we have shown that the relationship holds at all geospatial levels down to this level and thereby robustifed our general conclusion.

This analysis has been conducted in order to study the available objective and quantifiable data. However the very evident clinical and educational reality is that the real world situation is likely much worse than the scenario described in the present study and, like the iceberg, constitutes the predominant mass beneath the robust and convincing and unequivocal situation described herein.

References

1. Reece A. S., Hulse G.K. Epidemiological Associations of Various Substances and Multiple Cannabinoids with Autism in USA. Clinical Pediatrics: Open Access 2019;4:In Press.
2. Reece A.S., Hulse G.K. Effect of Cannabis Legalization on US Autism Incidence and Medium Term Projections. Clinical Pediatrics: Open Access 2019;4:1-17.
3. Tobler W. A Computer Movie Simulating Urban Growth in the Detroit Region. Economic Geography 1970;46 (Supplement):234-40.
4. Nevison C, Blaxill M, Zahorodny W. California Autism Prevalence Trends from 1931 to 2014 and Comparison to National ASD Data from IDEA and ADDM. J Autism Dev Disord 2018.
5. ElSohly MA, Mehmedic Z, Foster S, Gon C, Chandra S, Church JC. Changes in Cannabis Potency Over the Last 2 Decades (1995-2014): Analysis of Current Data in the United States. Biol Psychiatry 2016;79:613-9.
6. ElSohly MA, Ross SA, Mehmedic Z, Arafat R, Yi B, Banahan BF, 3rd. Potency trends of delta9-THC and other cannabinoids in confiscated marijuana from 1980-1997. Journal of forensic sciences 2000;45:24-30.
7. Millo G. Maximum likelihood estimation of spatially and serially correlated panels with random effects. Computational Statistics & Data Analysis 2014;71:914-33.
8. Becker MP, Collins PF, Lim KO, Muetzel RL, Luciana M. Longitudinal changes in white matter microstructure after heavy cannabis use. Developmental cognitive neuroscience 2015;16:23-35.
9. Calvigioni D, Hurd YL, Harkany T, Keimpema E. Neuronal substrates and functional consequences of prenatal cannabis exposure. Eur Child Adolesc Psychiatry 2014;23:931-41.
10. Cardenas A, Villalba A, de Juan Romero C, et al. Evolution of Cortical Neurogenesis in Amniotes Controlled by Robo Signaling Levels. Cell 2018;174:590-606 e21.
11. de Oliveira RW, Oliveira CL, Guimaraes FS, Campos AC. Cannabinoid signalling in embryonic and adult neurogenesis: possible implications for psychiatric and neurological disorders. Acta Neuropsychiatr 2018:1-16.
12. de Salas-Quiroga A, Diaz-Alonso J, Garcia-Rincon D, et al. Prenatal exposure to cannabinoids evokes long-lasting functional alterations by targeting CB1 receptors on developing cortical neurons. Proc Natl Acad Sci U S A 2015;112:13693-8.
13. DeRosse P, Ikuta T, Peters BD, Karlsgodt KH, Szeszko PR, Malhotra AK. Adding insult to injury: childhood and adolescent risk factors for psychosis predict lower fractional anisotropy in the superior longitudinal fasciculus in healthy adults. Psychiatry Res 2014;224:296-302.
14. Fine JD, Moreau AL, Karcher NR, et al. Association of Prenatal Cannabis Exposure With Psychosis Proneness Among Children in the Adolescent Brain Cognitive Development (ABCD) Study. JAMA Psychiatry 2019;76:762-4.
15. Gilbert MT, Sulik KK, Fish EW, Baker LK, Dehart DB, Parnell SE. Dose-dependent teratogenicity of the synthetic cannabinoid CP-55,940 in mice. Neurotoxicol Teratol 2016;58:15-22.
16. Hernandez-Cervantes R, Mendez-Diaz M, Prospero-Garcia O, Morales-Montor J. Immunoregulatory Role of Cannabinoids during Infectious Disease. Neuroimmunomodulation 2017;24:183-99.
17. Imperatore R, Palomba L, Morello G, et al. Formation of OX-1R/CB1R heteromeric complexes in embryonic mouse hypothalamic cells: Effect on intracellular calcium, 2-

arachidonoyl-glycerol biosynthesis and ERK phosphorylation. Pharmacol Res 2016;111:600-9.
18. Jansson LM, Jordan CJ, Velez ML. Perinatal Marijuana Use and the Developing Child. JAMA 2018;320:545-6.
19. Lorenzetti V, Solowij N, Whittle S, et al. Gross morphological brain changes with chronic, heavy cannabis use. Br J Psychiatry 2015;206:77-8.
20. Luby JL, Agrawal A, Belden A, Whalen D, Tillman R, Barch DM. Developmental Trajectories of the Orbitofrontal Cortex and Anhedonia in Middle Childhood and Risk for Substance Use in Adolescence in a Longitudinal Sample of Depressed and Healthy Preschoolers. Am J Psychiatry 2018:appiajp201817070777.
21. Maccarrone M, Guzman M, Mackie K, Doherty P, Harkany T. Programming of neural cells by (endo)cannabinoids: from physiological rules to emerging therapies. Nat Rev Neurosci 2014;15:786-801.
22. Madabhushi R, Pan L, Tsai LH. DNA damage and its links to neurodegeneration. Neuron 2014;83:266-82.
23. Mandolesi G, Bullitta S, Fresegna D, et al. Interferon-gamma causes mood abnormalities by altering cannabinoid CB1 receptor function in the mouse striatum. Neurobiology of disease 2017;108:45-53.
24. Navakkode S, Korte M. Pharmacological activation of CB1 receptor modulates long term potentiation by interfering with protein synthesis. Neuropharmacology 2014;79:525-33.
25. Renard J, Krebs MO, Le Pen G, Jay TM. Long-term consequences of adolescent cannabinoid exposure in adult psychopathology. Front Neurosci 2014;8:361.
26. Richardson KA, Hester AK, McLemore GL. Prenatal cannabis exposure - The "first hit" to the endocannabinoid system. Neurotoxicol Teratol 2016;58:5-14.
27. Romero J, Garcia-Palomero E, Berrendero F, et al. Atypical location of cannabinoid receptors in white matter areas during rat brain development. Synapse 1997;26:317-23.
28. Seleverstov O, Tobiasz A, Jackson JS, et al. Maternal alcohol exposure during mid-pregnancy dilates fetal cerebral arteries via endocannabinoid receptors. Alcohol (Fayetteville, NY 2017;61:51-61.
29. Skosnik PD, Cortes-Briones JA, Hajos M. It's All in the Rhythm: The Role of Cannabinoids in Neural Oscillations and Psychosis. Biol Psychiatry 2016;79:568-77.
30. Sun X, Deng W, Li Y, et al. Sustained Endocannabinoid Signaling Compromises Decidual Function and Promotes Inflammation-induced Preterm Birth. J Biol Chem 2016;291:8231-40.
31. Vargish GA, Pelkey KA, Yuan X, et al. Persistent inhibitory circuit defects and disrupted social behaviour following in utero exogenous cannabinoid exposure. Mol Psychiatry 2017;22:56-67.
32. Vecera J, Bartova E, Krejci J, et al. HDAC1 and HDAC3 underlie dynamic H3K9 acetylation during embryonic neurogenesis and in schizophrenia-like animals. J Cell Physiol 2018;233:530-48.
33. Volk DW, Lewis DA. The Role of Endocannabinoid Signaling in Cortical Inhibitory Neuron Dysfunction in Schizophrenia. Biol Psychiatry 2016;79:595-603.
34. Wu CS, Jew CP, Lu HC. Lasting impacts of prenatal cannabis exposure and the role of endogenous cannabinoids in the developing brain. Future Neurol 2011;6:459-80.
35. Zong Y, Zhou X, Cheng J, Yu J, Wu J, Jiang C. Cannabinoids Regulate the Diameter of Pericyte-Containing Retinal Capillaries in Rats. Cell Physiol Biochem 2017;43:2088-101.
36. Deverman BE, Patterson PH. Cytokines and CNS development. Neuron 2009;64:61-78.
37. Carpentier PA, Palmer TD. Immune influence on adult neural stem cell regulation and function. Neuron 2009;64:79-92.

38. Grissom NM, Herdt CT, Desilets J, Lidsky-Everson J, Reyes TM. Dissociable deficits of executive function caused by gestational adversity are linked to specific transcriptional changes in the prefrontal cortex. Neuropsychopharmacology 2015;40:1353-63.
39. Guennewig B, Bitar M, Obiorah I, et al. THC exposure of human iPSC neurons impacts genes associated with neuropsychiatric disorders. Transl Psychiatry 2018;8:89.
40. Martella G, Meringolo M, Trobiani L, De Jaco A, Pisani A, Bonsi P. The neurobiological bases of autism spectrum disorders: the R451C-neuroligin 3 mutation hampers the expression of long-term synaptic depression in the dorsal striatum. Eur J Neurosci 2018;47:701-8.
41. Siniscalco D, Bradstreet JJ, Cirillo A, Antonucci N. The in vitro GcMAF effects on endocannabinoid system transcriptionomics, receptor formation, and cell activity of autism-derived macrophages. J Neuroinflammation 2014;11:78.
42. Trifonov S, Houtani T, Shimizu J, et al. GPR155: Gene organization, multiple mRNA splice variants and expression in mouse central nervous system. Biochem Biophys Res Commun 2010;398:19-25.
43. Feinberg JI, Bakulski KM, Jaffe AE, et al. Paternal sperm DNA methylation associated with early signs of autism risk in an autism-enriched cohort. International journal of epidemiology 2015;44:1199-210.
44. Murphy SK, Itchon-Ramos N, Visco Z, et al. Cannabinoid exposure and altered DNA methylation in rat and human sperm. Epigenetics 2018.
45. Reece AS, Hulse G.K. Impacts of Cannabinoid Epigenetics on Human Development: Reflections on Murphy et. al. “Cannabinoid Exposure and Altered DNA Methylation in Rat and Human Sperm” Epigenetics 2018; 13: 1208-1221. Epigenetics 2019;In Press:1-16.
46. Skinner MK, Nilsson E, Sadler-Riggleman I, Beck D, Ben Maamar M, McCarrey JR. Transgenerational sperm DNA methylation epimutation developmental origins following ancestral vinclozolin exposure. Epigenetics 2019:1-19.
47. Acharya K.S., Schrott R., Grenier C., et al. Epigenetic Alterations in Cytochrome P450 Oxidoreductase (*Por*) in Sperm of Rats |Exposed to Tetrahydrocannabinol (THC). Scientific Reports 2019;In Press.
48. Foldy C, Malenka RC, Sudhof TC. Autism-associated neuroligin-3 mutations commonly disrupt tonic endocannabinoid signaling. Neuron 2013;78:498-509.
49. Radyushkin K, Hammerschmidt K, Boretius S, et al. Neuroligin-3-deficient mice: model of a monogenic heritable form of autism with an olfactory deficit. Genes Brain Behav 2009;8:416-25.
50. Sun C, Zhang L, Chen G. An unexpected role of neuroligin-2 in regulating KCC2 and GABA functional switch. Mol Brain 2013;6:23.
51. Anderson GR, Aoto J, Tabuchi K, et al. beta-Neurexins Control Neural Circuits by Regulating Synaptic Endocannabinoid Signaling. Cell 2015;162:593-606.
52. Hishimoto A, Liu QR, Drgon T, et al. Neurexin 3 polymorphisms are associated with alcohol dependence and altered expression of specific isoforms. Hum Mol Genet 2007;16:2880-91.
53. Wang H. Endocannabinoid Mediates Excitatory Synaptic Function of β-Neurexins. Commentary: β-Neurexins Control Neural Circuits by Regulating Synaptic Endocannabinoid Signaling. Frontiers in Neuroscience 2016;10.
54. Deng L, Ng L, Ozawa T, Stella N. Quantitative Analyses of Synergistic Responses between Cannabidiol and DNA-Damaging Agents on the Proliferation and Viability of Glioblastoma and Neural Progenitor Cells in Culture. J Pharmacol Exp Ther 2017;360:215-24.
55. Eisch AJ, Barrot M, Schad CA, Self DW, Nestler EJ. Opiates inhibit neurogenesis in the adult rat hippocampus. Proc Natl Acad Sci U S A 2000;97:7579-84.

56. McClean DK, Zimmerman AM. Action of delta 9-tetrahydrocannabinol on cell division and macromolecular synthesis in division-synchronized protozoa. Pharmacology 1976;14:307-21.
57. Noonan M.A., Eisch AJ. Regulation of Adult Neurogenesis by Cannabinoids. Chemistry Today 2006;24:84-8.
58. Wilkinson JD, Williamson EM. Cannabinoids inhibit human keratinocyte proliferation through a non-CB1/CB2 mechanism and have a potential therapeutic value in the treatment of psoriasis. J Dermatol Sci 2007;45:87-92.
59. Batalla A, Bhattacharyya S, Yucel M, et al. Structural and functional imaging studies in chronic cannabis users: a systematic review of adolescent and adult findings. PLoS One 2013;8:e55821.
60. Blanco-Hinojo L, Pujol J, Harrison BJ, et al. Attenuated frontal and sensory inputs to the basal ganglia in cannabis users. Addict Biol 2017;22:1036-47.
61. Chye Y, Solowij N, Ganella EP, et al. Role of orbitofrontal sulcogyral pattern on lifetime cannabis use and depressive symptoms. Prog Neuropsychopharmacol Biol Psychiatry 2017;79:392-400.
62. Chye Y, Solowij N, Suo C, et al. Orbitofrontal and caudate volumes in cannabis users: a multi-site mega-analysis comparing dependent versus non-dependent users. Psychopharmacology (Berl) 2017;234:1985-95.
63. Goodman MS, Bridgman AC, Rabin RA, et al. Differential effects of cannabis dependence on cortical inhibition in patients with schizophrenia and non-psychiatric controls. Brain Stimul 2017;10:275-82.
64. Lisdahl KM, Tamm L, Epstein JN, et al. The impact of ADHD persistence, recent cannabis use, and age of regular cannabis use onset on subcortical volume and cortical thickness in young adults. Drug Alcohol Depend 2016;161:135-46.
65. Lorenzetti V, Solowij N, Yucel M. The Role of Cannabinoids in Neuroanatomic Alterations in Cannabis Users. Biol Psychiatry 2016;79:e17-31.
66. Nicholls C, Bruno R, Matthews A. Chronic cannabis use and ERP correlates of visual selective attention during the performance of a flanker go/nogo task. Biol Psychol 2015;110:115-25.
67. Pfefferbaum A, Kwon D, Brumback T, et al. Altered Brain Developmental Trajectories in Adolescents After Initiating Drinking. Am J Psychiatry 2018;175:370-80.
68. Shollenbarger SG, Price J, Wieser J, Lisdahl K. Impact of cannabis use on prefrontal and parietal cortex gyrification and surface area in adolescents and emerging adults. Developmental cognitive neuroscience 2015;16:46-53.
69. Shollenbarger SG, Price J, Wieser J, Lisdahl K. Poorer frontolimbic white matter integrity is associated with chronic cannabis use, FAAH genotype, and increased depressive and apathy symptoms in adolescents and young adults. Neuroimage Clin 2015;8:117-25.
70. Tervo-Clemmens B, Simmonds D, Calabro FJ, Day NL, Richardson GA, Luna B. Adolescent cannabis use and brain systems supporting adult working memory encoding, maintenance, and retrieval. Neuroimage 2018;169:496-509.
71. Martel G, Uchida S, Hevi C, et al. Genetic Demonstration of a Role for Stathmin in Adult Hippocampal Neurogenesis, Spinogenesis, and NMDA Receptor-Dependent Memory. J Neurosci 2016;36:1185-202.
72. Tortoriello G, Morris CV, Alpar A, et al. Miswiring the brain: Delta9-tetrahydrocannabinol disrupts cortical development by inducing an SCG10/stathmin-2 degradation pathway. EMBO J 2014;33:668-85.
73. Meurette O, Mehlen P. Notch Signaling in the Tumor Microenvironment. Cancer Cell 2018;34:536-48.

74. Krishnamurthy N, Kurzrock R. Targeting the Wnt/beta-catenin pathway in cancer: Update on effectors and inhibitors. Cancer Treat Rev 2018;62:50-60.
75. Zhang Y, Jin X, Wang Z, Zhang X, Liu S, Liu G. Downregulation of SNHG1 suppresses cell proliferation and invasion by regulating Notch signaling pathway in esophageal squamous cell cancer. Cancer Biomark 2017;21:89-96.
76. Zhang J, Kuang Y, Wang Y, Xu Q, Ren Q. Notch-4 silencing inhibits prostate cancer growth and EMT via the NF-kappaB pathway. Apoptosis 2017;22:877-84.
77. Xiao W, Gao Z, Duan Y, Yuan W, Ke Y. Notch signaling plays a crucial role in cancer stem-like cells maintaining stemness and mediating chemotaxis in renal cell carcinoma. J Exp Clin Cancer Res 2017;36:41.
78. Locatelli M, Curigliano G. Notch inhibitors and their role in the treatment of triple negative breast cancer: promises and failures. Curr Opin Oncol 2017;29:411-27.
79. Lim JS, Ibaseta A, Fischer MM, et al. Intratumoural heterogeneity generated by Notch signalling promotes small-cell lung cancer. Nature 2017;545:360-4.
80. Li L, Tang P, Li S, et al. Notch signaling pathway networks in cancer metastasis: a new target for cancer therapy. Med Oncol 2017;34:180.
81. Ito T, Kudoh S, Ichimura T, Fujino K, Hassan WA, Udaka N. Small cell lung cancer, an epithelial to mesenchymal transition (EMT)-like cancer: significance of inactive Notch signaling and expression of achaete-scute complex homologue 1. Hum Cell 2017;30:1-10.
82. Ibrahim SA, Gadalla R, El-Ghonaimy EA, et al. Syndecan-1 is a novel molecular marker for triple negative inflammatory breast cancer and modulates the cancer stem cell phenotype via the IL-6/STAT3, Notch and EGFR signaling pathways. Molecular cancer 2017;16:57.
83. Solowij N, Michie PT, Fox AM. Differential impairments of selective attention due to frequency and duration of cannabis use. Biol Psychiatry 1995;37:731-9.
84. Hall W, Solowij N. Long-term cannabis use and mental health. Br J Psychiatry 1997;171:107-8.
85. Solowij N, Michie PT. Cannabis and cognitive dysfunction: parallels with endophenotypes of schizophrenia? J Psychiatry Neurosci 2007;32:30-52.
86. Solowij N, Battisti R. The chronic effects of cannabis on memory in humans: a review. Curr Drug Abuse Rev 2008;1:81-98.
87. Harding IH, Solowij N, Harrison BJ, et al. Functional connectivity in brain networks underlying cognitive control in chronic cannabis users. Neuropsychopharmacology 2012;37:1923-33.
88. Zalesky A, Solowij N, Yucel M, et al. Effect of long-term cannabis use on axonal fibre connectivity. Brain 2012;135:2245-55.
89. Solowij N, Yucel M, Respondek C, et al. Cerebellar white-matter changes in cannabis users with and without schizophrenia. Psychological medicine 2011;41:2349-59.
90. Ilyasov AA, Milligan CE, Pharr EP, Howlett AC. The Endocannabinoid System and Oligodendrocytes in Health and Disease. Front Neurosci 2018;12:733.
91. Marinelli C, Bertalot T, Zusso M, Skaper SD, Giusti P. Systematic Review of Pharmacological Properties of the Oligodendrocyte Lineage. Front Cell Neurosci 2016;10:27.
92. Bernal-Chico A, Canedo M, Manterola A, et al. Blockade of monoacylglycerol lipase inhibits oligodendrocyte excitotoxicity and prevents demyelination in vivo. Glia 2015;63:163-76.
93. Gomez O, Sanchez-Rodriguez A, Le M, Sanchez-Caro C, Molina-Holgado F, Molina-Holgado E. Cannabinoid receptor agonists modulate oligodendrocyte differentiation by activating PI3K/Akt and the mammalian target of rapamycin (mTOR) pathways. Br J Pharmacol 2011;163:1520-32.

94. Turunen PM, Louhivuori LM, Louhivuori V, Kukkonen JP, Akerman KE. Endocannabinoid Signaling in Embryonic Neuronal Motility and Cell-Cell Contact - Role of mGluR5 and TRPC3 Channels. Neuroscience 2018;375:135-48.
95. Arevalo-Martin A, Garcia-Ovejero D, Rubio-Araiz A, Gomez O, Molina-Holgado F, Molina-Holgado E. Cannabinoids modulate Olig2 and polysialylated neural cell adhesion molecule expression in the subventricular zone of post-natal rats through cannabinoid receptor 1 and cannabinoid receptor 2. Eur J Neurosci 2007;26:1548-59.
96. Alpar A, Tortoriello G, Calvigioni D, et al. Endocannabinoids modulate cortical development by configuring Slit2/Robo1 signalling. Nat Commun 2014;5:4421.
97. London NR, Li DY. Robo4-dependent Slit signaling stabilizes the vasculature during pathologic angiogenesis and cytokine storm. Curr Opin Hematol 2011;18:186-90.
98. London NR, Zhu W, Bozza FA, et al. Targeting Robo4-dependent Slit signaling to survive the cytokine storm in sepsis and influenza. Sci Transl Med 2010;2:23ra19.
99. Lu T, Newton C, Perkins I, Friedman H, Klein TW. Cannabinoid treatment suppresses the T-helper cell-polarizing function of mouse dendritic cells stimulated with Legionella pneumophila infection. J Pharmacol Exp Ther 2006;319:269-76.
100. Newton CA, Chou PJ, Perkins I, Klein TW. CB(1) and CB(2) cannabinoid receptors mediate different aspects of delta-9-tetrahydrocannabinol (THC)-induced T helper cell shift following immune activation by Legionella pneumophila infection. J Neuroimmune Pharmacol 2009;4:92-102.
101. Yeh ML, Gonda Y, Mommersteeg MT, et al. Robo1 modulates proliferation and neurogenesis in the developing neocortex. J Neurosci 2014;34:5717-31.
102. Aguado T, Palazuelos J, Monory K, et al. The endocannabinoid system promotes astroglial differentiation by acting on neural progenitor cells. J Neurosci 2006;26:1551-61.
103. Contreras X, Hippenmeyer S. Memo1 Tiles the Radial Glial Cell Grid. Neuron 2019;103:750-2.
104. Nakagawa N, Plestant C, Yabuno-Nakagawa K, et al. Memo1-Mediated Tiling of Radial Glial Cells Facilitates Cerebral Cortical Development. Neuron 2019;103:836-52 e5.
105. Portillo JC, Lopez Corcino Y, Miao Y, et al. CD40 in Retinal Muller Cells Induces P2X7-Dependent Cytokine Expression in Macrophages/Microglia in Diabetic Mice and Development of Early Experimental Diabetic Retinopathy. Diabetes 2017;66:483-93.
106. Diotel N, Vaillant C, Gueguen MM, et al. Cxcr4 and Cxcl12 expression in radial glial cells of the brain of adult zebrafish. The Journal of comparative neurology 2010;518:4855-76.
107. Mithal DS, Ren D, Miller RJ. CXCR4 signaling regulates radial glial morphology and cell fate during embryonic spinal cord development. Glia 2013;61:1288-305.
108. Ge Q, Maury E, Rycken L, et al. Endocannabinoids regulate adipokine production and the immune balance of omental adipose tissue in human obesity. International journal of obesity (2005) 2013;37:874-80.
109. Mukhopadhyay B, Schuebel K, Mukhopadhyay P, et al. Cannabinoid receptor 1 promotes hepatocellular carcinoma initiation and progression through multiple mechanisms. Hepatology 2015;61:1615-26.
110. Van Gelder MMHJ, Donders ART, Devine O, Roeleveld N, Reefhuis J. Using bayesian models to assess the effects of under-reporting of cannabis use on the association with birth defects, national birth defects prevention study, 1997-2005. Paediatric and perinatal epidemiology 2014;28:424-33.
111. Van Gelder MMHJ, Reefhuis J, Caton AR, Werler MM, Druschel CM, Roeleveld N. Maternal periconceptional illicit drug use and the risk of congenital malformations. Epidemiology 2009;20:60-6.

112. Kangsamaksin T, Murtomaki A, Kofler NM, et al. NOTCH decoys that selectively block DLL/NOTCH or JAG/NOTCH disrupt angiogenesis by unique mechanisms to inhibit tumor growth. Cancer Discov 2015;5:182-97.
113. Tanveer R, Gowran A, Noonan J, Keating SE, Bowie AG, Campbell VA. The endocannabinoid, anandamide, augments Notch-1 signaling in cultured cortical neurons exposed to amyloid-beta and in the cortex of aged rats. J Biol Chem 2012;287:34709-21.
114. Frampton G, Coufal M, Li H, Ramirez J, DeMorrow S. Opposing actions of endocannabinoids on cholangiocarcinoma growth is via the differential activation of Notch signaling. Exp Cell Res 2010;316:1465-78.
115. Kim D, Lim S, Park M, et al. Ubiquitination-dependent CARM1 degradation facilitates Notch1-mediated podocyte apoptosis in diabetic nephropathy. Cellular signalling 2014;26:1774-82.
116. Niu F, Zhao S, Xu CY, et al. Potentiation of the antitumor activity of adriamycin against osteosarcoma by cannabinoid WIN-55,212-2. Oncol Lett 2015;10:2415-21.
117. Xapelli S, Agasse F, Sarda-Arroyo L, et al. Activation of type 1 cannabinoid receptor (CB1R) promotes neurogenesis in murine subventricular zone cell cultures. PLoS One 2013;8:e63529.
118. Furukawa T, Mukherjee S, Bao ZZ, Morrow EM, Cepko CL. rax, Hes1, and notch1 promote the formation of Muller glia by postnatal retinal progenitor cells. Neuron 2000;26:383-94.
119. Redmond L, Oh SR, Hicks C, Weinmaster G, Ghosh A. Nuclear Notch1 signaling and the regulation of dendritic development. Nat Neurosci 2000;3:30-40.
120. Presente A, Andres A, Nye JS. Requirement of Notch in adulthood for neurological function and longevity. Neuroreport 2001;12:3321-5.
121. Li HS, Wang D, Shen Q, et al. Inactivation of Numb and Numblike in embryonic dorsal forebrain impairs neurogenesis and disrupts cortical morphogenesis. Neuron 2003;40:1105-18.
122. Klein AL, Zilian O, Suter U, Taylor V. Murine numb regulates granule cell maturation in the cerebellum. Dev Biol 2004;266:161-77.
123. Saura CA, Choi SY, Beglopoulos V, et al. Loss of presenilin function causes impairments of memory and synaptic plasticity followed by age-dependent neurodegeneration. Neuron 2004;42:23-36.
124. Huang EJ, Li H, Tang AA, et al. Targeted deletion of numb and numblike in sensory neurons reveals their essential functions in axon arborization. Genes Dev 2005;19:138-51.
125. Androutsellis-Theotokis A, Leker RR, Soldner F, et al. Notch signalling regulates stem cell numbers in vitro and in vivo. Nature 2006;442:823-6.
126. Yoon KJ, Koo BK, Im SK, et al. Mind bomb 1-expressing intermediate progenitors generate notch signaling to maintain radial glial cells. Neuron 2008;58:519-31.
127. Rash BG, Lim HD, Breunig JJ, Vaccarino FM. FGF signaling expands embryonic cortical surface area by regulating Notch-dependent neurogenesis. J Neurosci 2011;31:15604-17.
128. Rash BG, Tomasi S, Lim HD, Suh CY, Vaccarino FM. Cortical gyrification induced by fibroblast growth factor 2 in the mouse brain. J Neurosci 2013;33:10802-14.
129. Rusanescu G, Mao J. Notch3 is necessary for neuronal differentiation and maturation in the adult spinal cord. Journal of cellular and molecular medicine 2014;18:2103-16.
130. Luxan G, D'Amato G, de la Pompa JL. Intercellular Signaling in Cardiac Development and Disease: The NOTCH pathway. In: Nakanishi T, Markwald RR, Baldwin HS, Keller BB, Srivastava D, Yamagishi H, eds. Etiology and Morphogenesis of Congenital Heart Disease: From Gene Function and Cellular Interaction to Morphology. Tokyo2016:103-14.

131. Niessen K, Karsan A. Notch signaling in cardiac development. Circulation research 2008;102:1169-81.
132. Croquelois A, Domenighetti AA, Nemir M, et al. Control of the adaptive response of the heart to stress via the Notch1 receptor pathway. J Exp Med 2008;205:3173-85.
133. Collesi C, Zentilin L, Sinagra G, Giacca M. Notch1 signaling stimulates proliferation of immature cardiomyocytes. J Cell Biol 2008;183:117-28.
134. Campa VM, Gutierrez-Lanza R, Cerignoli F, et al. Notch activates cell cycle reentry and progression in quiescent cardiomyocytes. J Cell Biol 2008;183:129-41.
135. Xin M, Small EM, van Rooij E, et al. Essential roles of the bHLH transcription factor Hrt2 in repression of atrial gene expression and maintenance of postnatal cardiac function. Proc Natl Acad Sci U S A 2007;104:7975-80.
136. Kokubo H, Tomita-Miyagawa S, Hamada Y, Saga Y. Hesr1 and Hesr2 regulate atrioventricular boundary formation in the developing heart through the repression of Tbx2. Development 2007;134:747-55.
137. High FA, Zhang M, Proweller A, et al. An essential role for Notch in neural crest during cardiovascular development and smooth muscle differentiation. J Clin Invest 2007;117:353-63.
138. Walton CB, Ecker J, Anderson CD, Outten JT, Allison RZ, Shohet RV. Cardiac angiogenesis directed by stable Hypoxia Inducible Factor-1. Vasc Cell 2013;5:15.
139. Kangsamaksin T, Tattersall IW, Kitajewski J. Notch functions in developmental and tumour angiogenesis by diverse mechanisms. Biochemical Society transactions 2014;42:1563-8.
140. Rooney P, Connolly M, Gao W, et al. Notch-1 mediates endothelial cell activation and invasion in psoriasis. Exp Dermatol 2014;23:113-8.
141. Wu W, Tang L. [Research progress of vascular endothelial tip cells in diabetic retinopathy]. Zhonghua Yan Ke Za Zhi 2014;50:952-8.
142. Zheng Y, Hao Z, Ding Y, et al. Expression of delta-like 4 (Drosophila) and vascular endothelial growth factor A in colon cancer and association with tumour angiogenesis. J Int Med Res 2015;43:535-43.
143. Lv JY, Hu TY, Wang RY, Zhu JM, Wang G. Deciphering the anti-angiogenic effect of endostatin/cyclophosphamide to normalize tumor micrangium through notch signaling pathway in colon cancer. World J Surg Oncol 2016;14:10.
144. Carlson BM. Human Embryology and Developmental Biology. Philadelphia: Elsevier; 2014.
145. DeMorrow S, Francis H, Gaudio E, et al. The endocannabinoid anandamide inhibits cholangiocarcinoma growth via activation of the noncanonical Wnt signaling pathway. Am J Physiol Gastrointest Liver Physiol 2008;295:G1150-8.
146. Fiore D, Ramesh P, Proto MC, et al. Rimonabant Kills Colon Cancer Stem Cells without Inducing Toxicity in Normal Colon Organoids. Front Pharmacol 2017;8:949.
147. Hunt CPJ, Pouton CW, Haynes JM. Characterising the developmental profile of human embryonic stem cell-derived medium spiny neuron progenitors and assessing mature neuron function using a CRISPR-generated human DARPP-32(WT/eGFP-AMP) reporter line. Neurochem Int 2017;106:3-13.
148. Korem N, Lange R, Hillard CJ, Akirav I. Role of beta-catenin and endocannabinoids in the nucleus accumbens in extinction in rats exposed to shock and reminders. Neuroscience 2017;357:285-94.
149. Nallathambi R, Mazuz M, Namdar D, et al. Identification of Synergistic Interaction Between Cannabis-Derived Compounds for Cytotoxic Activity in Colorectal Cancer Cell Lines and Colon Polyps That Induces Apoptosis-Related Cell Death and Distinct Gene Expression. Cannabis Cannabinoid Res 2018;3:120-35.

150. Nalli Y, Dar MS, Bano N, et al. Analyzing the role of cannabinoids as modulators of Wnt/beta-catenin signaling pathway for their use in the management of neuropathic pain. Bioorganic & medicinal chemistry letters 2019;29:1043-6.
151. Petko J, Tranchina T, Patel G, Levenson R, Justice-Bitner S. Identifying novel members of the Wntless interactome through genetic and candidate gene approaches. Brain research bulletin 2018;138:96-105.
152. Proto MC, Fiore D, Piscopo C, et al. Inhibition of Wnt/beta-Catenin pathway and Histone acetyltransferase activity by Rimonabant: a therapeutic target for colon cancer. Sci Rep 2017;7:11678.
153. Vallee A, Lecarpentier Y, Guillevin R, Vallee JN. Effects of cannabidiol interactions with Wnt/beta-catenin pathway and PPARgamma on oxidative stress and neuroinflammation in Alzheimer's disease. Acta Biochim Biophys Sin (Shanghai) 2017;49:853-66.
154. Xian X, Tang L, Wu C, Huang L. miR-23b-3p and miR-130a-5p affect cell growth, migration and invasion by targeting CB1R via the Wnt/beta-catenin signaling pathway in gastric carcinoma. OncoTargets and therapy 2018;11:7503-12.
155. McKenzie MG, Cobbs LV, Dummer PD, et al. Non-canonical Wnt Signaling through Ryk Regulates the Generation of Somatostatin- and Parvalbumin-Expressing Cortical Interneurons. Neuron 2019;103:853-64 e4.
156. Shen J, Wang D, Wang X, et al. Neurovascular Coupling in the Dentate Gyrus Regulates Adult Hippocampal Neurogenesis. Neuron 2019;103:878-90 e3.
157. Wilderman MJ, Armstead WM. Relationship between nitric oxide and opioids in hypoxia-induced pial artery vasodilation. The American journal of physiology 1996;270:H869-74.
158. Tayfun Uzbay I, Oglesby MW. Nitric oxide and substance dependence. Neuroscience and biobehavioral reviews 2001;25:43-52.
159. Homayoun H, Sayyah M, Dehpour AR. The additive effect of opioids and nitric oxide in increasing pentylenetetrazole-induced seizure threshold in cholestatic mice. Journal of gastroenterology and hepatology 2002;17:96-101.
160. Pol O. The involvement of the nitric oxide in the effects and expression of opioid receptors during peripheral inflammation. Current medicinal chemistry 2007;14:1945-55.
161. Saric A, Balog T, Sobocanec S, Marotti T. Endomorphin 1 activates nitric oxide synthase 2 activity and downregulates nitric oxide synthase 2 mRNA expression. Neuroscience 2007;144:1454-61.
162. Rodriguez-Munoz M, Garzon J. Nitric oxide and zinc-mediated protein assemblies involved in mu opioid receptor signaling. Molecular neurobiology 2013;48:769-82.
163. Rahmati B, Beik A. Prevention of morphine dependence and tolerance by Nepeta menthoides was accompanied by attenuation of Nitric oxide overproduction in male mice. J Ethnopharmacol 2017;199:39-51.
164. Someya E, Mori A, Sakamoto K, Ishii K, Nakahara T. Stimulation of mu-opioid receptors dilates retinal arterioles by neuronal nitric oxide synthase-derived nitric oxide in rats. European journal of pharmacology 2017;803:124-9.
165. Da Silva Santos R, Galdino G. Endogenous systems involved in exercise-induced analgesia. J Physiol Pharmacol 2018;69:3-13.
166. Mansouri MT, Naghizadeh B, Ghorbanzadeh B, Alboghobeish S, Houshmand G, Amirgholami N. Venlafaxine Attenuates the Development of Morphine Tolerance and Dependence: Role of L-Arginine/Nitric Oxide/cGMP Pathway. Endocr Metab Immune Disord Drug Targets 2018;18:362-70.
167. Mehanna MM, Domiati S, Nakkash Chmaisse H, El Mallah A. Antinociceptive effect of tadalafil in various pain models: Involvement of opioid receptors and nitric oxide cyclic GMP pathway. Toxicology and applied pharmacology 2018;352:170-5.

168. Martin-Moreno AM, Reigada D, Ramirez BG, et al. Cannabidiol and other cannabinoids reduce microglial activation in vitro and in vivo: relevance to Alzheimer's disease. Mol Pharmacol 2011;79:964-73.
169. Borrelli F, Fasolino I, Romano B, et al. Beneficial effect of the non-psychotropic plant cannabinoid cannabigerol on experimental inflammatory bowel disease. Biochemical pharmacology 2013;85:1306-16.
170. Bujalska-Zadrozny M, de Corde A, Pawlik K. Influence of nitric oxide synthase or cyclooxygenase inhibitors on cannabinoids activity in streptozotocin-induced neuropathy. Pharmacol Rep 2015;67:209-16.
171. Carletti F, Gambino G, Rizzo V, Ferraro G, Sardo P. Cannabinoid and nitric oxide signaling interplay in the modulation of hippocampal hyperexcitability: Study on electrophysiological and behavioral models of temporal lobe epilepsy in the rat. Neuroscience 2015;303:149-59.
172. Hassanpour S, Zendehdel M, Babapour V, Charkhkar S. Endocannabinoid and nitric oxide interaction mediates food intake in neonatal chicken. British poultry science 2015;56:443-51.
173. Kokona D, Thermos K. Synthetic and endogenous cannabinoids protect retinal neurons from AMPA excitotoxicity in vivo, via activation of CB1 receptors: Involvement of PI3K/Akt and MEK/ERK signaling pathways. Exp Eye Res 2015;136:45-58.
174. Lisboa SF, Gomes FV, Silva AL, et al. Increased Contextual Fear Conditioning in iNOS Knockout Mice: Additional Evidence for the Involvement of Nitric Oxide in Stress-Related Disorders and Contribution of the Endocannabinoid System. Int J Neuropsychopharmacol 2015;18.
175. Zou S, Kumar U. Colocalization of cannabinoid receptor 1 with somatostatin and neuronal nitric oxide synthase in rat brain hippocampus. Brain Res 2015;1622:114-26.
176. Zou S, Somvanshi RK, Paik S, Kumar U. Colocalization of cannabinoid receptor 1 with somatostatin and neuronal nitric oxide synthase in rat brain hypothalamus. J Mol Neurosci 2015;55:480-91.
177. Maroso M, Szabo GG, Kim HK, et al. Cannabinoid Control of Learning and Memory through HCN Channels. Neuron 2016;89:1059-73.
178. Al Suleimani YM, Al Mahruqi AS. The endogenous lipid N-arachidonoyl glycine is hypotensive and nitric oxide-cGMP-dependent vasorelaxant. European journal of pharmacology 2017;794:209-15.
179. Carletti F, Gambino G, Rizzo V, Ferraro G, Sardo P. Neuronal nitric oxide synthase is involved in CB/TRPV1 signalling: Focus on control of hippocampal hyperexcitability. Epilepsy research 2017;138:18-25.
180. Iyer MR, Cinar R, Katz A, et al. Design, Synthesis, and Biological Evaluation of Novel, Non-Brain-Penetrant, Hybrid Cannabinoid CB1R Inverse Agonist/Inducible Nitric Oxide Synthase (iNOS) Inhibitors for the Treatment of Liver Fibrosis. J Med Chem 2017;60:1126-41.
181. Lopez-Dyck E, Andrade-Urzua F, Elizalde A, et al. ACPA and JWH-133 modulate the vascular tone of superior mesenteric arteries through cannabinoid receptors, BKCa channels, and nitric oxide dependent mechanisms. Pharmacol Rep 2017;69:1131-9.
182. Aban CE, Accialini PL, Etcheverry T, Leguizamon GF, Martinez NA, Farina MG. Crosstalk Between Nitric Oxide and Endocannabinoid Signaling Pathways in Normal and Pathological Placentation. Front Physiol 2018;9:1699.
183. Schacht JP, Hutchison KE, Filbey FM. Associations between cannabinoid receptor-1 (CNR1) variation and hippocampus and amygdala volumes in heavy cannabis users. Neuropsychopharmacology 2012;37:2368-76.

184. James A, James C, Thwaites T. The brain effects of cannabis in healthy adolescents and in adolescents with schizophrenia: a systematic review. Psychiatry Res 2013;214:181-9.
185. Filbey FM, McQueeny T, Kadamangudi S, Bice C, Ketcherside A. Combined effects of marijuana and nicotine on memory performance and hippocampal volume. Behav Brain Res 2015;293:46-53.
186. Buchy L, Mathalon DH, Cannon TD, et al. Relation between cannabis use and subcortical volumes in people at clinical high risk of psychosis. Psychiatry Res Neuroimaging 2016;254:3-9.
187. Yucel M, Lorenzetti V, Suo C, et al. Hippocampal harms, protection and recovery following regular cannabis use. Transl Psychiatry 2016;6:e710.
188. Chye Y, Suo C, Yucel M, den Ouden L, Solowij N, Lorenzetti V. Cannabis-related hippocampal volumetric abnormalities specific to subregions in dependent users. Psychopharmacology (Berl) 2017;234:2149-57.
189. Koenders L, Lorenzetti V, de Haan L, et al. Longitudinal study of hippocampal volumes in heavy cannabis users. Journal of psychopharmacology (Oxford, England) 2017;31:1027-34.
190. Batalla A, Lorenzetti V, Chye Y, et al. The Influence of DAT1, COMT, and BDNF Genetic Polymorphisms on Total and Subregional Hippocampal Volumes in Early Onset Heavy Cannabis Users. Cannabis Cannabinoid Res 2018;3:1-10.
191. Beale C, Broyd SJ, Chye Y, et al. Prolonged Cannabidiol Treatment Effects on Hippocampal Subfield Volumes in Current Cannabis Users. Cannabis Cannabinoid Res 2018;3:94-107.
192. Chye Y, Lorenzetti V, Suo C, et al. Alteration to hippocampal volume and shape confined to cannabis dependence: a multi-site study. Addict Biol 2019;24:822-34.
193. Chi Y, Sauve AA. Nicotinamide riboside, a trace nutrient in foods, is a vitamin B3 with effects on energy metabolism and neuroprotection. Curr Opin Clin Nutr Metab Care 2013;16:657-61.
194. Gomez CA, Sutin J, Wu W, et al. Phasor analysis of NADH FLIM identifies pharmacological disruptions to mitochondrial metabolic processes in the rodent cerebral cortex. PLoS One 2018;13:e0194578.
195. Hollis F, van der Kooij MA, Zanoletti O, Lozano L, Canto C, Sandi C. Mitochondrial function in the brain links anxiety with social subordination. Proc Natl Acad Sci U S A 2015;112:15486-91.
196. Moon J, Kim HR, Shin MG. Rejuvenating Aged Hematopoietic Stem Cells Through Improvement of Mitochondrial Function. Ann Lab Med 2018;38:395-401.
197. Rennie G, Chen AC, Dhillon H, Vardy J, Damian DL. Nicotinamide and neurocognitive function. Nutr Neurosci 2015;18:193-200.
198. Wang HF, Li Q, Feng RL, Wen TQ. Transcription levels of sirtuin family in neural stem cells and brain tissues of adult mice. Cell Mol Biol (Noisy-le-grand) 2012;Suppl.58:OL1737-43.
199. Bayrakdar ET, Armagan G, Uyanikgil Y, Kanit L, Koylu E, Yalcin A. Ex vivo protective effects of nicotinamide and 3-aminobenzamide on rat synaptosomes treated with Abeta(1-42). Cell Biochem Funct 2014;32:557-64.
200. Braidy N, Berg J, Clement J, et al. Role of Nicotinamide Adenine Dinucleotide and Related Precursors as Therapeutic Targets for Age-Related Degenerative Diseases: Rationale, Biochemistry, Pharmacokinetics, and Outcomes. Antioxid Redox Signal 2018.
201. Braidy N, Grant R, Sachdev PS. Nicotinamide adenine dinucleotide and its related precursors for the treatment of Alzheimer's disease. Current opinion in psychiatry 2018;31:160-6.

202. Gong B, Pan Y, Vempati P, et al. Nicotinamide riboside restores cognition through an upregulation of proliferator-activated receptor-gamma coactivator 1alpha regulated beta-secretase 1 degradation and mitochondrial gene expression in Alzheimer's mouse models. Neurobiology of aging 2013;34:1581-8.
203. Hou Y, Lautrup S, Cordonnier S, et al. NAD(+) supplementation normalizes key Alzheimer's features and DNA damage responses in a new AD mouse model with introduced DNA repair deficiency. Proc Natl Acad Sci U S A 2018;115:E1876-E85.
204. Min SW, Sohn PD, Li Y, et al. SIRT1 Deacetylates Tau and Reduces Pathogenic Tau Spread in a Mouse Model of Tauopathy. J Neurosci 2018;38:3680-8.
205. Turunc Bayrakdar E, Uyanikgil Y, Kanit L, Koylu E, Yalcin A. Nicotinamide treatment reduces the levels of oxidative stress, apoptosis, and PARP-1 activity in Abeta(1-42)-induced rat model of Alzheimer's disease. Free Radic Res 2014;48:146-58.
206. Bartova A, Birmingham MK. Effect of delta9-tetrahydrocannabinol on mitochondrial NADH-oxidase activity. J Biol Chem 1976;251:5002-6.
207. Benard G, Massa F, Puente N, et al. Mitochondrial CB(1) receptors regulate neuronal energy metabolism. Nat Neurosci 2012;15:558-64.
208. Hebert-Chatelain E, Desprez T, Serrat R, et al. A cannabinoid link between mitochondria and memory. Nature 2016;539:555-9.
209. Hebert-Chatelain E, Reguero L, Puente N, et al. Cannabinoid control of brain bioenergetics: Exploring the subcellular localization of the CB1 receptor. Mol Metab 2014;3:495-504.
210. Koch M, Varela L, Kim JG, et al. Hypothalamic POMC neurons promote cannabinoid-induced feeding. Nature 2015;519:45-50.
211. Mahoney JM, Harris RA. Effect of 9 -tetrahydrocannabinol on mitochondrial processes. Biochemical pharmacology 1972;21:1217-26.
212. Wolff V, Schlagowski AI, Rouyer O, et al. Tetrahydrocannabinol induces brain mitochondrial respiratory chain dysfunction and increases oxidative stress: a potential mechanism involved in cannabis-related stroke. Biomed Res Int 2015;2015:323706.
213. Alberts B., Johnson A., Lewis J., Raff M., Roberts K., Walter P., eds. Molecular Biology of the Cell. Second ed. New York: Garland Science; 2008.
214. Morimoto S, Tanaka Y, Sasaki K, et al. Identification and characterization of cannabinoids that induce cell death through mitochondrial permeability transition in Cannabis leaf cells. J Biol Chem 2007;282:20739-51.
215. Shoyama Y, Sugawa C, Tanaka H, Morimoto S. Cannabinoids act as necrosis-inducing factors in Cannabis sativa. Plant Signal Behav 2008;3:1111-2.
216. Gant J. Scientists are baffled by spatter of babies born without hands or arms in France, as investigation fails to discover a cause. Daily Mail. London, U.K.: Daily Mail; 2019.
217. Agence France-Presse in Paris. France to investigate cause of upper limb defects in babies. The Guardian. London The Guardian; 2018.
218. Willsher K. Baby arm defects prompt nationwide investigation in France. Guardian. London: The Guardian; 2018.
219. Forrester MB, Merz RD. Risk of selected birth defects with prenatal illicit drug use, Hawaii, 1986-2002. Journal of toxicology and environmental health 2007;70:7-18.
220. Babies born with deformed hands spark investigation in Germany. CNN News, 2019. (Accessed 5th October 2019, 2019, at https://edition.cnn.com/2019/09/16/health/hand-deformities-babies-gelsenkirchen-germany-intl-scli-grm/index.html.)
221. Brents L. Correlates and consequences of Prenatal Cannabis Exposure (PCE): Identifying and Characterizing Vulnerable Maternal Populations and Determining Outcomes

in Exposed Offspring In: Preedy V.R., ed. Handbook of Cannabis and Related Pathologies: Biology, Pharmacology, Diagnosis and Treatment. London: Academic Press; 2017:160-70.

TABLES

Table 1.: Panel Regressions – National Level

Model Type	Dependent Variable	Lagged Instrumental Variables	Parameter	Parameter				Model Parameters				
				Estimate	Std. Error	t value	Pr(>|t|)	Adj. R-Squared	Chi.Squ.	dF	P	
National Autism Rate												
Interactive Models												
Panel Model												
4 Lags			*plm(LAutRt~cigmon*log(mrjmon)*anlyr+bngalc+log(cocyr)*									
plm	Log(Autism_Rate)	lag(mrjmon, 0:4)	cigmon:log(mrjmon)	396.2095	88.6624	4.4687	0.000008	0.95674	292.515	5	<2.2E-16	***
twoway FX		lag(cigmon, 0:4)	log(mrjmon)	-88.7064	20.2318	-4.3845	0.000012					***
instrumental method			log(cocyr)	9.7895	2.2743	4.3043	0.000017					***
=amemiya			cigmon	937.0985	218.3632	4.2915	0.000018					***
model=			bngalc	-75.5216	20.3622	-3.7089	0.000208					***
pooling												
6 Lags												
Panel Model			*plm(LAutRt~cigmon+DCan1825+DCan2634*anlyr+log(cocyr)*									
plm	Log(Autism_Rate)	lag(mrjmon, 0:6)	cigmon	-203.0643	29.1959	-6.9552	3.52E-12	0.99018	812.726	6	<2.2E-16	***
twoway FX		lag(cigmon, 0:6)	log(cocyr)	37.8761	5.6152	6.7453	1.53E-11					***
instrumental method		lag(Δ9THC, 0:6)	DCan2634:anlyr	60368.8224	9447.9465	6.3896	1.66E-10					***
=amemiya		lag(CBG, 0:6)	DCan2634	-3115.6405	495.7087	-6.2852	3.27E-10					***
			anlyr	-3195.2865	516.637	-6.1848	6.22E-10					***
			DCan1825	580.1553	94.5944	6.1331	8.62E-10					***

6 Lags												
Panel Model - Cannabis: Tobacco Interaction			***plm(LAutRt~cigmon*DCan1825+DCan2634+anlyr+log(cocyr)***									
plm	Log(Autism_Rate)	lag(mrjmon, 0:6)	cigmon	3508.1943	476.375	7.3644	1.78E-13	0.99292	1129.1	7	<2.2E-16	***
twoway FX		lag(cigmon, 0:6)	DCan1825	10926.8916	1449.149	7.5402	4.69E-14					***
instrumental method		lag(Δ9THC, 0:6)	anlyr	1762.2046	219.5965	8.0247	1.02E-15					***
=amemiya		lag(CBG, 0:6)	cigmon:DCan1825	-49883.3748	6610.4042	-7.5462	4.48E-14					***
			log(cocyr)	-56.8796	7.9647	-7.1414	9.24E-13					***
			bngalc	226.4019	34.9574	6.4765	9.39E-11					***
			DCan2634	40.508	19.4992	2.0774	0.03776					*
6 Lags, 6 Instruments												
Panel Model			***plm(LAutRt~cigmon+DCan1825+DCan2634*anlyr+log(cocyr)***									
plm	Log(Autism_Rate)	lag(mrjmon, 0:6)	log(cocyr)	29.6125	5.4668	5.4168	6.07E-08	0.98154	432.448	7	<2.2E-16	***
twoway FX		lag(cigmon, 0:6)	cigmon	-176.6468	34.0351	-5.1901	2.10E-07					***
instrumental method		lag(Δ9THC, 0:6)	anlyr	7009.5056	1451.7631	4.8283	0.000001					***
=amemiya		lag(CBG, 0:6)	log(DCan2634):anlyr	2335.2522	493.4054	4.7329	0.000002					***
		lag(log(DCan2634), 0:4)	log(DCan2634)	-119.5497	25.362	-4.7137	0.000002					***
		lag(DCan1825, 0:4)	DCan1825	456.4964	97.3048	4.6914	0.000003					***
			bngalc	-52.45	21.4357	-2.4469	0.014411					*

Table 2.: Spatial Lag Model Regressions – Regional Level

Model Type	Dependent Variable	Parameter	Parameter				Model				
			Estimate	Std. Error	t value	Pr(>|t|)	Parameter	Statistic	P-value		
Spatial Lag	Autism_Rate	*spml(asinh(AutRtReg)~Region,lag=TRUE*									
		Region_Mid-West	0.1852	0.0538	3.4415	0.00058	phi	1.00E-08		***	***
		Region_North-East	0.4350	0.0538	8.0838	6.28E-16	lambda	0.9174	<2.0E-16	***	***
		Region_West	0.1850	0.0538	3.4374	0.00059				***	

Table 3.: Spatial Regression by Substances – Regional Level

General			Parameter	Parameter				Model				
Model Type	Technique	Dependent Variable		Estimate	Std. Error	t value	Pr(>|t|)	Parameter	Statistic	P-value		
SARAR			*log(AutRt)~log(cigmon)*log(mrjmon)*(abodalc)+log(anlyr)+log(cocyr)*									
	spml	AutRt	log(manlyr)	-0.99172	0.14502	-6.8384	8.01E-12	phi	1.00E-08	NA	***	
			log(mmrjmon)	8.83296	1.68745	5.2345	1.65E-07	rho	0.6521	4.53E-08	***	***
			log(mmrjmon):mAbdAlc	-98.0816	21.14819	-4.6378	0.000004	lambda	0.7196	<2e-16	***	***
			log(mcigmon):log(mmrjmon)	3.23837	1.05199	3.0783	0.002082				**	
			log(mcigmon):log(mmrjmon):mAbdAlc	-34.70781	12.79269	-2.7131	0.006666				**	
			mAbdAlc	-144.77873	56.43446	-2.5654	0.010305				*	
SARAR			*log(AutRt)~log(cigmon)*log(mrjmon)*log(anlyr)+(abodalc)+log(cocyr)*									
	spml	AutRt	mcocyr	18.0038	5.4322	3.3143	0.0009188	phi	1.00E-08	0.4143	***	
			log(mcigmon):log(mmrjmon):log(manlyr)	-24.3723	9.353	-2.6058	0.0091654	rho	0.9687	<2e-16	**	***
			log(mcigmon):log(mmrjmon)	-74.2647	28.7746	-2.5809	0.0098541	lambda	-0.2806	0.5175	**	
			log(mmrjmon):log(manlyr)	-33.1224	13.4706	-2.4589	0.0139374				*	
			log(mmrjmon)	-100.6919	41.5017	-2.4262	0.0152575				*	
			log(mcigmon):log(manlyr)	-66.0977	27.4019	-2.4122	0.0158583				*	
			log(mcigmon)	-201.6794	84.4054	-2.3894	0.0168753				*	
			log(manlyr)	-91.4219	39.5662	-2.3106	0.0208546				*	
			mAbdAlc	9.9389	1.1361	8.7483	< 2.2e-16				***	

Table 4.: Autism Spatial Regressions – Regional

General				Parameter	Parameter				Model				
Model Type	Technique	Dependent Variable	Instrumental Variables	Parameter	Estimate	Std. Error	t value	Pr(>|t|)	Parameter	Statistic	P-value		
Interactive Models													
2 Lags													
SEM2SRRE				***log(AutRt)~log(cigmon)*log(mrjmon)*log(anlyr)+(abodalc)+log(cocyr)***									
+SAR	spreml	AutismRate	lag(log(THCRt), 0:2)	log(mmrjmon)	0.1229	0.0572	2.1468	0.03181	phi	0.7601	0.6259	*	
			lag(log(CBGRt), 0:2)						psi	0.9908	< 2.2e-16		***
			lag(log(AutismRt), 1:2)						rho	-0.8805	0.0003		***
4 Lags													
SEM2SRRE				***log(AutRt)~log(cigmon)*log(mrjmon)*log(anlyr)+(abodalc)+log(cocyr)***									
+SAR	spreml	AutismRate	lag(log(THCRt), 0:4)	mAbdAlc	6.3759	0.6118	10.4212	<2e-16	phi	4.82E-08	NA	***	
			lag(log(CBGRt), 0:4)	log(manlyr)	548.5112	66.0752	8.3013	<2e-16	rho	-0.5409	NA	***	
			lag(log(AutismRt), 1:4)	log(mcigmon)	1111.3397	134.0059	8.2932	<2e-16	lambda	-0.2832	NA	***	
				log(mcigmon):log(manlyr)	367.6514	44.3659	8.2868	<2e-16				***	
				log(mmrjmon)	541.0568	65.3968	8.2734	<2e-16				***	
				log(mmrjmon):log(manlyr)	178.5970	21.6523	8.2484	<2e-16				***	
				log(mcigmon):log(mmrjmon)	357.2873	43.5731	8.1997	2.41E-16				***	
				log(mcigmon):log(mmrjmon):log(manlyr)	118.1826	14.4326	8.1886	2.64E-16				***	
				mcocyr	-5.5914	1.4544	-3.8445	0.0001208				***	
6 Lags													
SEM2SRRE				***log(AutRt)~log(cigmon)*log(mrjmon)*log(anlyr)+(abodalc)+log(cocyr)***									
+SAR	spreml	AutismRate	lag(log(THCRt), 0:6)										
			lag(log(CBGRt), 0:6)	log(manlyr)	740.5144	24.4080	30.339	<2e-16	phi	1.3E-07	1	***	
			lag(log(AutismRt), 1:6)	log(mcigmon)	1491.3069	49.8193	29.934	<2e-16	psi	-0.993545	<2e-16	***	***
				log(mcigmon):log(manlyr)	494.3370	16.5167	29.930	<2e-16	rho	0.531139	<2e-16	***	***
				log(mmrjmon)	723.6168	24.3891	29.670	<2e-16				***	
				log(mmrjmon):log(manlyr)	239.4310	8.0846	29.616	<2e-16				***	
				log(mcigmon):log(mmrjmon)	475.7265	16.3914	29.023	<2e-16				***	
				log(mcigmon):log(mmrjmon):log(manlyr)	157.6794	5.4370	29.001	<2e-16				***	
				mAbdAlc	1.0628	0.0958	11.089	<2e-16				***	
				mcocyr	-9.6481	0.5249	-18.382	<2e-16				***	

Table 5.: OLS Regression – State Level

Parameter	Parameter				Model Parameters				
	Estimate	Std. Error	t value	Pr(>|t|)	R-Squared	F	dF	P	
log(AutRt) ~ PC1 + log(mrjmon)									
PC1	-0.2747	0.0235	-11.71	<2e-16	0.282	98.2	2,493	<2.0E-16	***
log(mrjmon)	1.0962	0.0902	12.16	<2e-16					***
log(AutRt) ~ cigmon + abodalc + log(anlyr) + log(cocyr) + log(mrjmon)									
cigmon	-4.1922	0.6266	-6.691	6.1E-11	0.3206	47.73	5,490	<2.0E-16	***
abodalc	-11.5664	1.8587	-6.223	1.1E-09					***
log(cocyr)	-0.5292	0.0824	-6.419	3.2E-10					***
log(mrjmon)	0.9279	0.0931	9.965	<2.0E-16					***

Parameter	Parameter					Model Parameters			
	Value	Std.Error	DF	t-value	p-value	AIC	BIC	logLik	
log(AutRt)~PC1 + log(mrjmon), random=~1|State									
PC1	-0.3017	0.0191	444	-15.7954	0.0000	354.7809	375.7834	-172.3904	***
log(mrjmon)	1.1795	0.1127	444	10.4696	0.0000				***
log(AutRt) ~ cigmon + abodalc + log(anlyr) + log(cocyr) + log(mrjmon), random =~1|State									
cigmon	-7.4827	0.8656	441	-8.6449	0.0000	222.6718	256.2271	-103.3359	***
abodalc	-9.6339	2.0254	441	-4.7565	0.0000				***
log(anlyr)	0.6297	0.1339	441	4.7024	0.0000				***
log(cocyr)	-0.6596	0.0704	441	-9.3668	0.0000				***
log(mrjmon)	0.8011	0.1068	441	7.5005	0.0000				***

Table 6.: Results of LaGrange Multiplier Tests from GeoDa

Test	MI/DF	Value	P-Value
Moran's I	0.23	28.735	0.0000
Lagrange Multiplier - Lag	1	178.841	0.0000
Robust LM Lag	1	10.942	0.0009
Lagrange Multiplier - Error	1	556.614	0.0000
Robust Error	1	388.715	0.0000
Lagrange Multiplier - SARMA	2	567.556	0.0000

Table 7.: OLS Regressions with Principal Components

Parameter	Parameter				Model Parameters				
	Estimate	Std. Error	t value	Pr(>|t|)	R-Squared	F	dF	P	
Linear Model									
lm(log(AutRt)~PC1 = log(mrjmon))									
PC1	-0.27589	0.02341	-11.79	<2e-16	0.2808	98.39	2,497	<2.0E-16	***
log(mrjmon)	1.08406	0.0893	12.14	<2e-16					***
Lag									
spgm(log(AutRt) ~ PC1 + log(mrjmon))									
PC1	-0.132794	0.021784	-6.096	1.09E-09					***
log(mrjmon)	0.49867	0.113345	4.3996	1.09E-05					***
Spatial Error									
spgm(log(AutRt) ~ PC1 * log(mrjmon))									
lambda	0.9906	0.0473	20.9563	<2e-16					
PC1	-0.2591	0.1238	-2.0932	0.0363					*
PC1:log(mrjmon)	-0.0891	0.0444	-2.0069	0.0448					
Residual variance (sigma squared): 0.92801, (sigma: 0.96333)									
SARMA									
spgm(log(AutRt) ~ PC1 + log(mrjmon) - PC1)									
lambda	1.025464	0.018093	56.6773	<2.0E-16					***
log(mrjmon)	-0.123075	0.063698	-1.9322	0.05334					.

Table 8.: Spatial Regressions with Principal Components

Parameter	Parameter			
	Estimate	Std. Error	t value	Pr(>|t|)
Interactive Models				
OLS				
lm(log(AutRt)~cigmon*log(mrjmon)*(abodalc)+log(anlyr)+log(cocyr)				
log(cocyr)	-0.4961	0.0796	-6.233	9.80E-10
cigmon:log(mrjmon)	12.7247	2.2613	5.627	3.1E-08
cigmon	35.0032	6.5149	5.373	1.2E-07
cigmon:abodalc	-370.6772	79.3021	-4.674	3.8E-06
cigmon:log(mrjmon):abodalc	-115.4399	27.6657	-4.173	0.00004
SPGM				
OLS w 2 Endogenous Variables				
spgm(log(AutRt)~cigmon*log(mrjmon)*(abodalc)+log(anlyr)+log(cocyr)				
log(d9THCRt)	1.9736	0.0904	21.829	<2.0E-16
cigmon:abodalc	-146.3070	32.7233	-4.471	7.8E-06
cigmon:log(mrjmon):abodalc	-46.4296	11.6404	-3.989	0.00007
log(mrjmon)	-0.8371	0.2761	-3.032	0.00243
SARAR				
spgm(log(AutRt)~cigmon*log(mrjmon)*(abodalc)+log(anlyr)+log(cocyr)				
lambda	0.8472	0.0327	25.919	<2.0E-16
cigmon:abodalc	-93.6156	28.1087	-3.331	0.00087
log(mrjmon)	0.6538	0.2142	3.052	0.00228
cigmon:log(mrjmon):abodalc	-26.1061	9.7082	-2.689	0.00717

SARAR w 5 Endogenous & Instrumental Variables				
spgm(log(AutRt)~cigmon*log(mrjmon)*(abodalc)+log(anlyr)+log(cocyr)				
lambda	0.7430	0.0898	8.278	<2.0E-16
cigmon:abodalc	-91.0827	27.0962	-3.362	0.00078
cigmon:log(mrjmon):abodalc	-29.0080	9.2524	-3.135	0.00172
log(d9THCRt)	0.4999	0.1649	3.031	0.00244
log(cocyr)	0.1316	0.0497	2.647	0.00813
Error				
spgm(log(AutRt)~cigmon*log(mrjmon)*(abodalc)+log(anlyr)+log(cocyr)				
log(cocyr)	-0.4200	0.0736	-5.704	1.2E-08
cigmon:log(mrjmon):abodalc	-144.1570	30.0759	-4.793	1.6E-06
cigmon:abodalc	-365.9616	86.4525	-4.233	2.3E-05
log(mrjmon):abodalc	24.0915	6.5993	3.651	0.00026
cigmon:log(mrjmon)	6.0794	1.7614	3.451	0.00056
abodalc	50.5362	19.0216	2.657	0.00789
cigmon	11.2367	5.6727	1.981	0.04761
Error w 5 Endogenous & Instrumental Variables				
spgm(log(AutRt)~cigmon*log(mrjmon)*(abodalc)+log(anlyr)+log(cocyr)				
log(d9THCRt)	1.9391	0.1453	13.350	<2.0E-16
log(mrjmon)	-1.6102	0.3204	-5.025	5.0E-07
cigmon:abodalc	-140.2022	31.0562	-4.515	6.3E-06
cigmon:log(mrjmon):abodalc	-45.7265	11.0677	-4.132	0.00004
log(CBGRt)	-0.3005	0.1245	-2.413	0.01582
log(cocyr)	0.1513	0.0635	2.382	0.01722
log(CBCRt)	0.7170	0.3408	2.104	0.03540

General			Parameters					Model				
Model Type	Technique	Dependent Variable	Parameter	Estimate	Std. Error	t value	P-Value	Parameters	Value	P-Value		
SARAR			*log(AutRt)~log(cigmon)*log(mrjmon)*(abodalc)+log(anlyr)+log(cocyr)*									
	spml	AutRt	cigmon	-4.2894	0.7639	-5.6151	0.00000				***	
			abodalc	-9.4348	1.8064	-5.2230	0.00000				***	
			log(mrjmon)	0.4761	0.1029	4.6259	0.00000				***	
			log(cocyr)	-0.3593	0.0719	-4.9960	0.00000				***	
			log(anlyr)	0.3520	0.1225	2.8746	0.00405				**	
Error			*log(AutRt)~log(cigmon)*log(mrjmon)*(abodalc)+log(anlyr)+log(cocyr)*									
	spml	AutRt	cigmon:log(mrjmon)	1.9416	0.5127	3.7873	0.00015	phi	4.038143	4.20E-06	**	
			cigmon:abodalc	-73.2933	20.1974	-3.6289	0.00028	rho	-0.536384	1.03E-13	*	
			log(anlyr)	0.2258	0.0727	3.1034	0.00191	lambda	0.79238	<2.0E-16	***	
			cigmon:log(mrjmon):abodalc	-39.0231	13.3130	-2.9312	0.00338				***	
			log(mrjmon):abodalc	4.8343	1.8066	2.6759	0.00745				**	
			log(cocyr)	-0.0962	0.0387	-2.4877	0.01286				**	
SARAR			*log(AutRt)~log(cigmon)*log(mrjmon)*(abodalc)+log(anlyr)+log(cocyr)*									
	spgm	AutRt	cigmon:abodalc	-93.6156	28.1087	-3.3305	0.00087	lambda	0.84719	<2e-16	***	***
			log(mrjmon)	0.6538	0.2142	3.0518	0.00228				**	
			cigmon:log(mrjmon):abodalc	-26.1061	9.7082	-2.6891	0.00717				**	
Error			*log(AutRt)~log(cigmon)*log(mrjmon)*(abodalc)+log(anlyr)+log(cocyr)*									
	spgm	AutRt	cigmon	-4.2894	0.7639	-5.6151	1.97E-08				***	
			log(mrjmon)	0.4761	0.1029	4.6259	3.73E-06				***	
			abodalc	-9.4348	1.8064	-5.2230	1.76E-07				***	
			log(anlyr)	0.3520	0.1225	2.8746	0.004046				**	
			log(cocyr)	-0.3593	0.0719	-4.9960	5.86E-07				***	

Table 9.: Additive Spatial Models

Parameter	Parameter						
	Estimate	Std. Error	t value	Pr(>|t|)			
Additive Models							
Spatial Lag							
spml(log(AutRt)~cigmon+abodalc+log(anlyr)+log(cocyr)+log(mrjmon)							
phi	4.2374	0.9401	4.5075	6.56E-06	***	Error variance parameters:	
lambda	0.6987	0.0278	25.1600	<2.0E-16	***	Spatial	autoregressi coefficient:
cigmon	-3.7064	0.5828	-6.3602	2.02E-10	***		
abodalc	-7.6577	1.3126	-5.8342	5.40E-09	***		
log(anlyr)	0.2630	0.0925	2.8435	0.004462	**		
log(mrjmon)	0.2169	0.0774	2.8026	0.00507	**		
Spatial Error							
spml(log(AutRt)~cigmon+abodalc+log(anlyr)+log(cocyr)+log(mrjmon)-log(cocyr),							
phi	4.0965	0.9742	4.2050	2.61E-05	***	Error variance parameters:	
rho	0.8462	0.0207	40.9570	<2.0E-16	***		
cigmon	-1.7980	0.6342	-2.8351	0.004582	**		
abodalc	-6.8487	1.4117	-4.8515	1.23E-06	***		
log(anlyr)	0.2499	0.0974	2.5655	0.010303	*		
log(cocyr)	0.1428	0.0627	2.2783	0.022708	*		
SARMA							
spml(log(AutRt)~cigmon+abodalc+log(anlyr)+log(cocyr)+log(mrjmon)-log(cocyr),							
phi	6.6371	1.7649	3.7606	0.0001695	***	Error variance parameters:	
rho	0.9452	0.0108	87.9187	<2.0E-16	***		
lambda	-0.6966	0.0822	-8.4712	<2.0E-16	***	Spatial	autoregressi coefficient:
cigmon	-1.0617	0.5316	-1.9974	0.04578	*		
abodalc	-5.0443	1.1708	-4.3083	0.00002	***		
log(anlyr)	0.2422	0.0769	3.1493	0.00164	**		

Table 10.: Interactive Spatial Models

Parameter	Parameter				
	Estimate	Std. Error	t value	Pr(>|t|)	
Interactive Models					
spml					
Lag					
*spml(log(AutRt)~abodalc+cigmon*log(mrjmon)*log(anlyr)+log(cocyr)*					
phi	4.5077	1.0027	4.4956	6.94E-06	***
lambda	0.6751	0.0313	21.5660	<2.0E-16	***
abodalc	-7.2830	1.4166	-5.1412	0.00000	***
cigmon	-21.5657	4.3985	-4.9030	0.00000	***
log(mrjmon)	1.8615	0.3992	4.6626	3.1E-06	***
log(cocyr)	-0.1026	0.0500	-2.0548	0.03990	*
cigmon:log(mrjmon)	-7.7418	1.6288	-4.7529	2.0E-06	***
cigmon:log(mrjmon):log(anlyr)	-0.4038	0.1168	-3.4555	0.00055	***
Error					
*spml(log(AutRt)~abodalc+cigmon*log(mrjmon)*log(anlyr)+log(cocyr)*					
phi	4.43158	1.06293	4.1692	3.06E-05	***
rho	0.85295	0.02092	40.772	<2.0E-16	***
abodalc	-6.574674	1.394089	-4.7161	2.40E-06	***
cigmon	-39.632582	10.001601	-3.9626	0.00007	***
cigmon:log(mrjmon)	-14.348168	3.539817	-4.0534	0.00005	***
log(mrjmon)	1.404577	0.387294	3.6266	0.00029	***
cigmon:log(mrjmon):log(anlyr)	-2.914581	1.110374	-2.6249	0.00867	**
cigmon:log(anlyr)	-7.441016	3.14591	-2.3653	0.01802	*
log(cocyr)	0.138061	0.063571	2.1718	0.02987	*
SARMA					
*spml(log(AutRt)~abodalc+cigmon*log(mrjmon)*log(anlyr)+log(cocyr)*					
phi	6.0893	1.3921	4.3741	1.22E-05	***
rho	-0.6729	0.0950	-7.0842	1.40E-12	***
lambda	0.8385	0.0234	35.7930	<2.0E-16	***
abodalc	-4.2045	1.0160	-4.1385	0.00003	***
cigmon	-148.5336	61.9994	-2.3957	0.01659	*
log(mrjmon)	12.6082	5.2911	2.3829	0.01718	*
cigmon:log(mrjmon)	-50.7085	21.3014	-2.3805	0.01729	*
cigmon:log(mrjmon):log(anlyr)	-15.1881	6.9284	-2.1922	0.02837	*
log(anlyr)	10.9676	5.0100	2.1891	0.02859	*
log(mrjmon):log(anlyr)	3.7457	1.7180	2.1802	0.02924	*
cigmon:log(anlyr)	-43.8304	20.2234	-2.1673	0.03021	*

Parameter	Parameter					
	Estimate	Std. Error	t value	Pr(>|t|)		
Interactive Models						
spgm						
Lag						
spgm(log(AutRt)~abodalc+cigmon*log(mrjmon)*log(anlyr)+log(cocyr)						
lambda	0.986899	0.051324	19.2287	<2.0E-16		Spatial
abodalc	-5.786124	1.429294	-4.0482	0.00005	***	
cigmon	-15.796453	4.445966	-3.553	0.00038	***	
cigmon:log(mrjmon)	-5.177465	1.56734	-3.3033	0.00096	***	
log(mrjmon)	1.267041	0.40852	3.1015	0.00193	**	
log(cocyr)	0.167628	0.061647	2.7191	0.00655	**	
Error						
spgm(log(AutRt)~abodalc+cigmon*log(mrjmon)*log(anlyr)+log(cocyr)-log(mrjmon):log(anlyr)-log(anlyr)-cigmon:log(anlyr)						
abodalc	-10.4312	1.8336	-5.6890	1.28E-08	***	
log(cocyr)	-0.2844	0.0744	-3.8216	0.00013	***	
log(mrjmon)	1.9138	0.5075	3.7708	0.00016	***	
cigmon	-20.0926	5.5540	-3.6176	0.00030	***	
cigmon:log(mrjmon)	-7.1503	2.0362	-3.5115	0.00045	***	
cigmon:log(mrjmon):log(anlyr)	-0.5028	0.1604	-3.1357	0.00171	**	
SARMA						
spgm(log(AutRt)~abodalc+cigmon*log(mrjmon)*log(anlyr)+log(cocyr)						
lambda	0.95158	0.025191	37.7742	<2.0E-16	***	Spatial
cigmon	-141.856277	59.353829	-2.39	0.01685	*	
cigmon:log(mrjmon)	-48.041995	20.385678	-2.3567	0.01844	*	
log(mrjmon)	11.739886	5.060145	2.3201	0.02034	*	
cigmon:log(anlyr)	-43.257354	19.357301	-2.2347	0.02544	*	
log(anlyr)	10.699003	4.789731	2.2337	0.0255	*	
cigmon:log(mrjmon):log(anlyr)	-14.692519	6.63103	-2.2157	0.02671	*	
log(mrjmon):log(anlyr)	3.598374	1.642603	2.1907	0.02848	*	
abodalc	-2.07897	0.992094	-2.0955	0.03612	*	

Table 11.: Significance of the Changes

GMErrorsar

Parameter	Parameter				Model	
	Estimate	Std. Error	t value	Pr(>|t|)	Parameter	Statistic
dmrjmonA:dabodalcA	41530.067	11723	3.5426	0.00040	Lambda	-0.2689
dcigmonA:dmrjmonA:dabodalcA	-479233.385	167935.974	-2.8537	0.00432	z	-0.4716
					ML Varian	605.92
					GM Argmi	593.64

Errorsarlm

Parameter	Parameter				Model		
	Estimate	Std. Error	t value	Pr(>|t|)	Parameter	Statistic	P-value
dmrjmonA:dabodalcA	167572.3	47485.8	3.5289	0.00042	Lambda	-0.5854	0.03497
dcigmonA:dmrjmonA:dabodalcA	-1748861.1	649300.2	-2.6935	0.00707	z	-2.4052	0.01616
dmrjmonA	-3868.1	1562.7	-2.4752	0.01332	Wald	5.785	0.01616
dabodalcA	-1748.9	856.8	-2.0411	0.04124	LogLik	-228.32	
					ML Varian	501.09	
					AIC	474.64	

Table 12: OLS Regression of the Changes 1994-2011

Model Type	Dependent Variable	Parameter	Parameter				Model Parameters				
			Estimate	Std. Error	t value	Pr(>|t|)	Adjusted R-Squared	F	dF	P	
Linear		*lm(log(AutRt)~Year)*									
Exponential	AutRt	Year	1.81E-01	3.00E-03	60.18	<2e-16	0.7799	3622	1,1021	<2e-16	***
Linear		*lm(log(AutRt)~Status*									
Exponential	AutRt	Status_Decriminalised	0.44145	0.10024	4.404	1.17E-05	0.4612	25.71	2,1020	1.28E-11	***
		Status_Medical	0.75843	0.12127	6.254	5.87E-10					***
Linear		*lm(log(AutRt)~Year+Status*									
Exponential	AutRt	Status_Decriminalised	2.85E-01	4.74E-02	6.001	2.72E-09	0.7871	1,261.00	3,1019	<2e-16	***
		Status_Medical	3.56E-03	5.87E-02	0.061	0.952					
Linear		*lm(log(AutRt)~Year*Status*									
Exponential	AutRt	Year	1.80E-01	3.03E-03	59.575	<2e-16	0.7871	1,261.00	3,1019	<2e-16	***
		Year:Status_Decriminalised	1.42E-04	2.37E-05	6.002	2.70E-09					***
Quadratic		*lm(log(AutRt)~poly(Year,degree=2)*Status)*									
Exponential	AutRt	Year	36.61922	0.55254	66.274	<2e-16	0.8215	1177	4,1018	<2e-16	***
		$Year^2$	-7.65663	0.54535	-14.04	<2e-16					***
		Status_Decriminalised	0.29654	0.04344	6.827	1.49E-11					***

Table 13.: LM Tests

Test	MI/DF	Value	P-Value
Moran's I	0.0574	11.6224	0.00000
Lagrange Multiplier - Lag	1	101.8425	0.00000
Robust LM Lag	1	2.0397	0.15324
Lagrange Multiplier - Error	1	116.276	0.00000
Robust Error	1	16.4733	0.00005
Lagrange Multiplier - SARMA	2	118.3158	0.00000

Table 14.: Spatially Lagged spreml Models of Cannabis Legal Status

General				Parameter	Parameter				Model				
Model Type	Technique	Dependent Variable	Lagged Variable		Estimate	Std. Error	t value	Pr(>|t|)	Parameter	Statistic	P-value		
Interactive Models													
2 Lags													
SEM2SRRE				*log(AutRt)~Status*									
+SAR	spreml	AutismRate	lag(log(AutRt), 1:2)	Legal_Status	7.38004	2.16613	3.407	0.000657	phi	0.000002	NA	***	
									psi	0.962170	< 2.2e-16		***
									rho	-0.877650	< 2.2e-16		***
									lambda	0.861574	< 2.2e-16		
4 Lags													
SEM2SRRE				*log(AutRt)~Status*									
+SAR	spreml	AutismRate	lag(log(AutRt), 1:4)	Legal_Status	7.58305	2.2676	3.3441	0.000826	phi	1.95E-07	1		
									psi	0.958700	< 2.2e-16	***	***
									rho	-0.883240	< 2.2e-16		***
									lambda	0.860488	< 2.2e-16		
6 Lags													
SEM2SRRE				*log(AutRt)~Status*									
+SAR	spreml	AutismRate	lag(log(AutRt), 1:6)	Legal_Status	7.72938	2.37342	3.2566	0.001127	phi	0.000001	NA		
									psi	0.957790	< 2.2e-16	**	***
									rho	-0.873810	< 2.2e-16		***
									lambda	0.855205	< 2.2e-16		***
8 Lags													
SEM2SRRE				*log(AutRt)~Status*									
+SAR	spreml	AutismRate	lag(log(AutRt), 1:8)	Legal_Status	7.8614	2.4359	3.2272	0.001250	phi	0.000006	NA	**	
									psi	0.957120	< 2.2e-16		***
									rho	-0.871390	< 2.2e-16		***
									lambda	0.857060	< 2.2e-16		***

Table 15.: Spatial Models 1994-2011

General			Parameters					Model				
Model Type	Technique	Dependent Variable	Parameter	Estimate	Std. Error	t value	P-Value	Parameters	Value	P-Value		
SARAR												
		spml(AutRt~Status, lag=TRUE,spatial.error="kkp")										
	spml	Autism_Rate	StatusDecriminalised	20.4010	3.1544	6.4676	9.96E-11	phi	1.6017	7.36E-06	***	***
			StatusMedical	10.8493	1.5170	7.1519	8.56E-13	rho	-0.9520	<2e-16	***	***
								lambda	0.9396	<2e-16		***
		spgm(AutRt~Status, lag=TRUE, spatial.error=TRUE)										
	spgm	Autism_Rate	StatusDecriminalised	18.2614	3.4334	5.3187	1.05E-07	lambda	0.9726	<2e-16	***	***
			StatusMedical	6.6898	2.0011	3.3431	0.00083				***	
Error												
		spml(AutRtStatus, lag=FALSE,spatial.error="kkp")										
	spml	Autism_Rate	StatusDecriminalised	21.0633	4.5339	4.6457	3.39E-06	phi	1.2519	3.42E-06	***	***
			StatusMedical	6.7664	2.2501	3.0072	0.00264	rho	0.8201	<2e-16	***	***
		spgm(AutRt~Status, lag=FALSE,spatial.error=TRUE)										
	spgm	Autism_Rate	StatusDecriminalised	21.5860	4.7288	4.5648	5.00E-06				***	
			StatusMedical	7.5654	2.3604	3.2051	0.00135				**	

Figure Legends

Figure 1: National Autism Rate USA 1994-2011

Figure 2.: Cumulative National Autism numbers USA, 1994-2011

Figure 3.: US National Level Drug Use 2000-2017

Figure 4.: Relative Autism Rate by Region 1992-2011

Figure 5.: Absolute Autism Rate by Region

Figure 6.: Regional Autism Rate, 1994-2011

Figure 7.: US Relative Autism Rate by State 1992-2011

Figure 8.: US Absolute Autism Rate by State 1992-2011

Figure 9.: Bivariate Plots of Cannabis and Autism Emergence 2000 – 2011

Figure 10.: Bivariate Autism and Cigarette Emergence Maps 2000 – 2011

Figure 11.: K clustering of Autism Rate – from GeoDa

Figure 12.: Hinge and Natural Breaks Maps – from GeoDa

Figure 13.: Dorlings Cartogram Autism USA

Figure 14.: Dorlings Cartograms – Autism, Cannabis, THC and Cannabidiol Exposures

Figure 29.: Autism Rate by Cannabis Legal Status for IDEA and ADDM Datasets.

Figure 30.: Change in Autism Rate 1995-2011 by Cannabis Legal Status.

F1

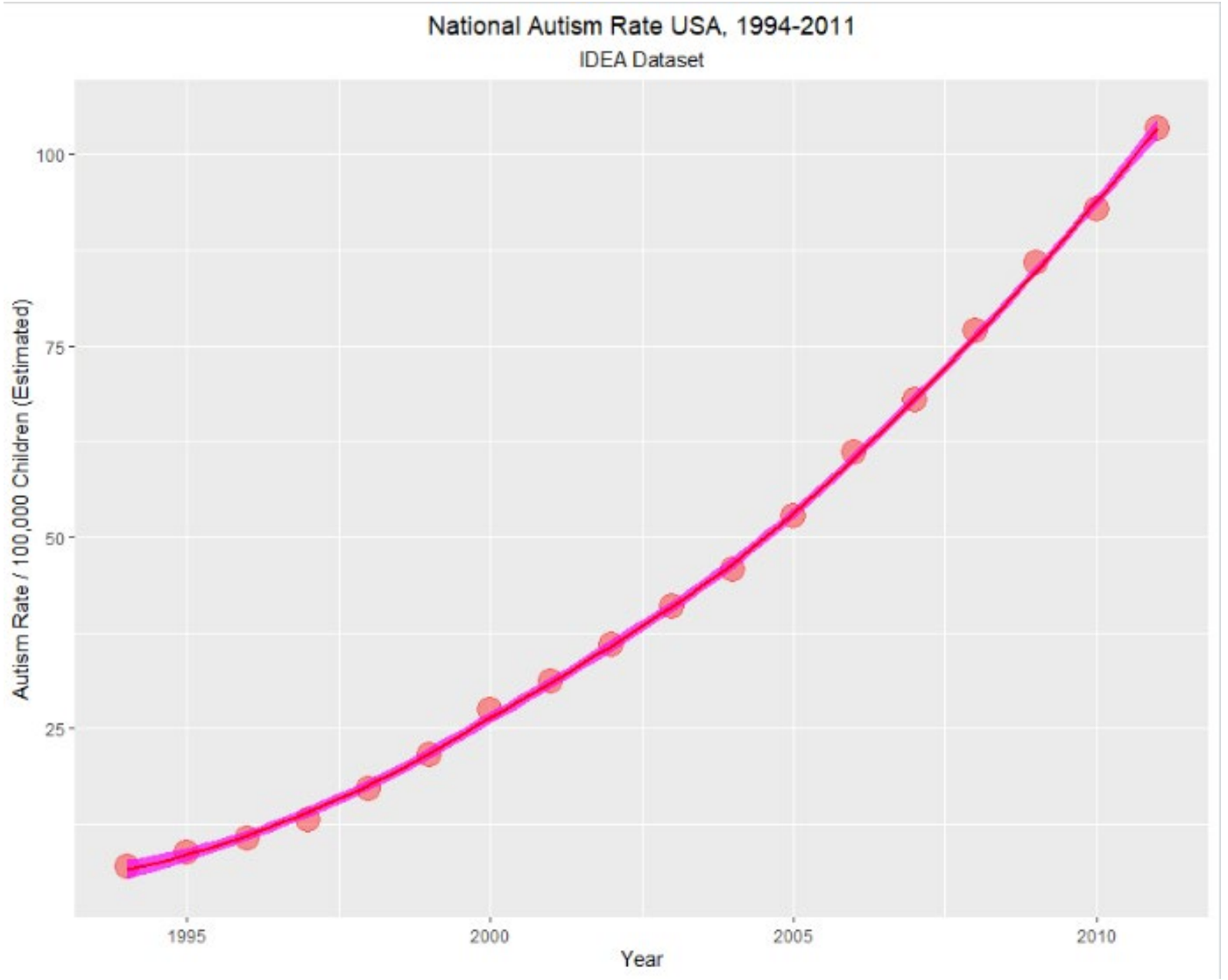
National Autism Rate USA, 1994-2011
IDEA Dataset
Autism Rate / 100,000 Children (Estimated)
100
75
50
25
1995
2000
2005
2010
Year

F2

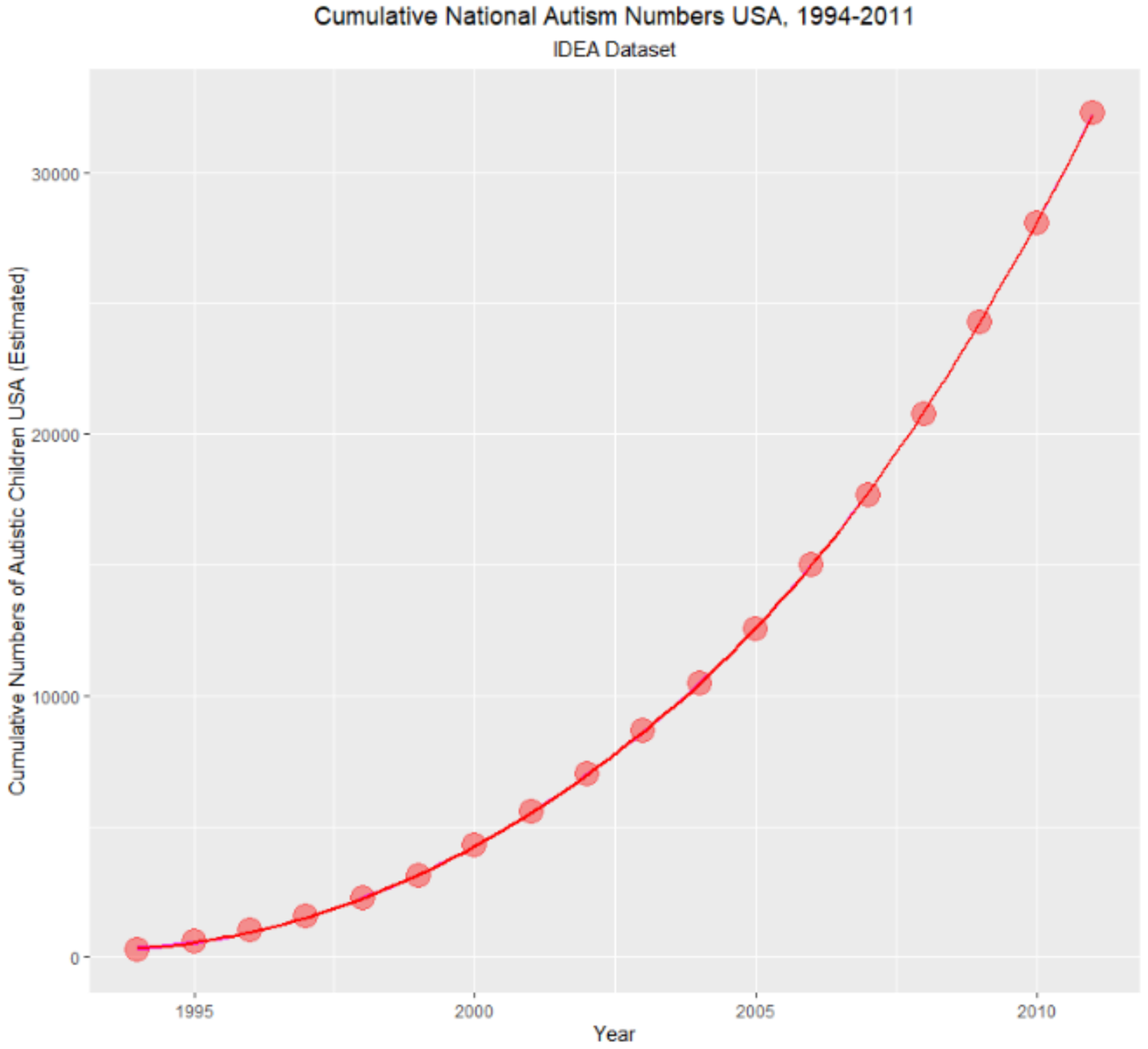
Cumulative National Autism Numbers USA, 1994-2011
IDEA Dataset
Cumulative Numbers of Autistic Children USA (Estimated)
30000
20000
10000
0
1995
2000
2005
2010
Year

F3 US National Level Drug Use

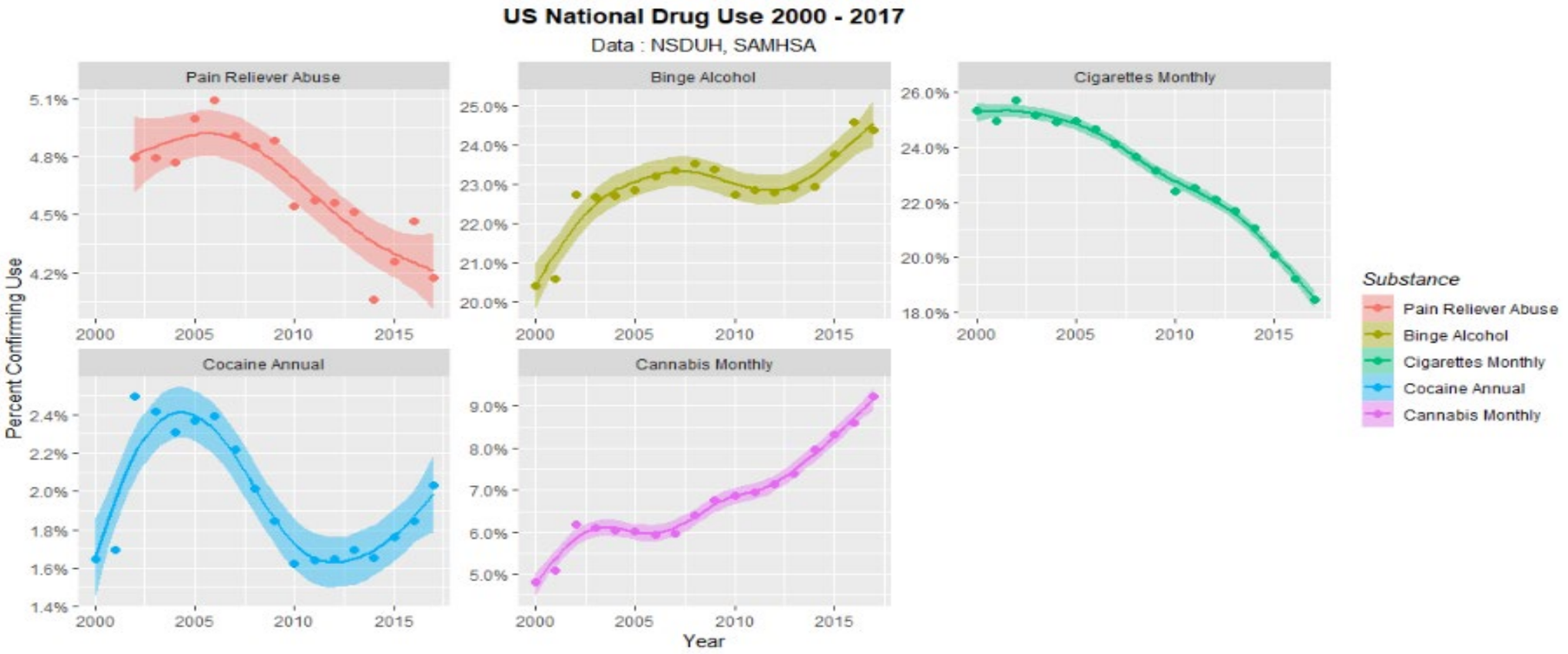

F4 - Autism Rate by Region - Relative

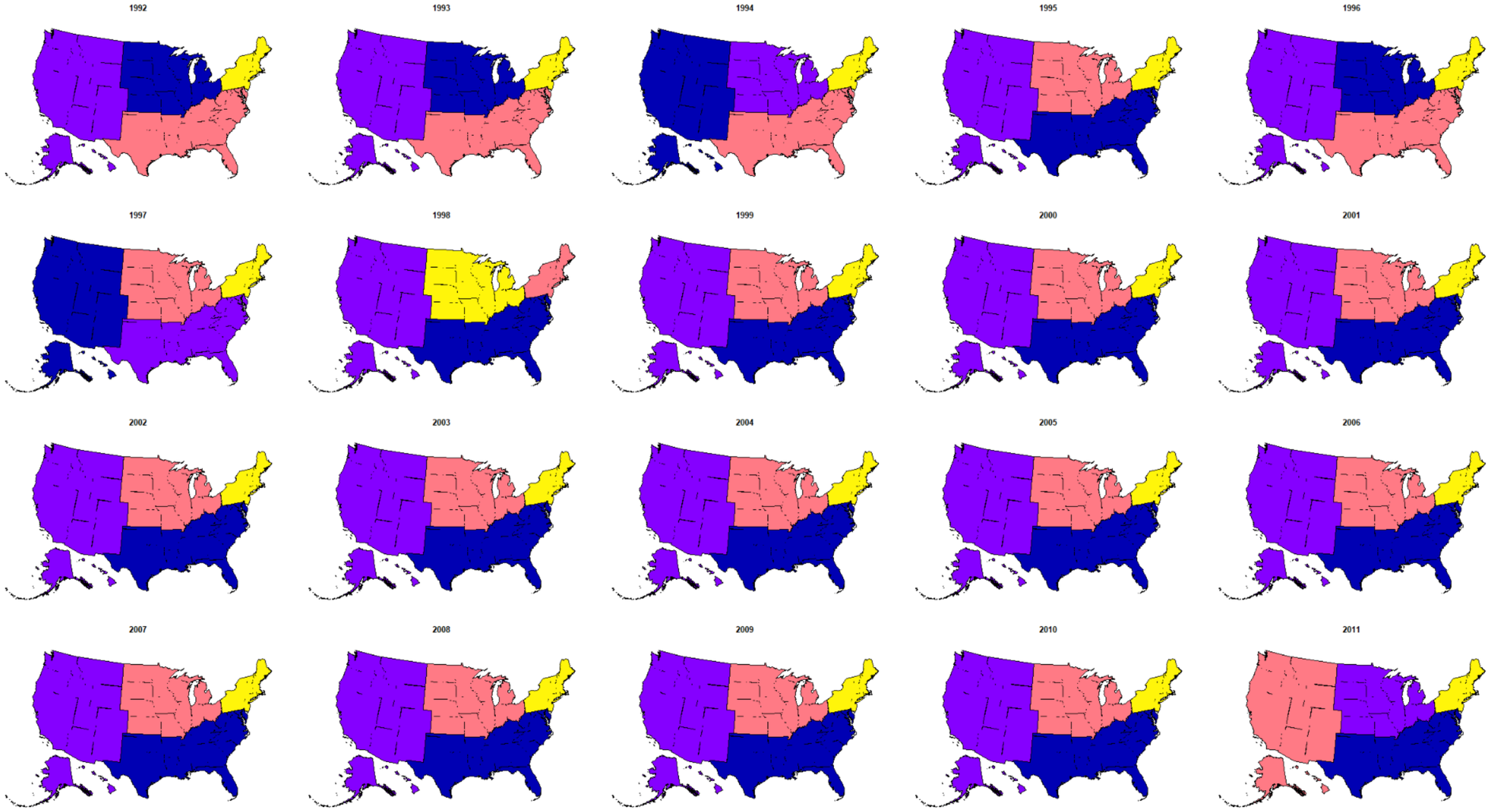

F5 - Autism by Region - Absolute

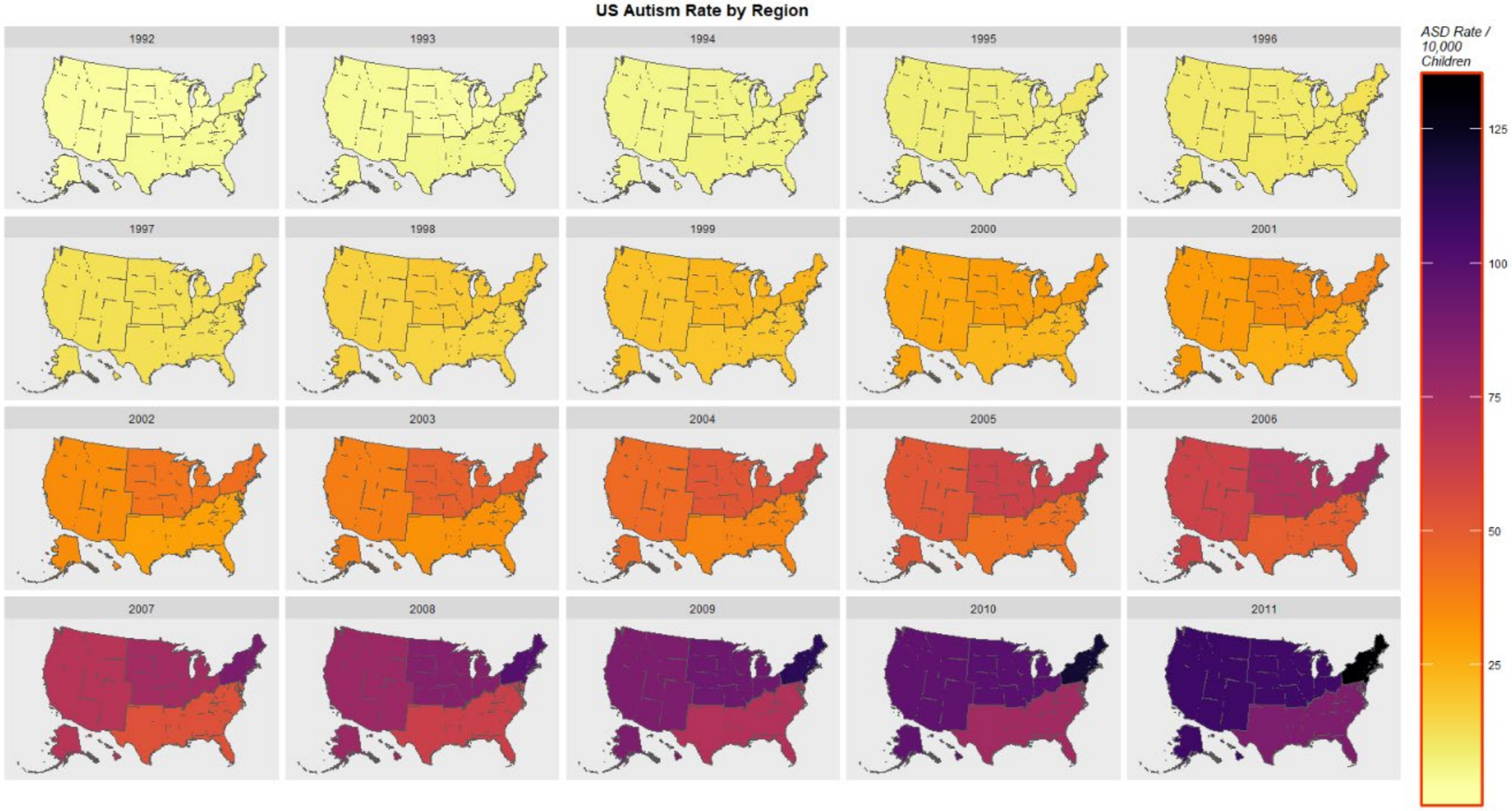

F6

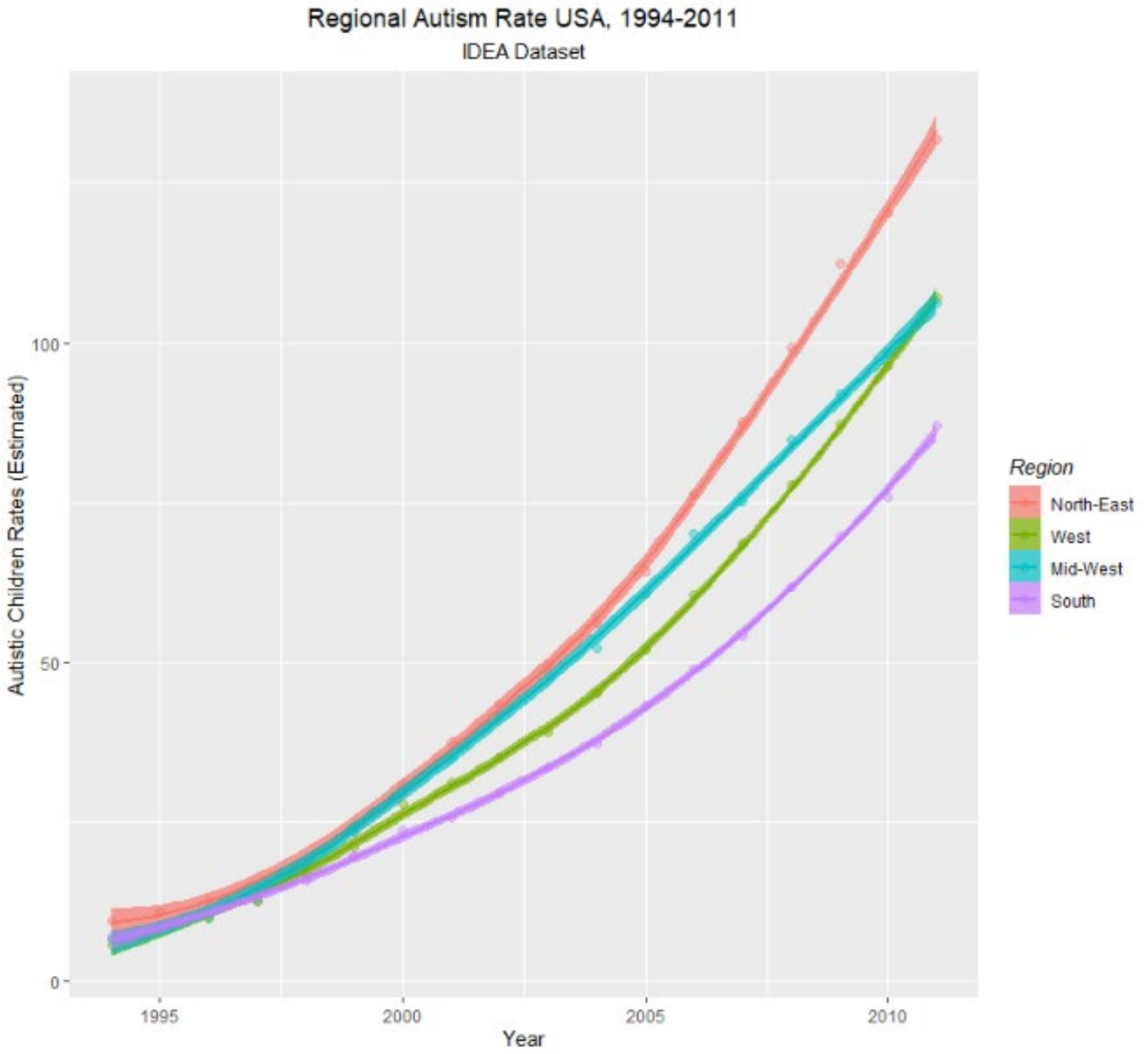
Regional Autism Rate USA, 1994-2011
IDEA Dataset
Autistic Children Rates (Estimated)
100
50
0
1995
2000
2005
2010
Year
Region
North-East
West
Mid-West
South

F7 - Autism Rate ~ 20 Years

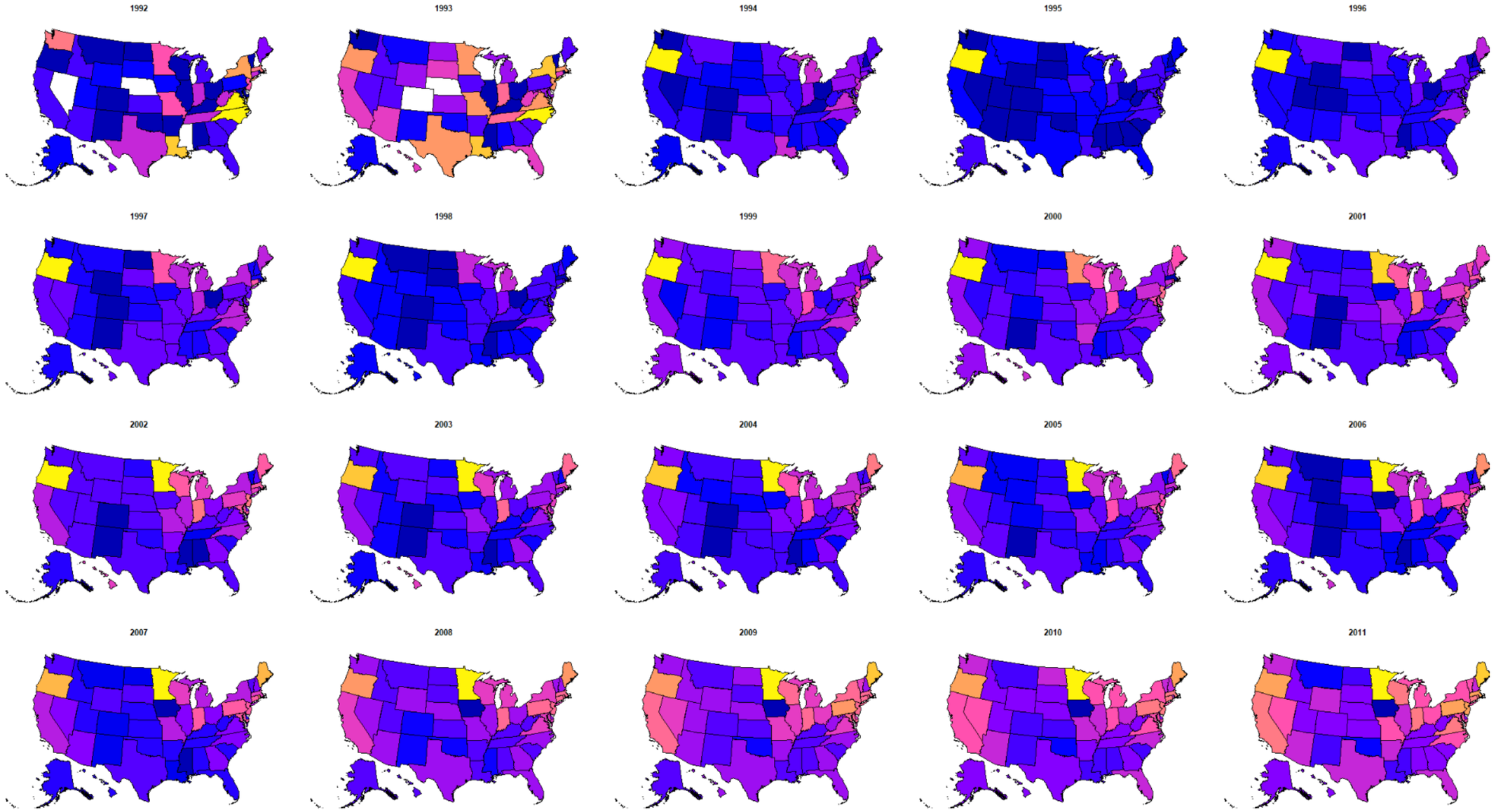

F8 - Autism by State

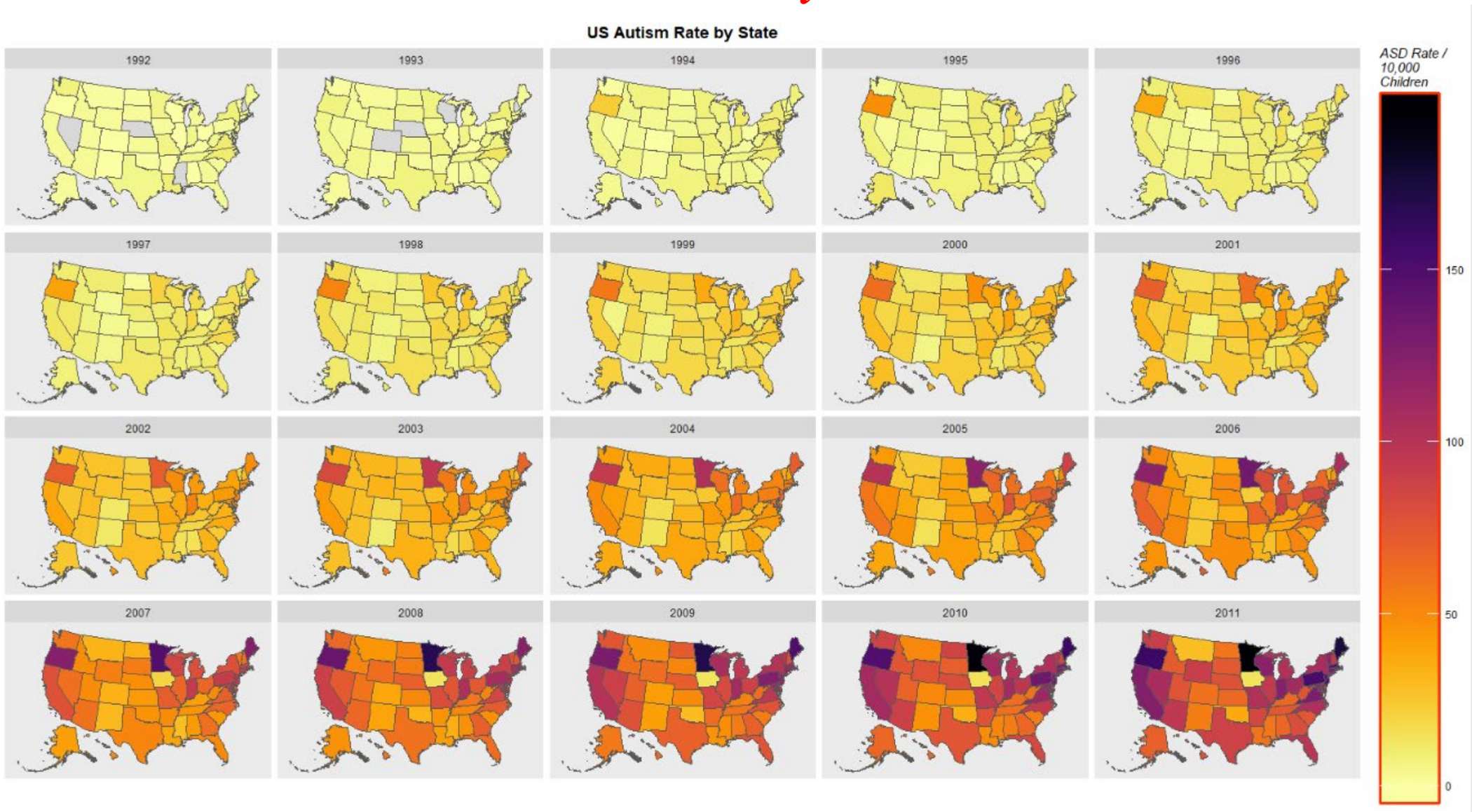

F9 - Bivariate Autism and Cannabis Emergence Maps

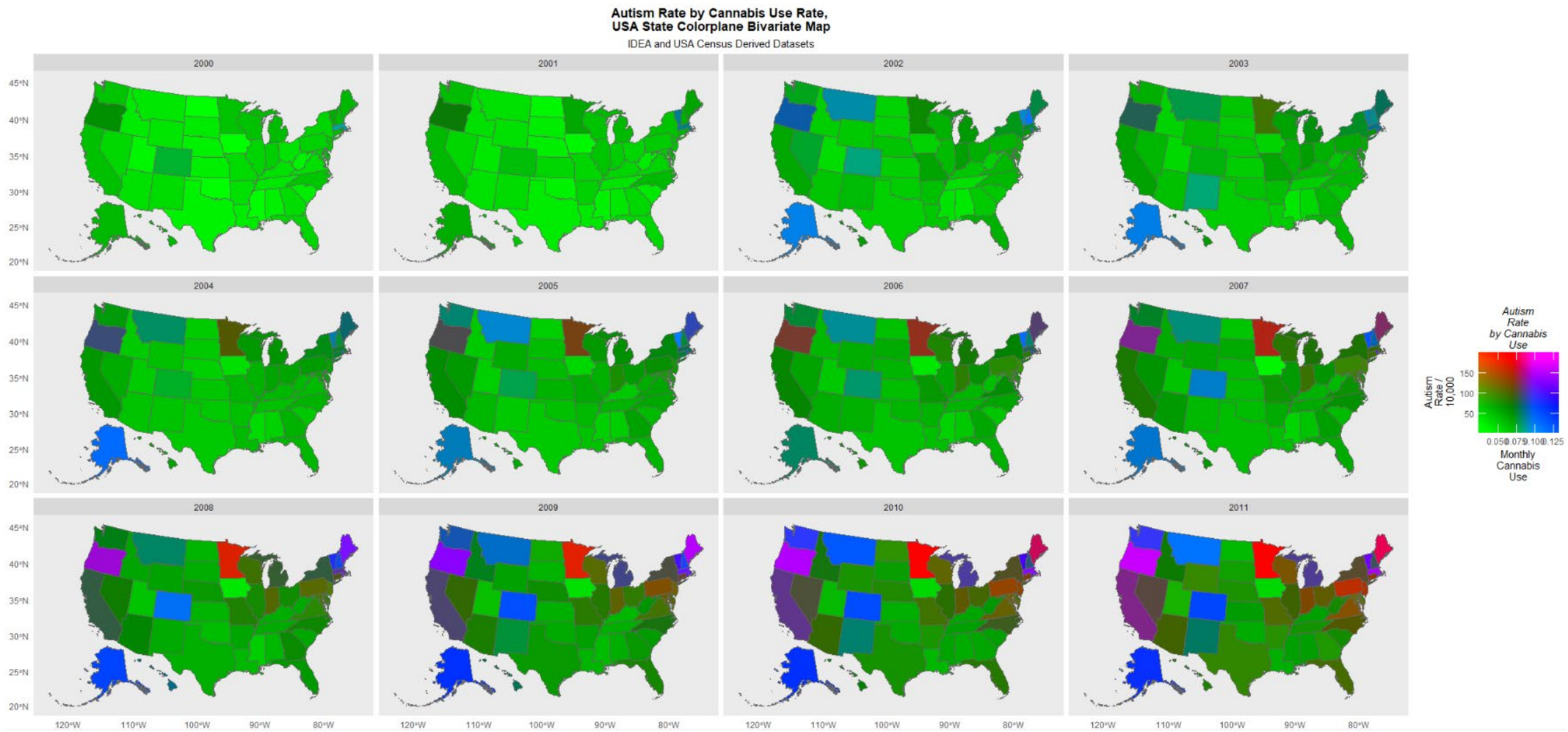

F10 - Bivariate Autism and Cigarette Emergence Maps

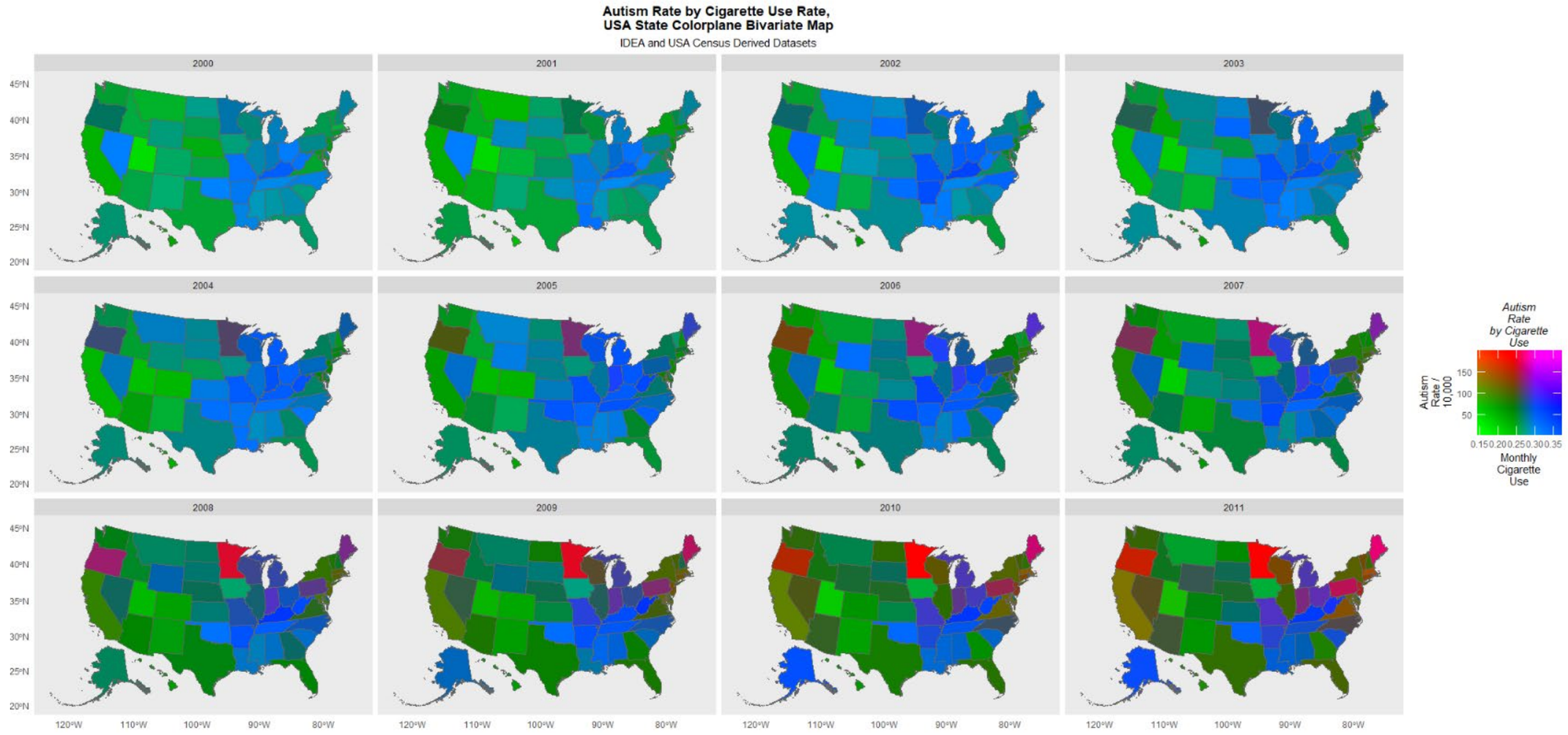

F11 - K-Clusters

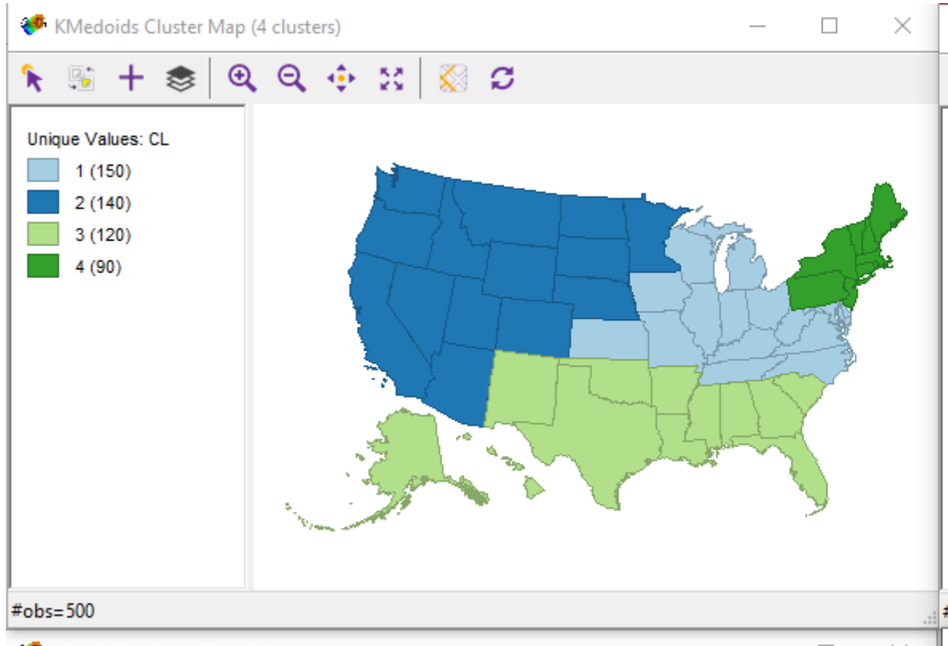

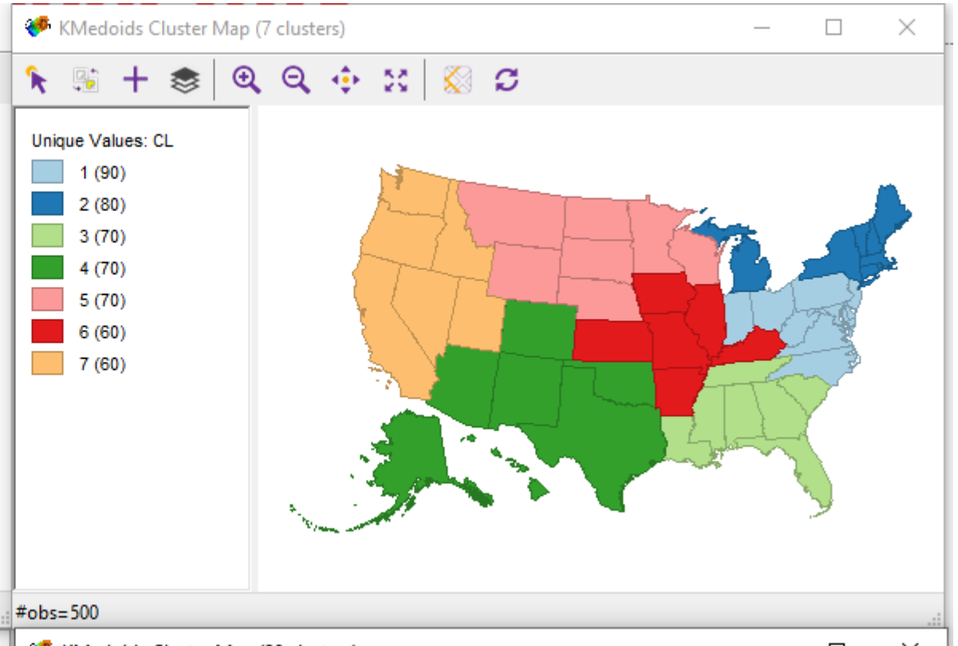

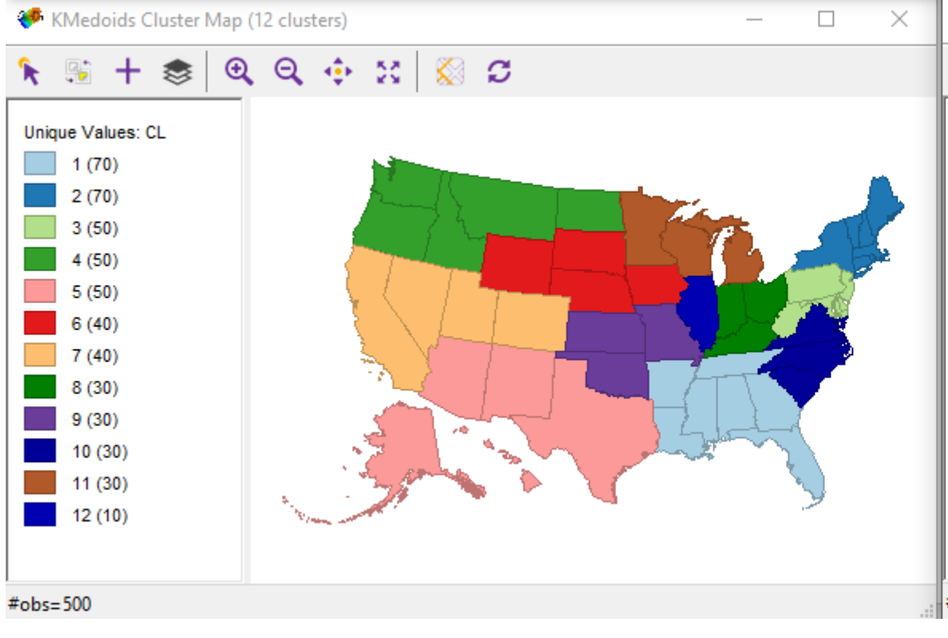

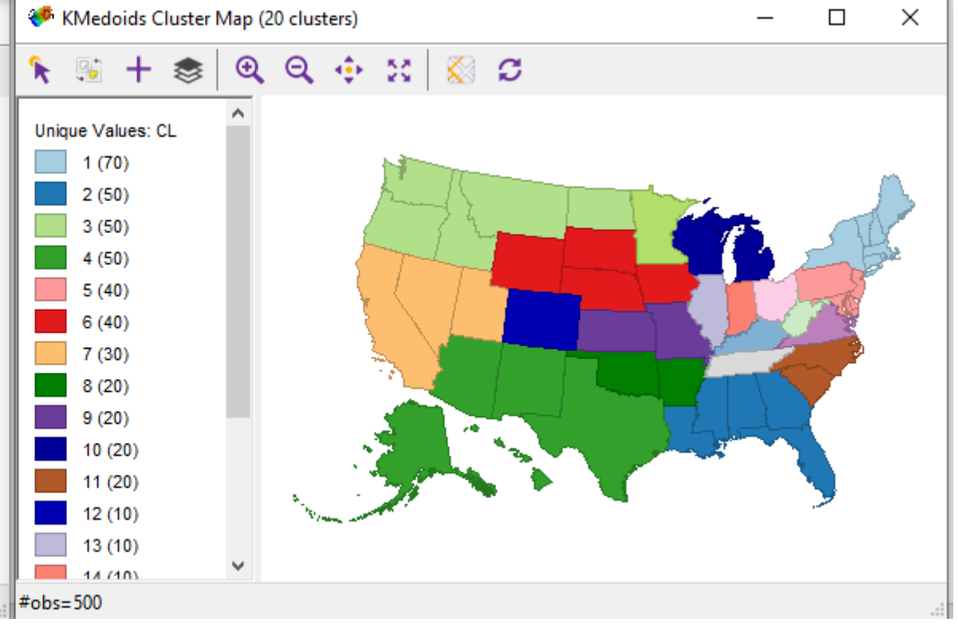

F12 - Hinge & Natural Breaks Map-Graphs

A

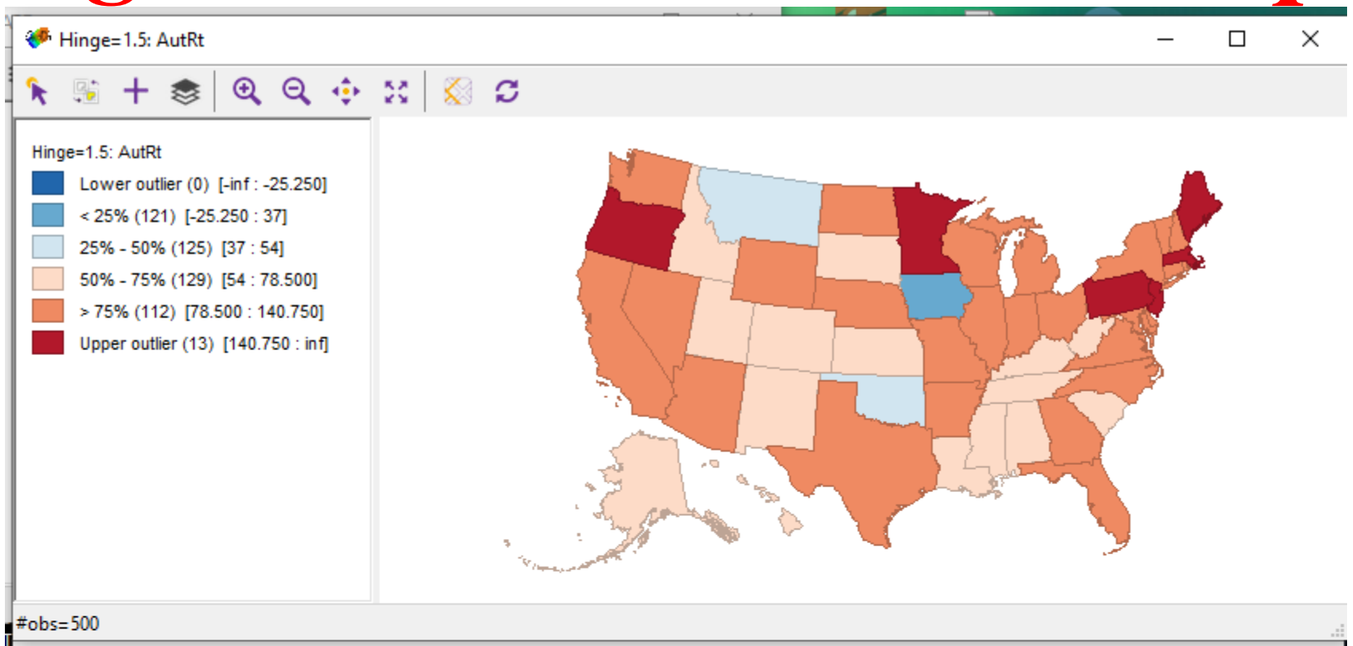

B

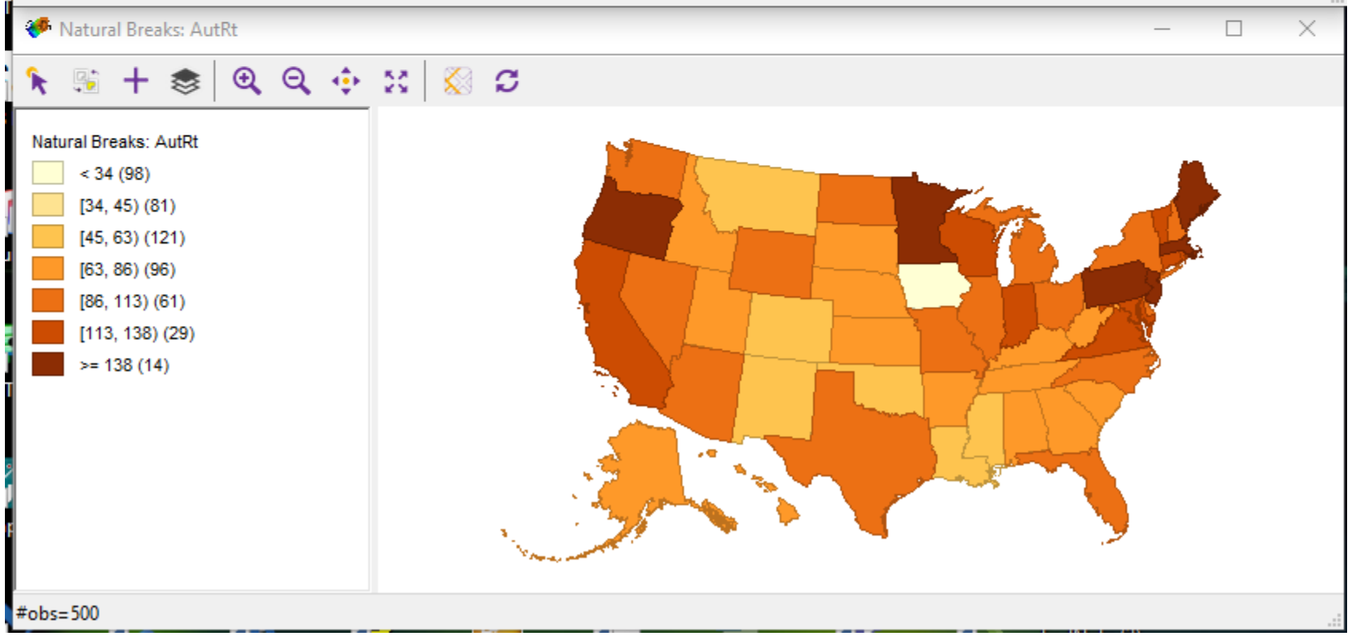

F13 - Dorlings Cartogram Autism USA

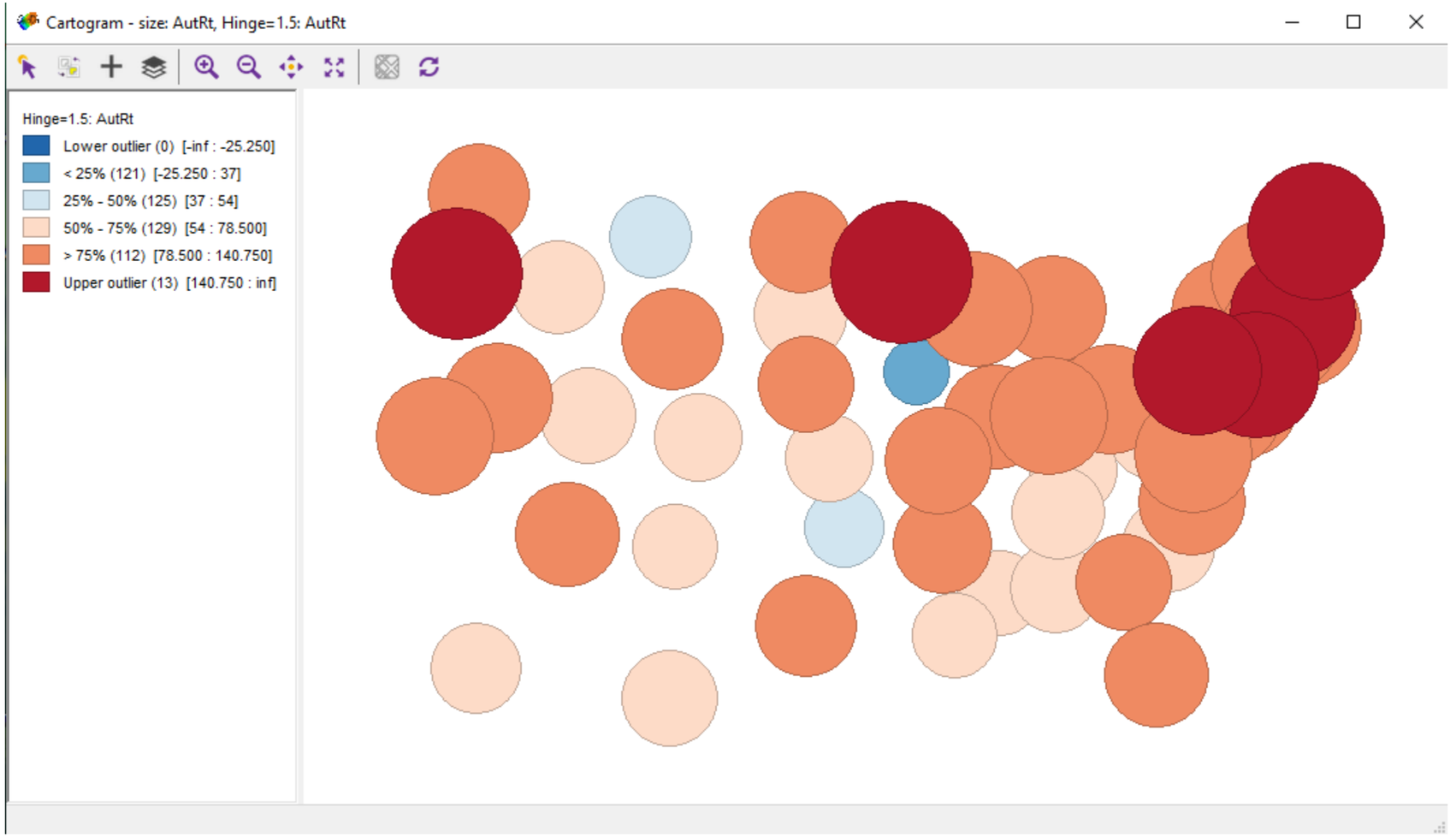

F14 - Cartograms – Autism ~ Cannabis, THC and CBD Exposure

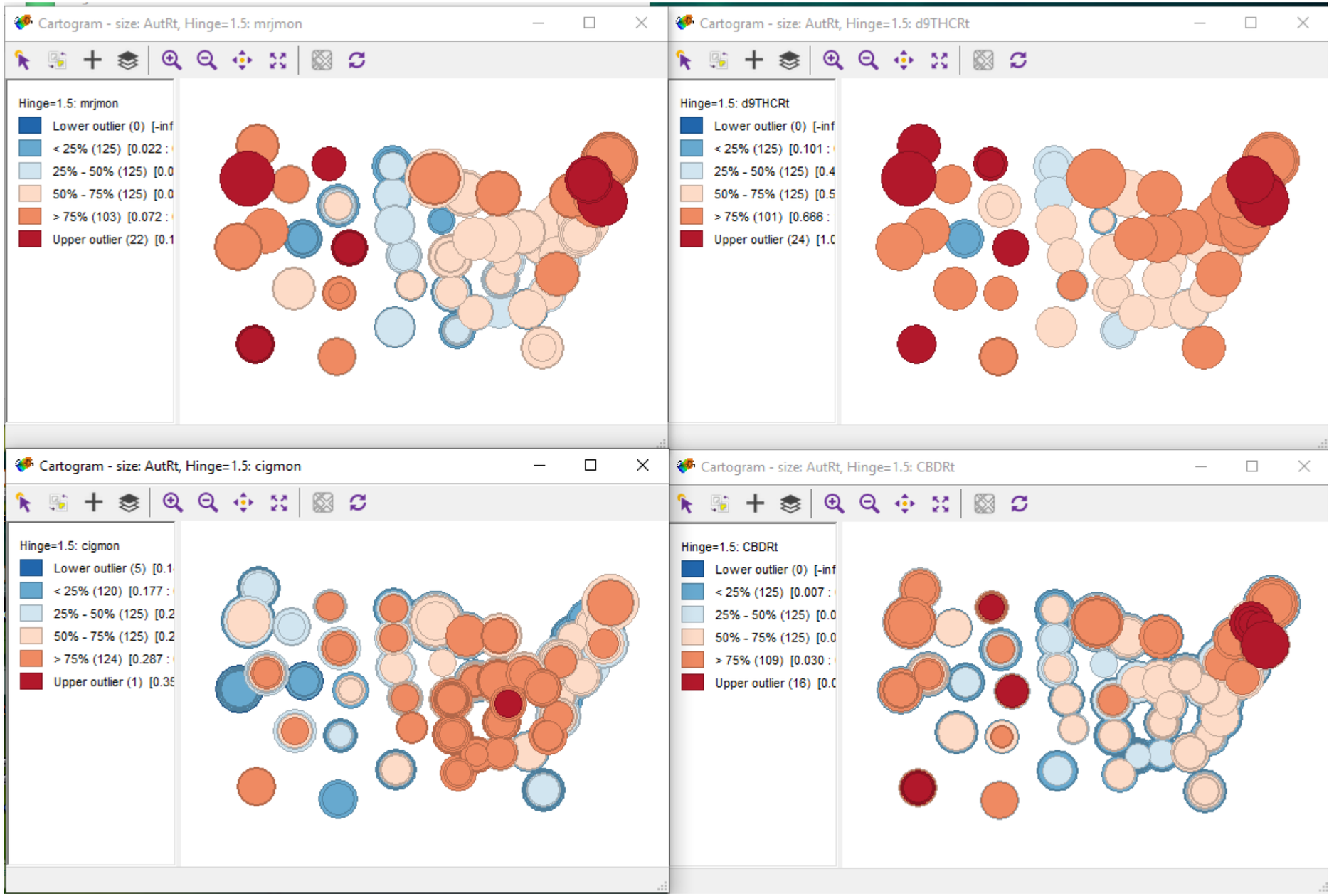

F15 - Scatterplot Matrix – ASD ~ Cigs, Alc, Cocaine

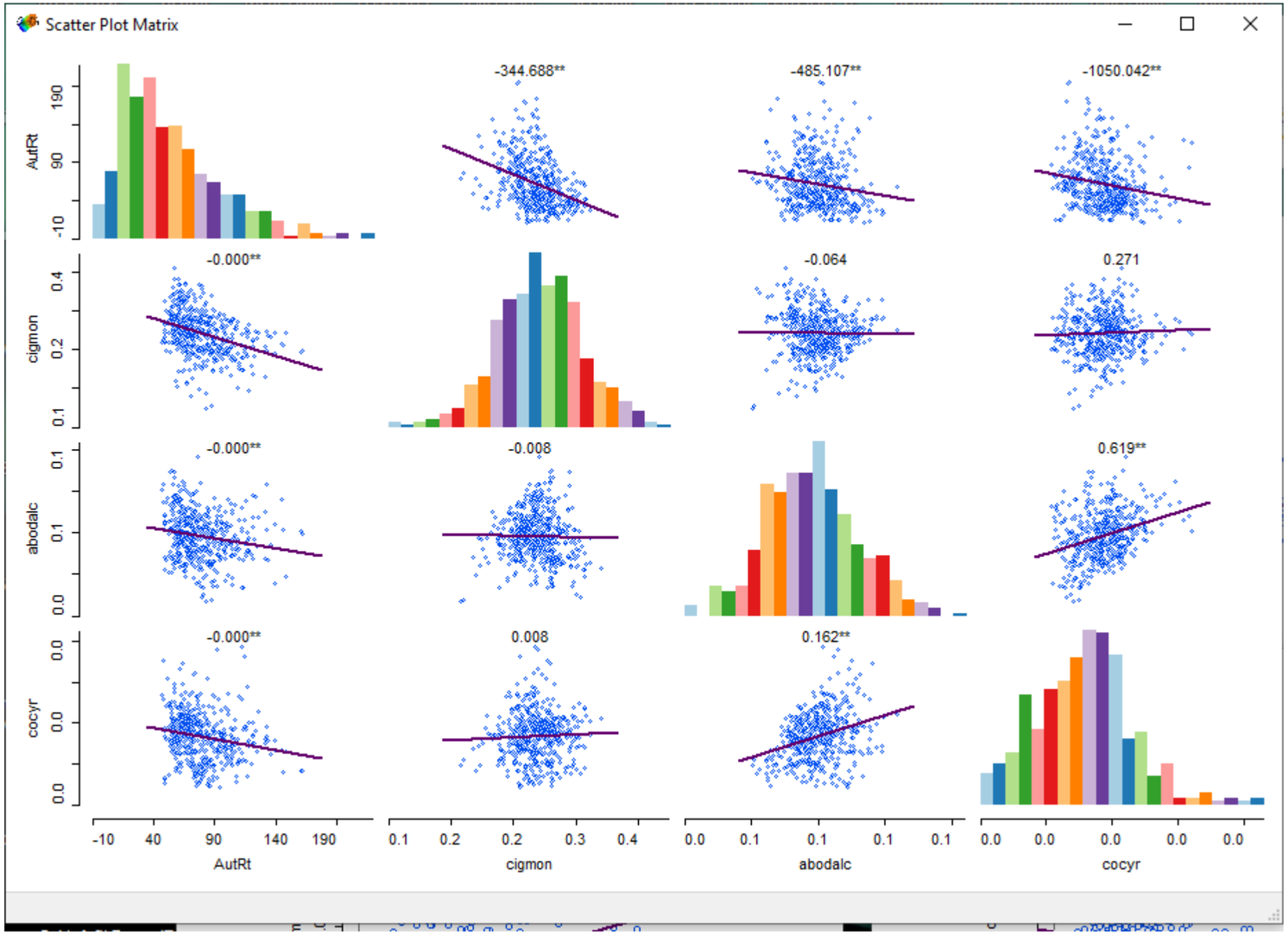

F16 - Scatterplot Matrix – ASD ~ Mrj, THC, CBD

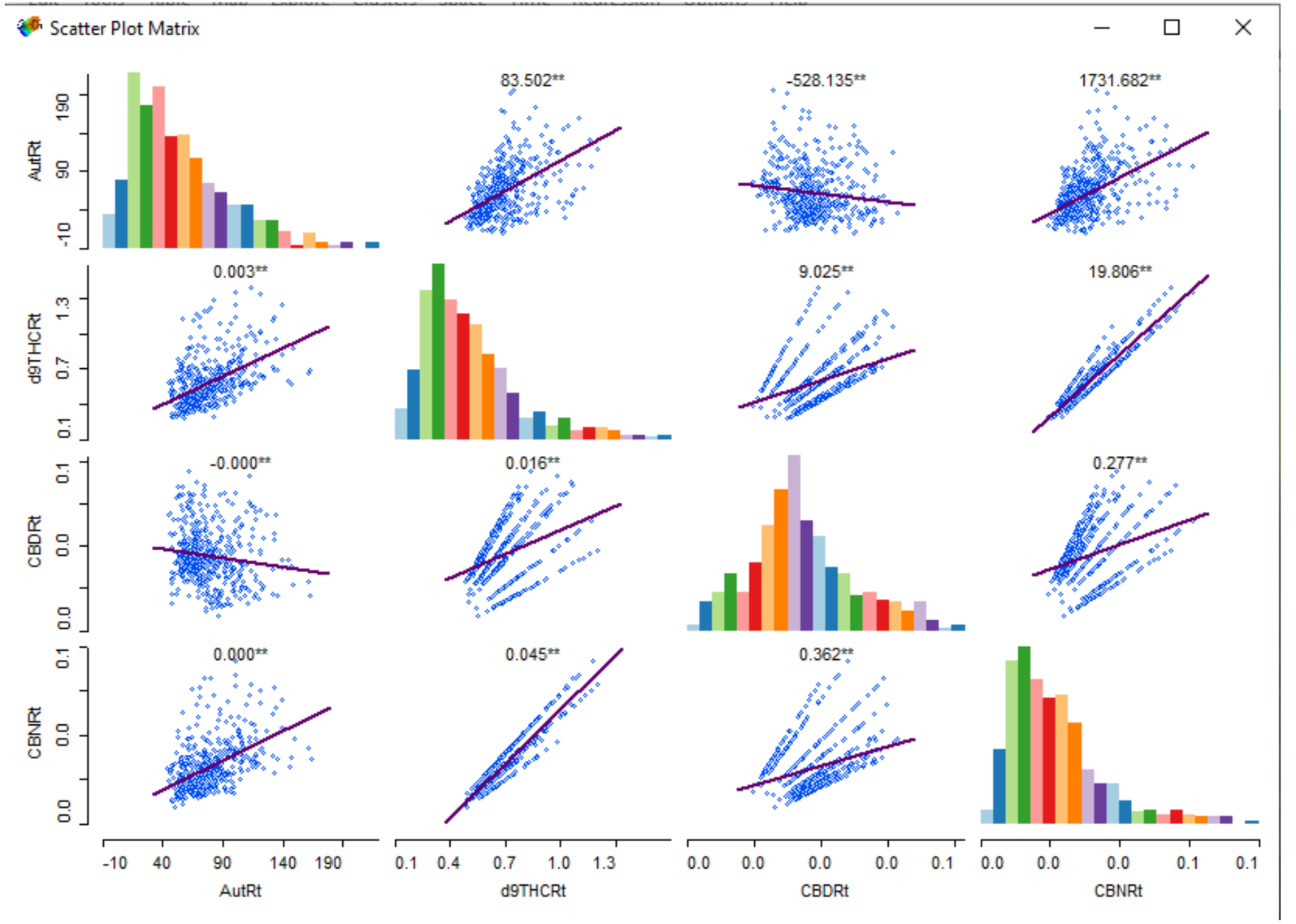

F17 - ASD ~ THC

A

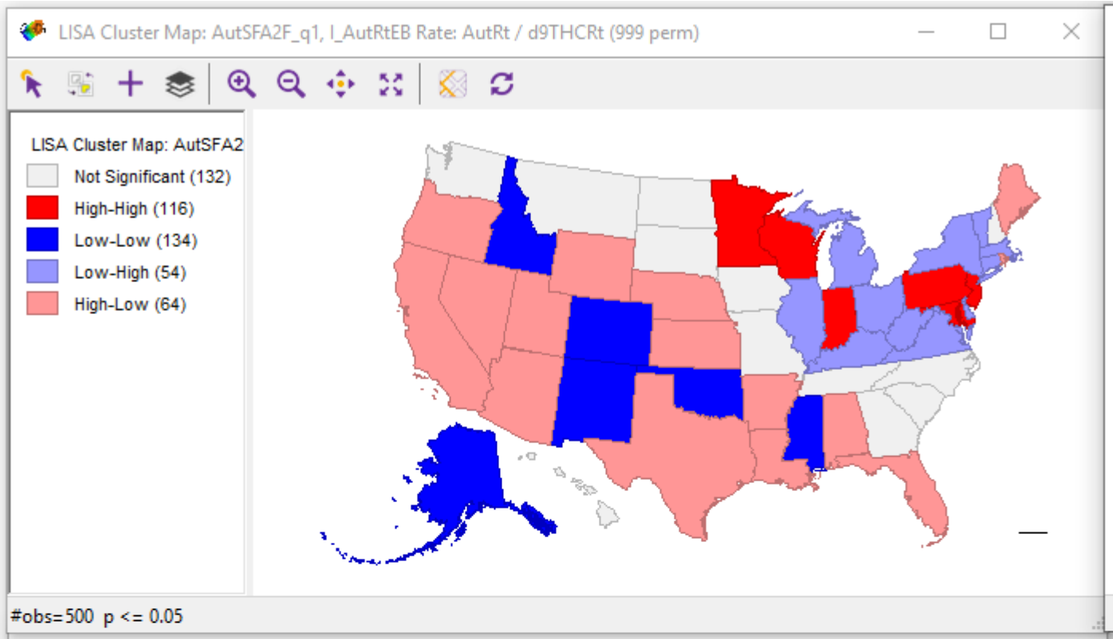

B

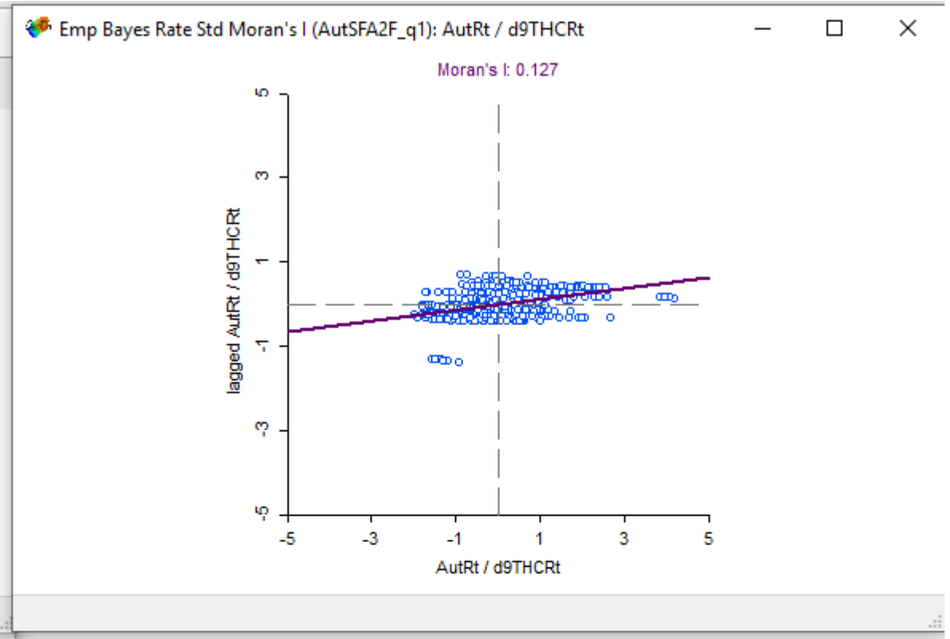

C

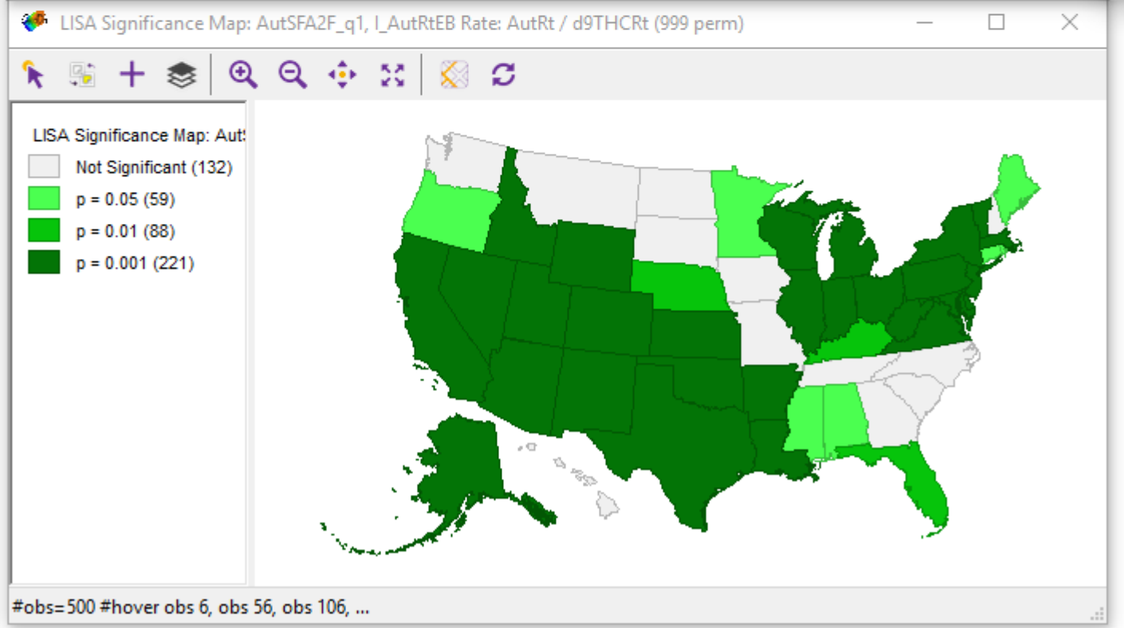

F18 - Bi-LISA Cluster Map - Autism v THC

A

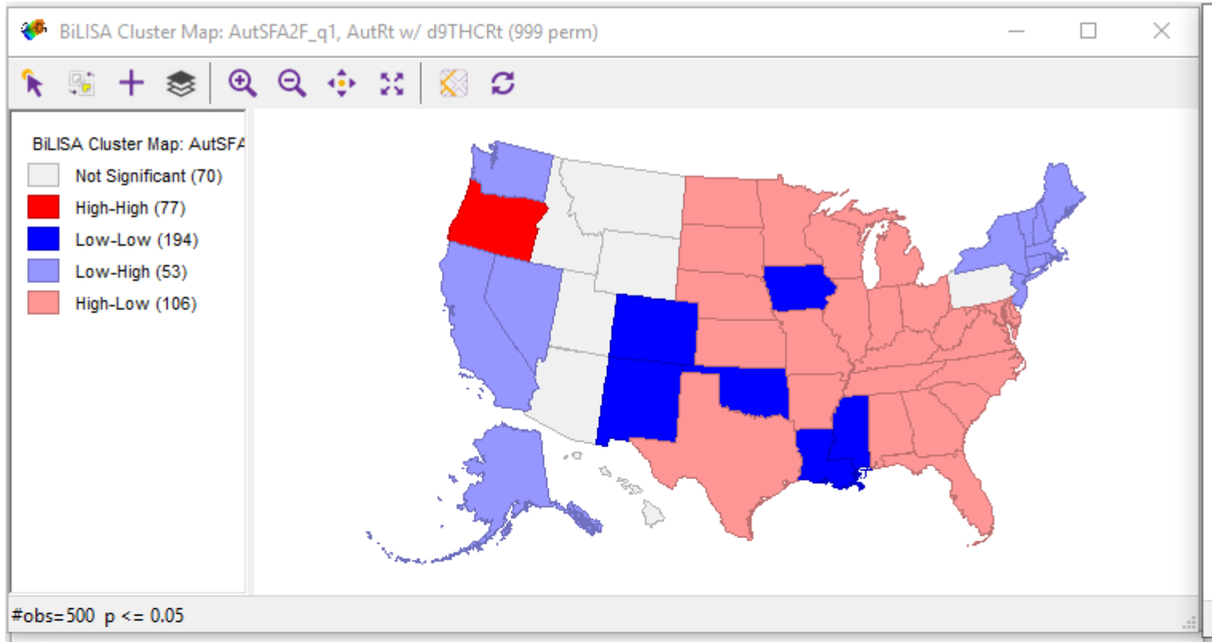

B

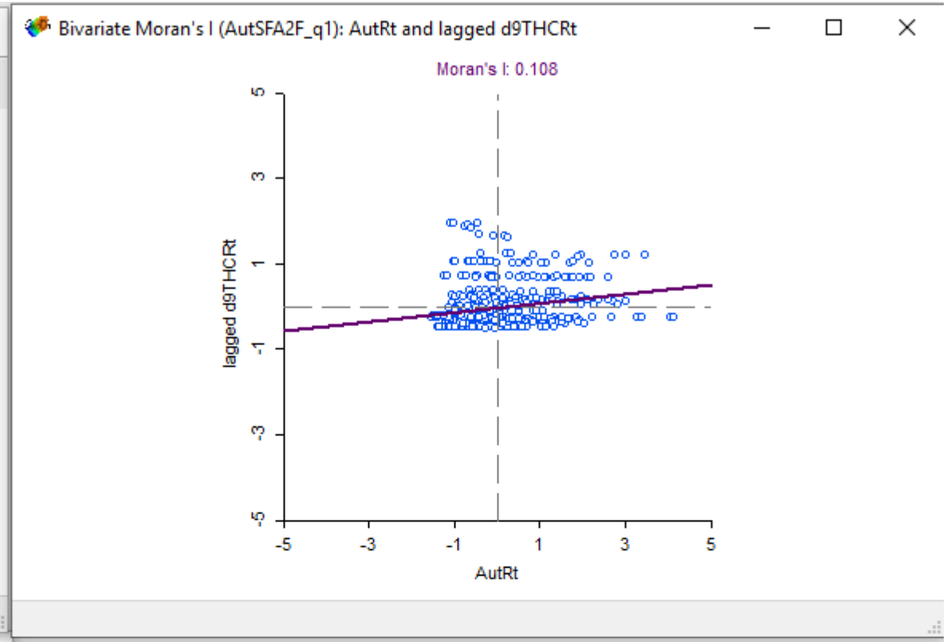

C

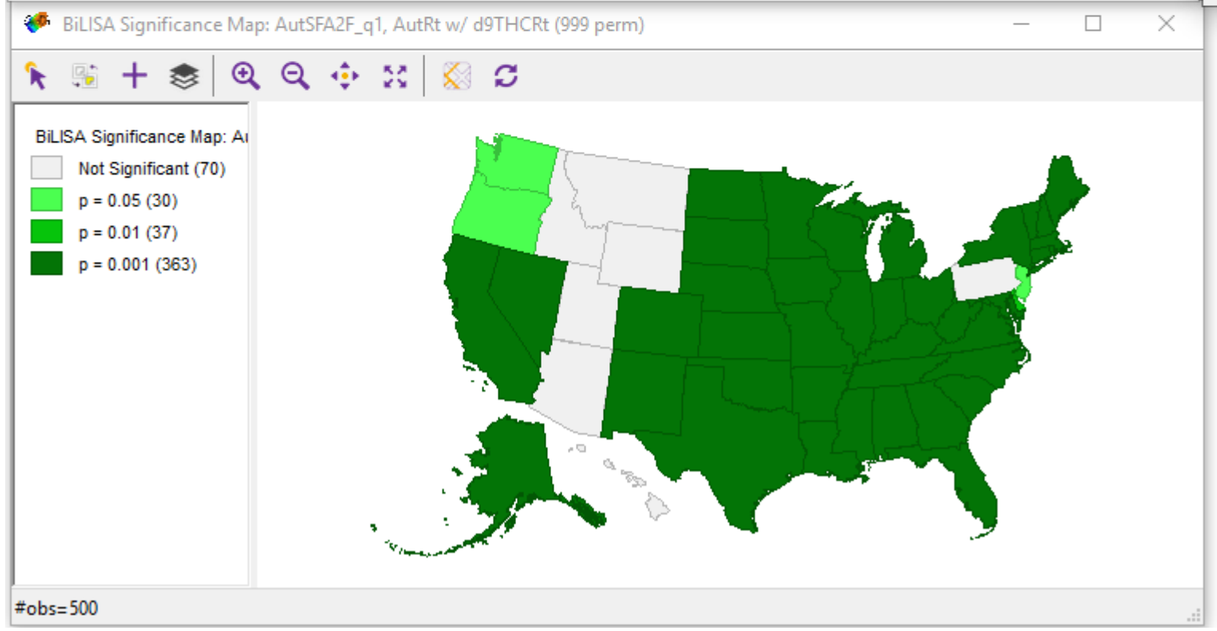

F19 - Autism ~ Time ~ THC Concentration

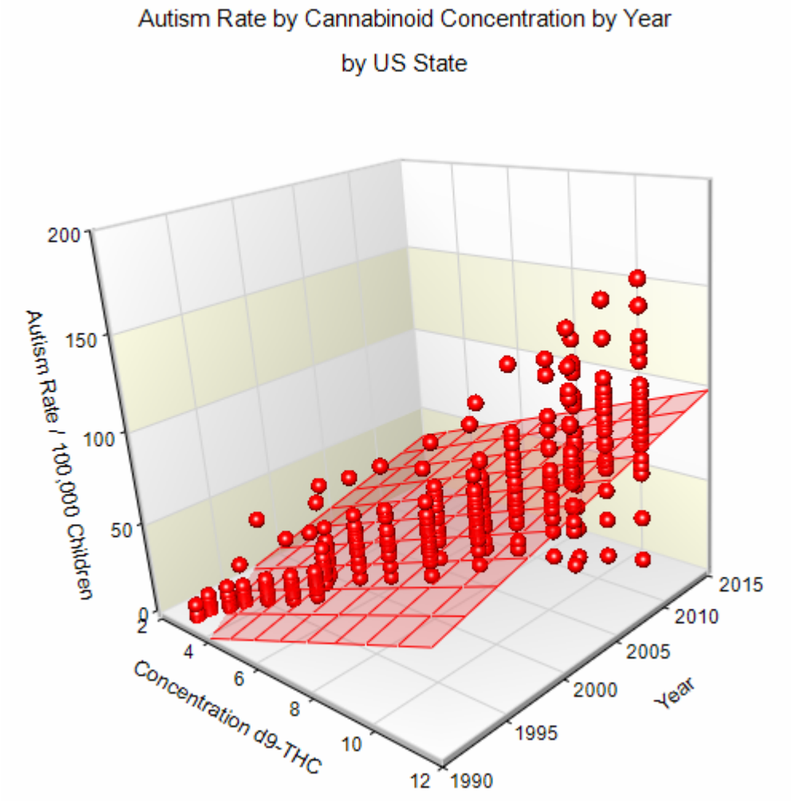

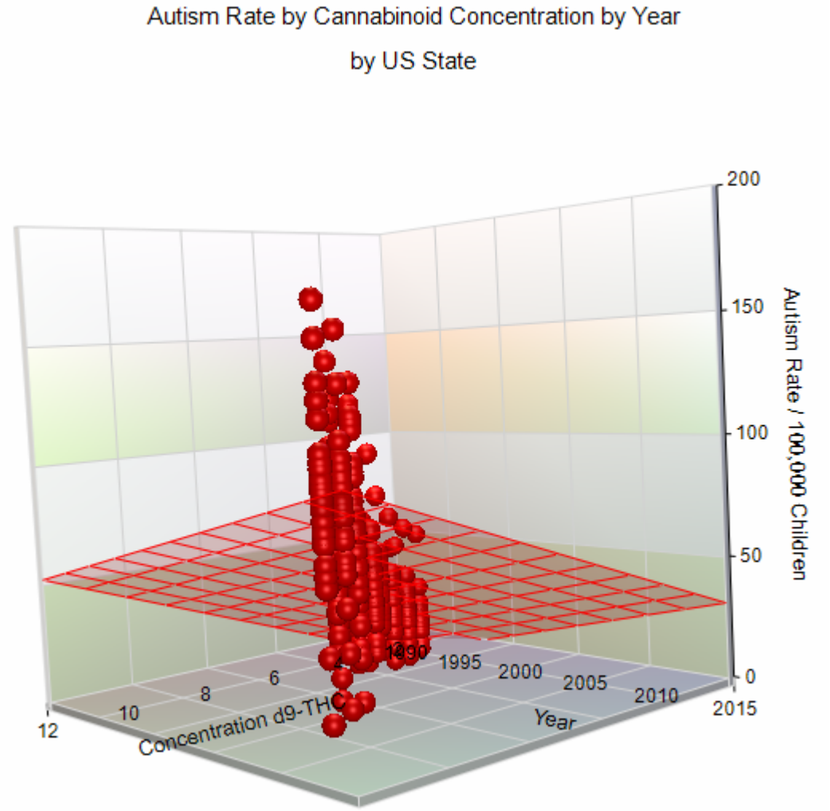

NCSS Software

F20 - 3D Smoothed Regression Surface

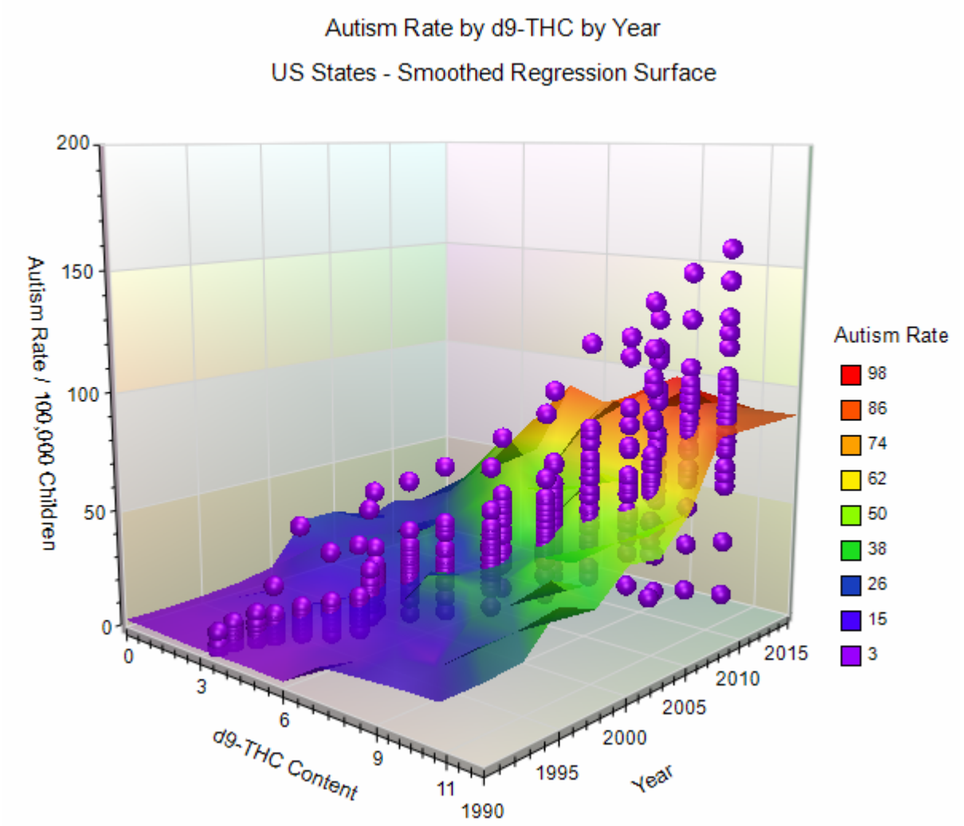

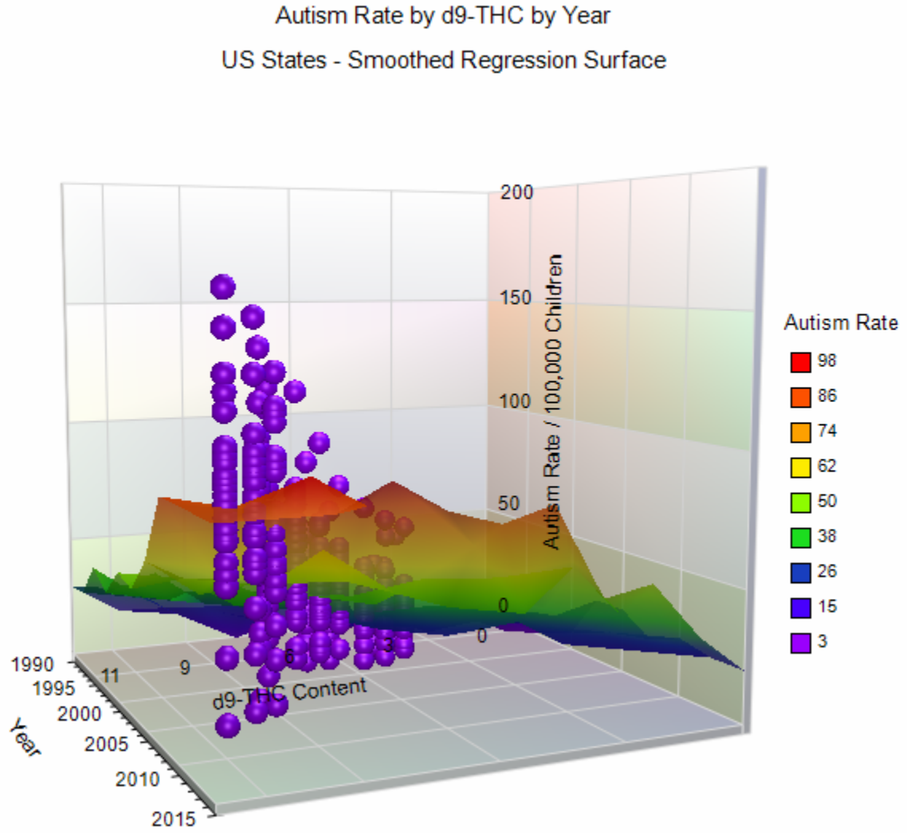

NCSS Software

F21 - 3-D Relationships – THC, Time & Autism

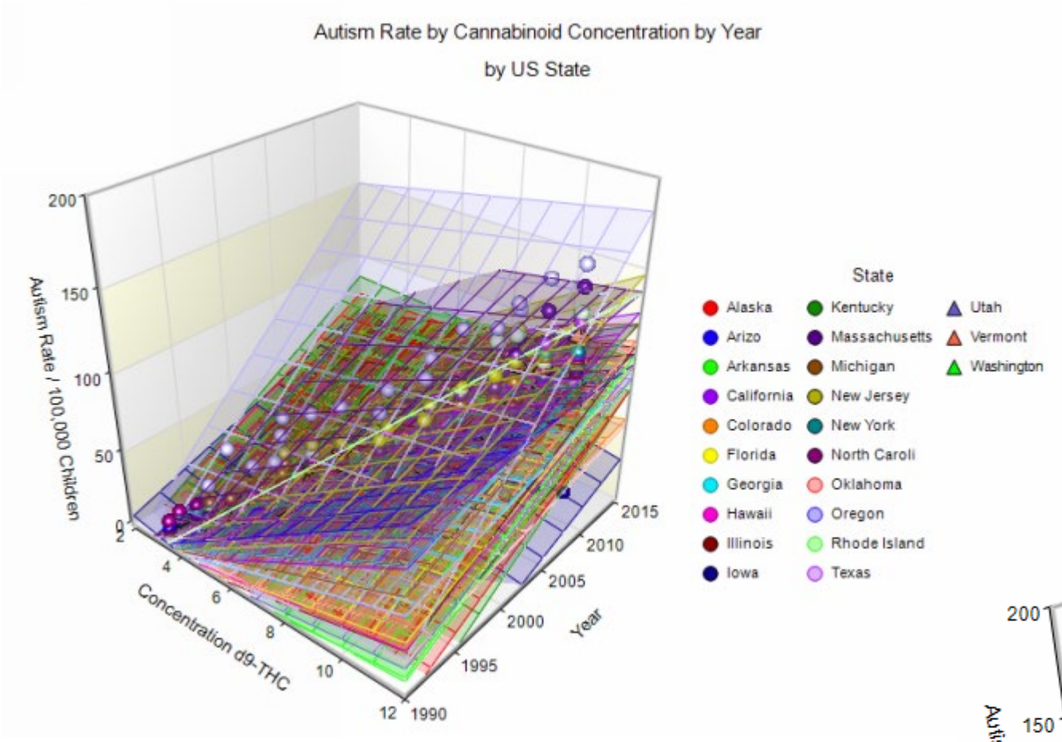

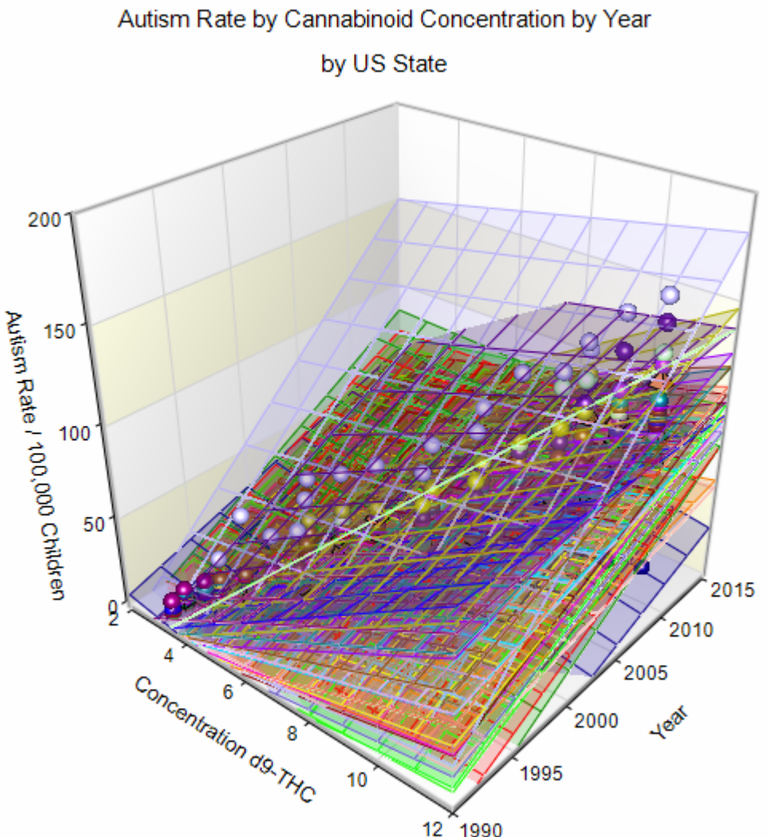

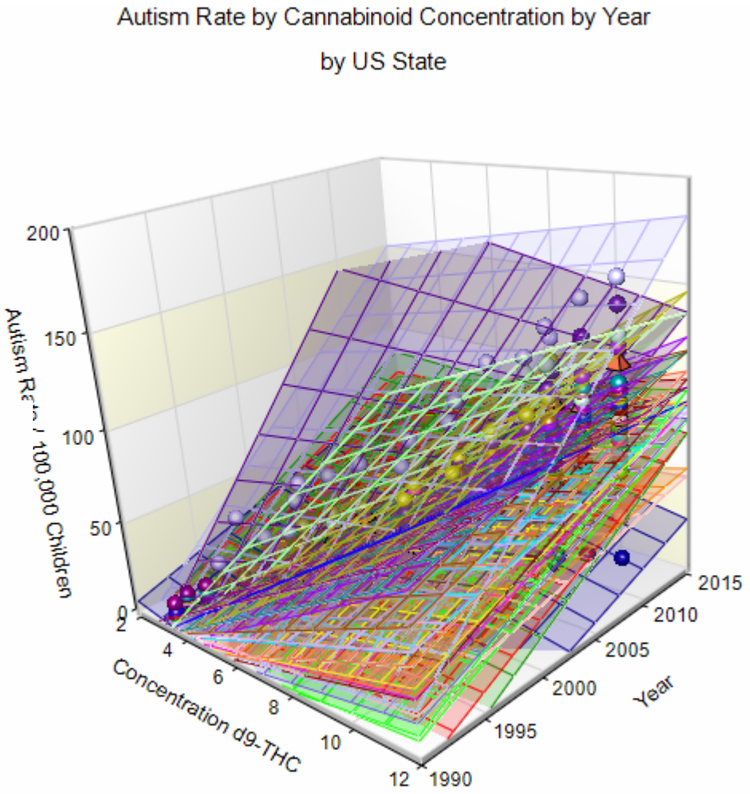

NCSS Software

F22 - Autism by THC by Time

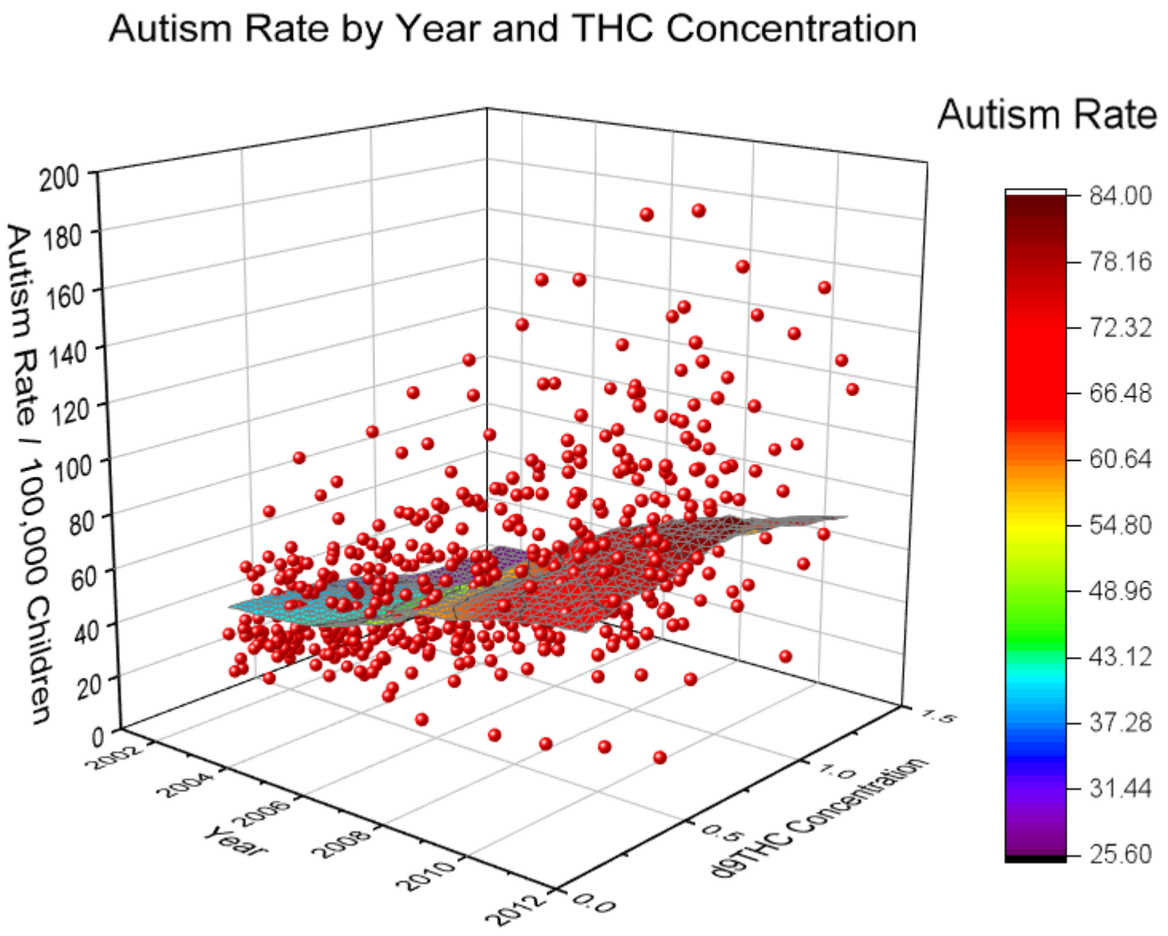

Adjacent Median Smoothing

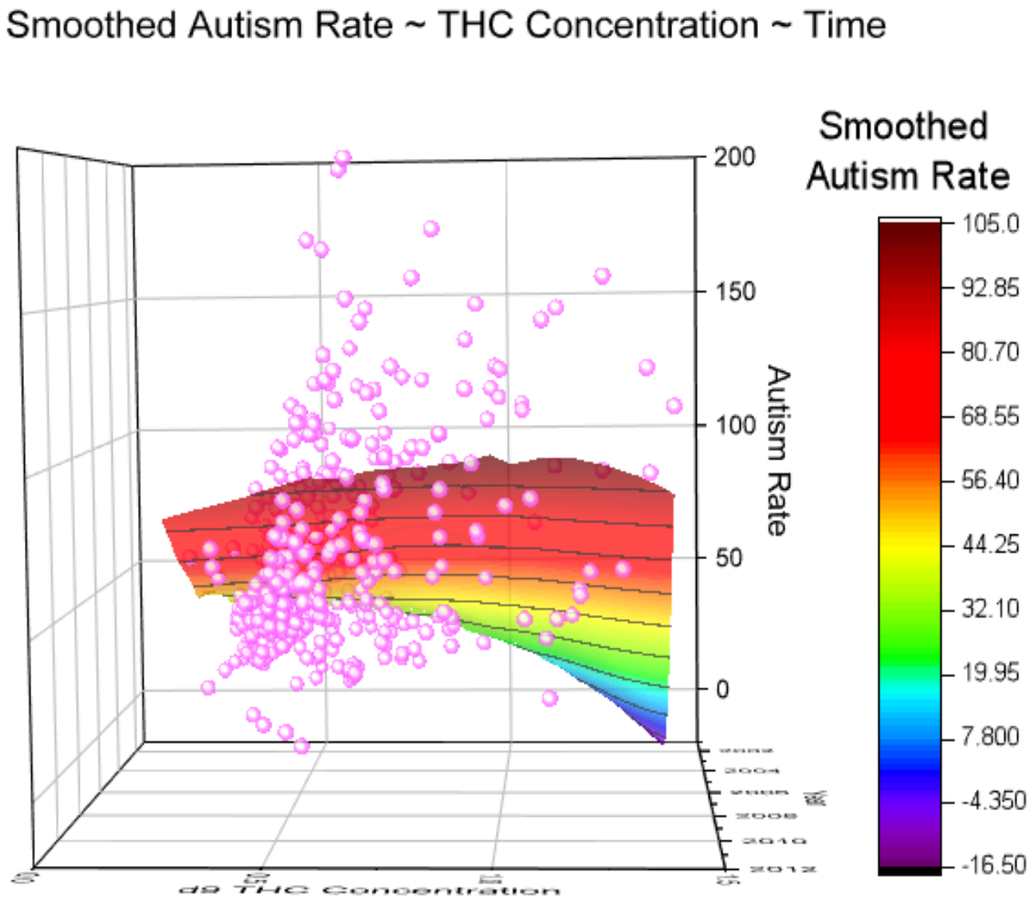

Negative Exponential Smoothing

OriginLab Software

F23 - Variography - Autism

Variogram model - SpaceStat

Dataset: AutRt Variogram model name: Variogram model

Point dataset for custom-weighted centroids: <none> Export centroids

Model definition | Deconvolution settings

Estimator: Traditional

Weight dataset: <specify> Population denominator: 1

Current time interval: [1 Jan 2001, 1 Jan 2002)

Plot | Map | Cloud

Lag count: 10 Lag: 297833 Tolerance: 148917 Reset lags

Angle count: 1 Start angle: 0 Angle lag: 0 Tolerance: 90

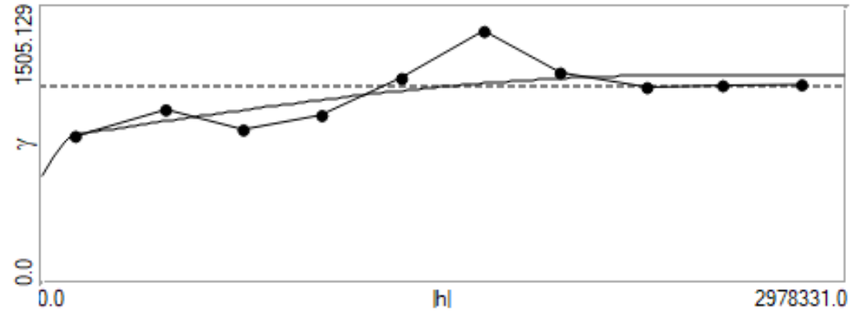

Show variance Show model Skip factor: 1 Display: All angles

Distance (|h|): 2297762 Semivariance (γ): 209.3226 Data pairs: 10700

Variogram model parameters

Nugget: 580.909540730585

Number of basic models: 2

Model 1 | Model 2

Type: Spherical

Sill: 197.37971

Ellipse parameters

Angle: 0.0

Min range: 127317.83

Max range: 127317.83

Export model Auto-fit model

MSS error: 0.063668

Current time interval: [1 Jan 2001, 1 Jan 2002)

Plot | Map | Cloud

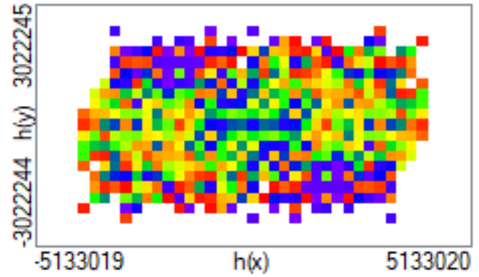

X bins: 20

Y bins: 11

Bin size: 250391

(unit: Meter)

Smooth map

Distance: 0.0

Angle: 0.0

Observations: 0.0

Model definition | Deconvolution settings

Estimator: Traditional

Weight dataset: <specify> Population denominator: 1

Current time interval: [1 Jan 2001, 1 Jan 2002)

Plot | Map | Cloud

Maximum distance (unit: Meter) 2.97833e+06 Angle: 0 Tolerance: 90

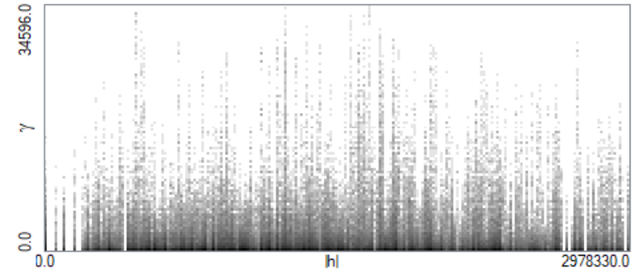

Show frequency raster Resolution: 2

Distance (|h|): 455589.7 Semivariance (γ): 1132.152

F24 - Variography – Monthly Cannabis Use

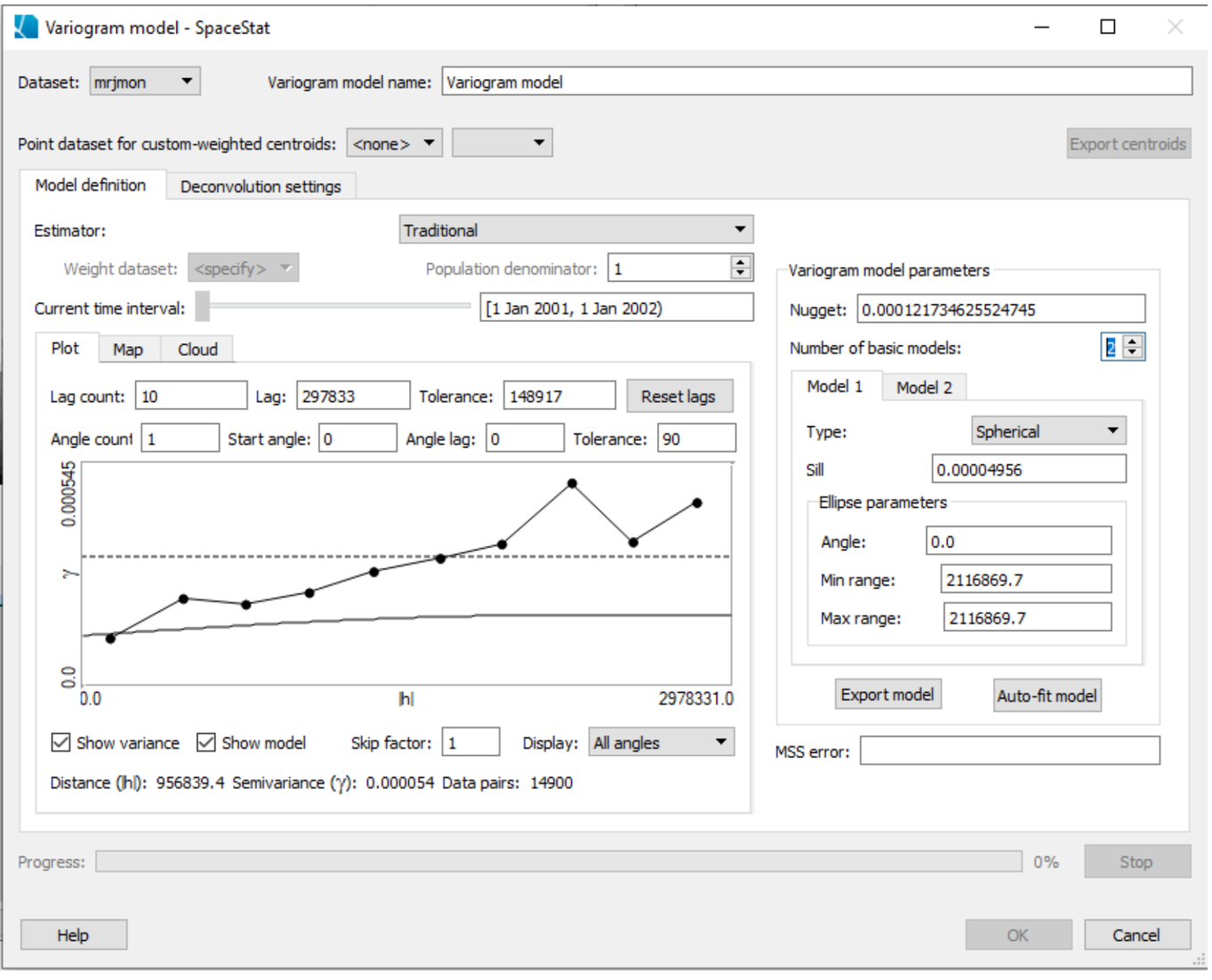

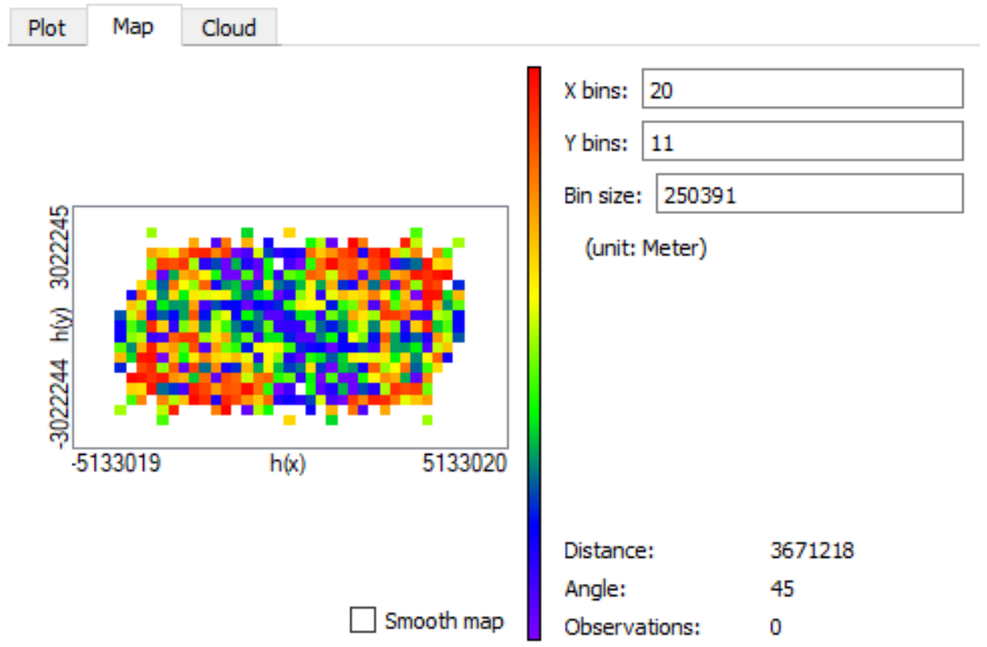

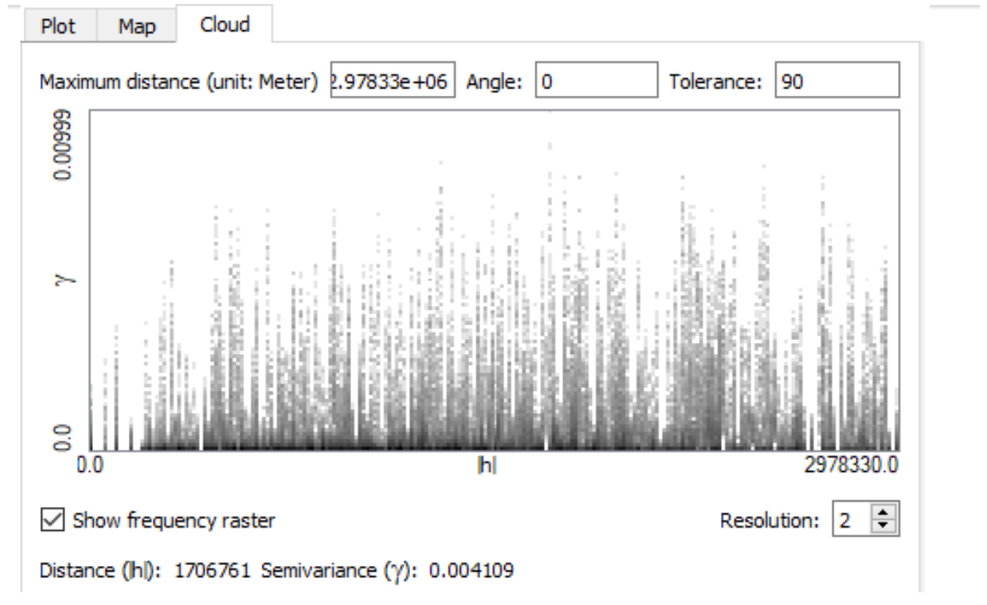

F25 - Variography – Δ9-THC Consumption (Estimated)

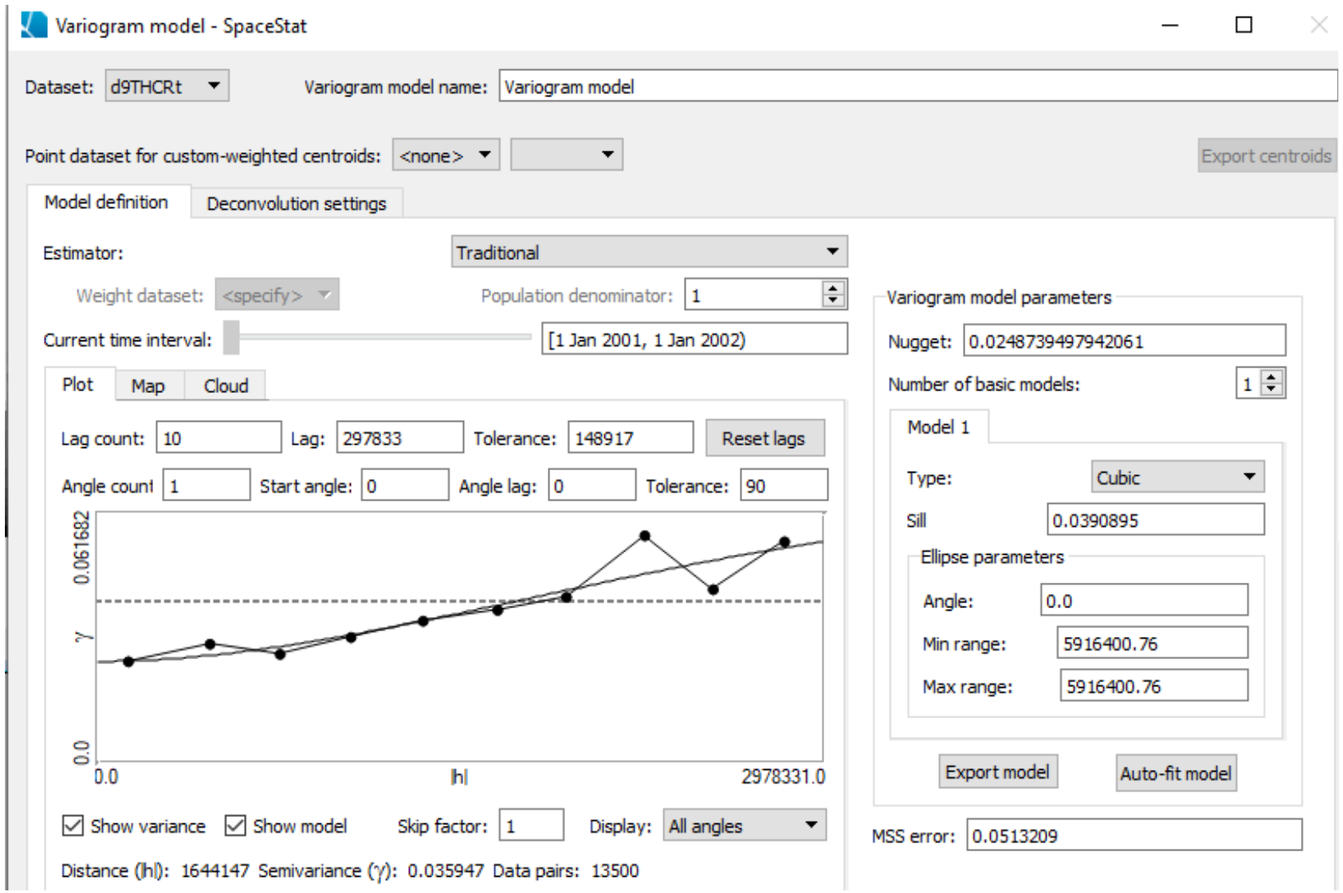

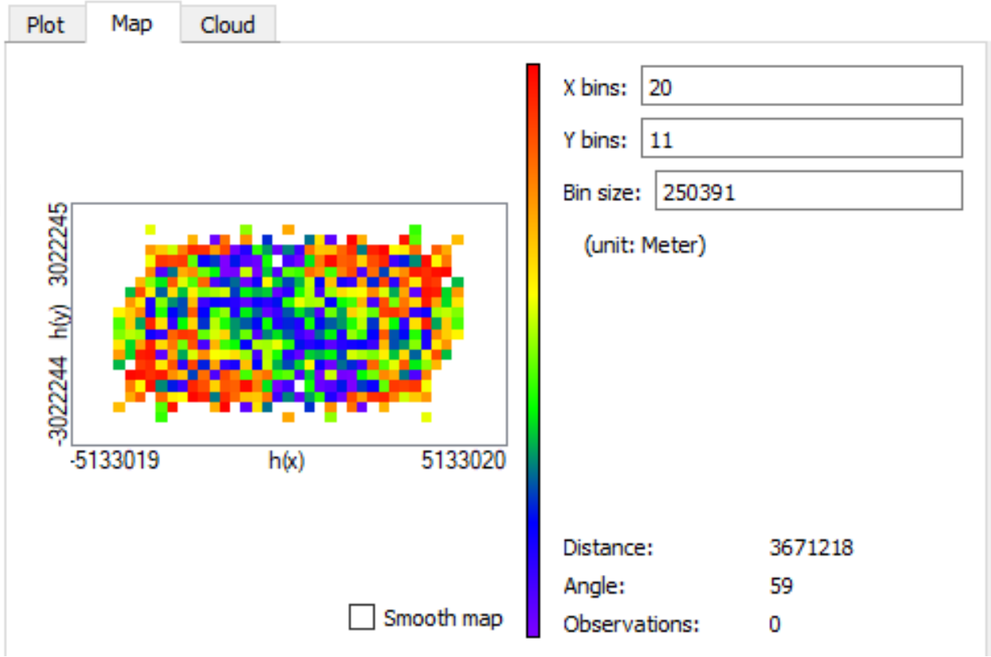

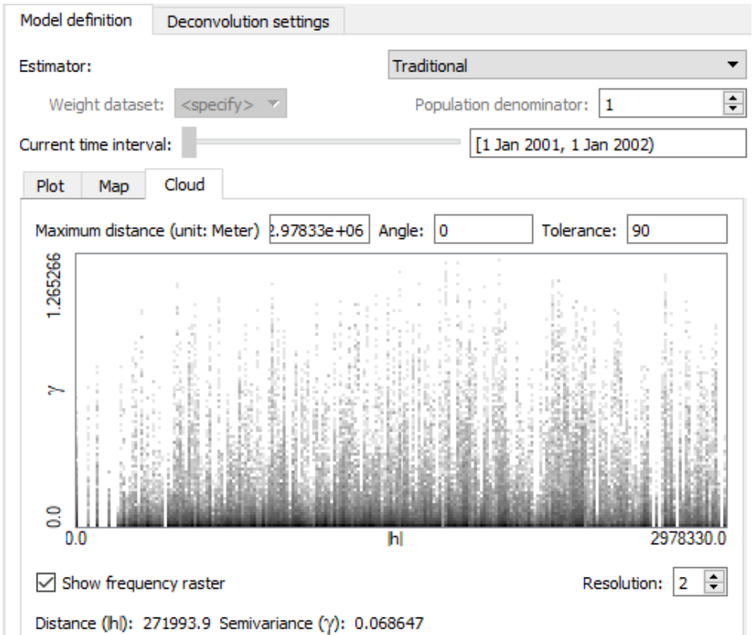

F26 - Changes in Autism

Difference_1992-2011

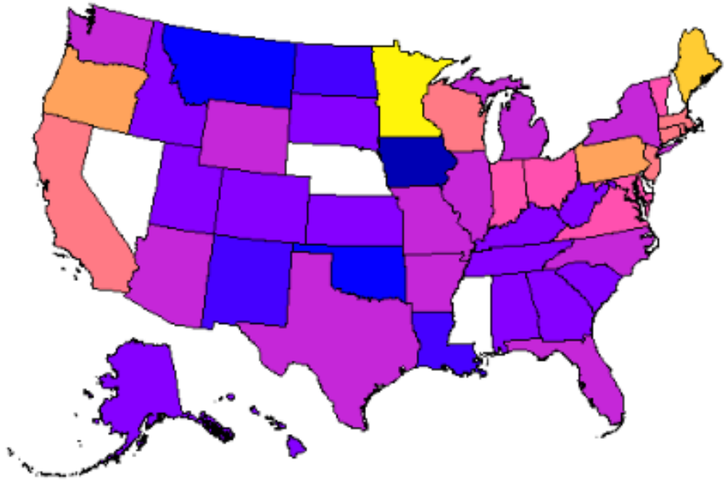

Difference_1994-2011

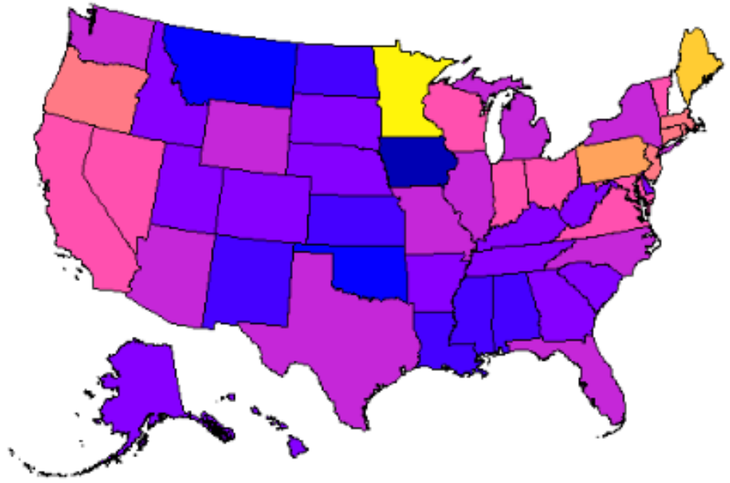

Difference_1995-2011

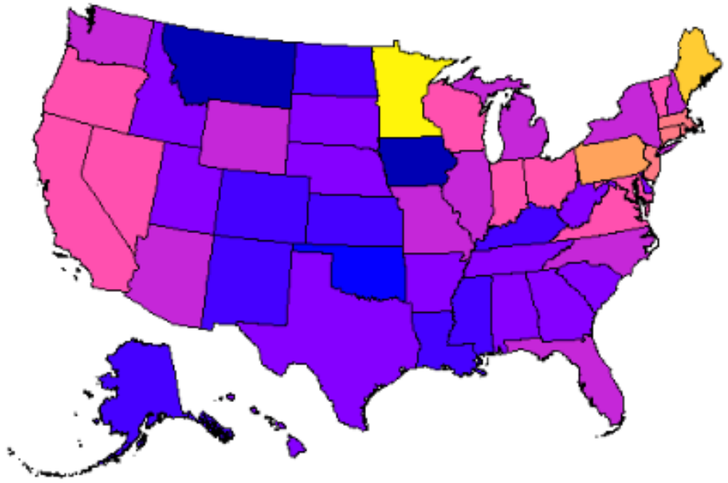

Difference_1996-2011

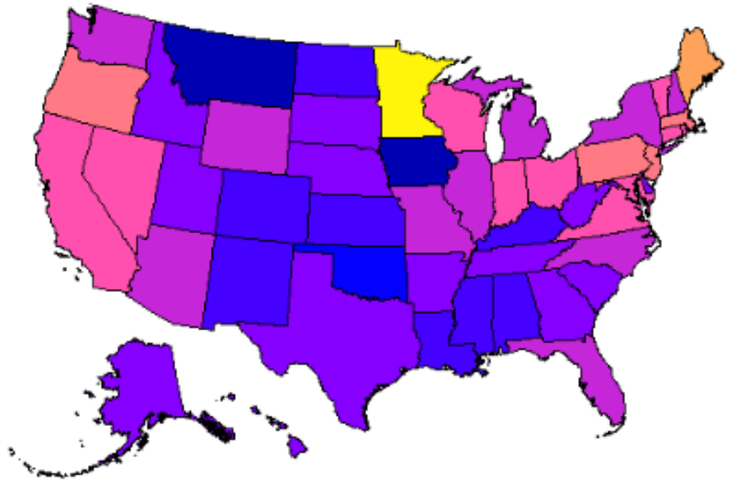

F27 - Change Autism Rate 2002-2011

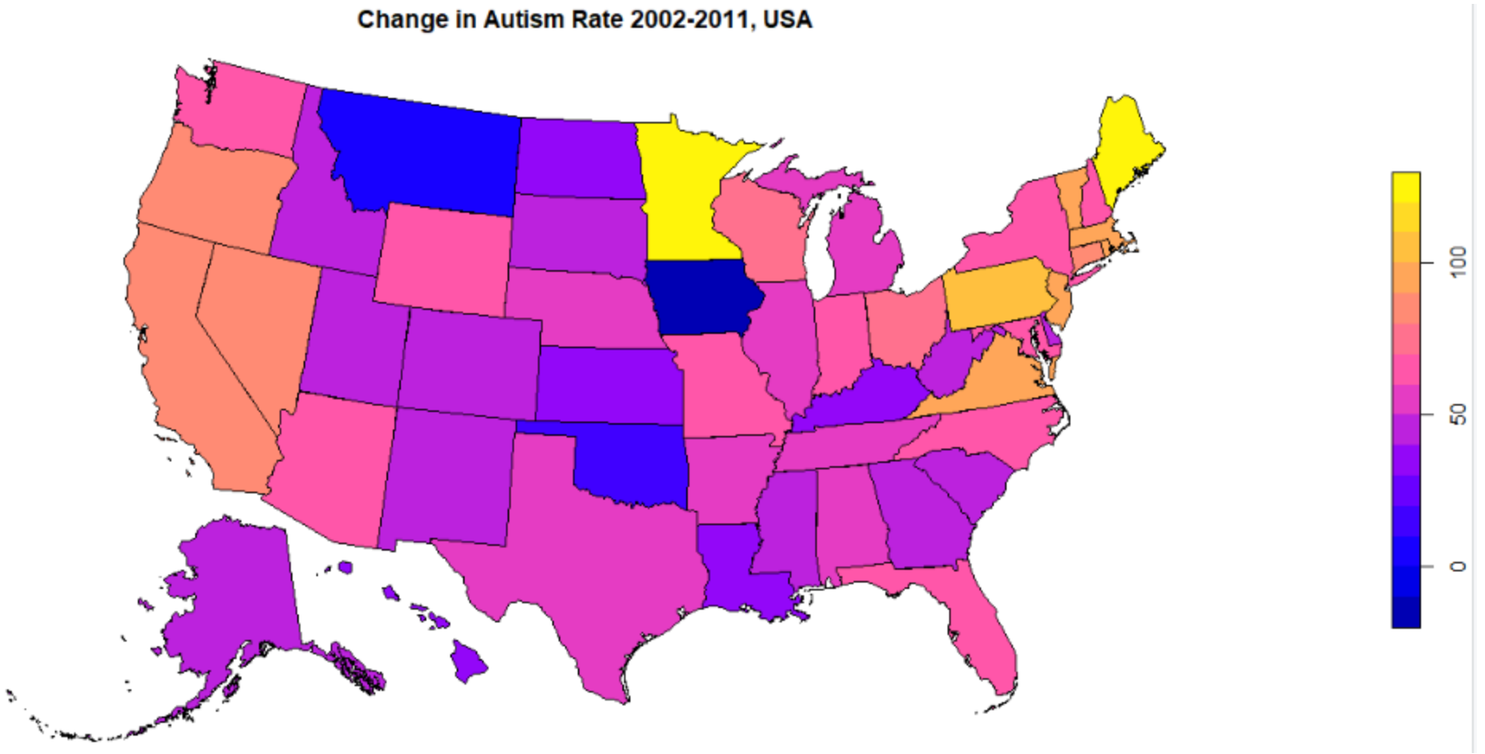

F28 - Changes Autism & Drug Use 2002-2011

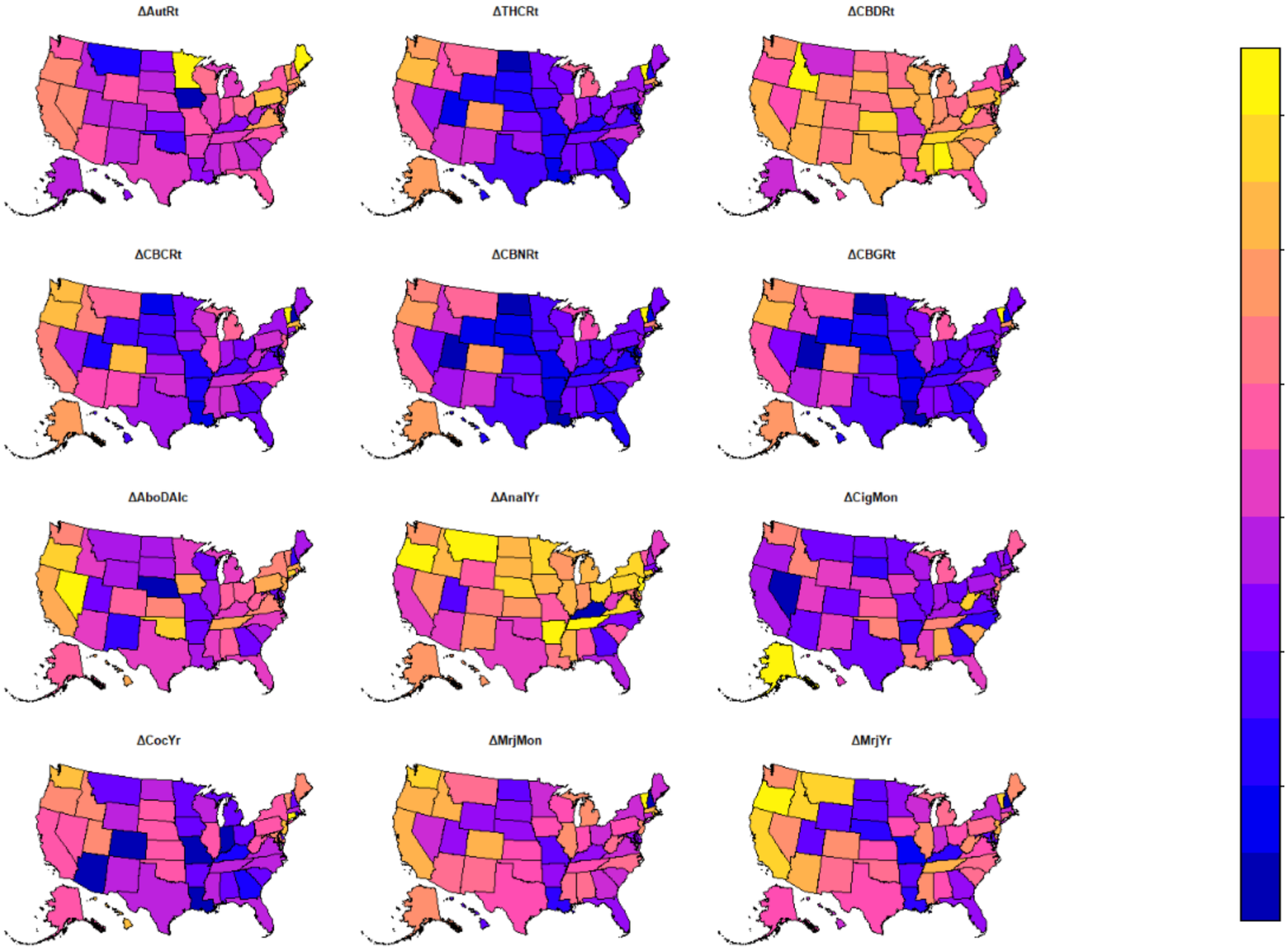

F29 - Status

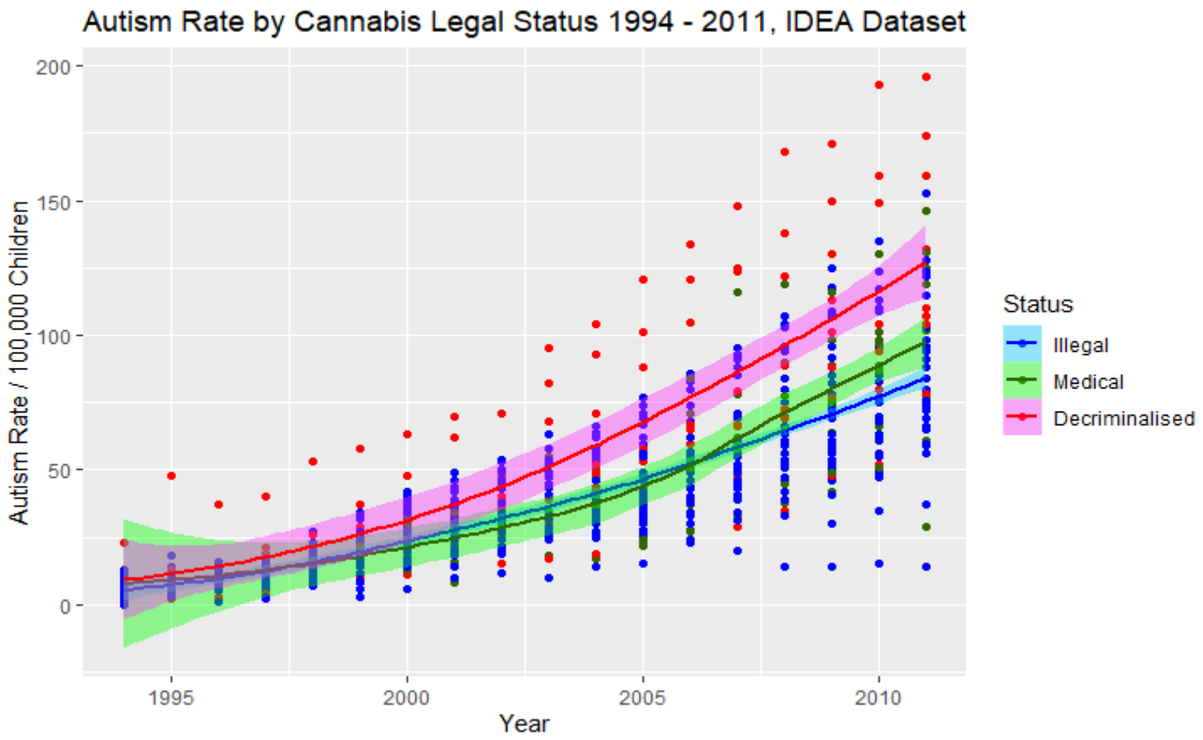
Autism Rate by Cannabis Legal Status 1994 - 2011, IDEA Dataset
Autism Rate / 100,000 Children
200
150
100
50
0
1995
2000
2005
2010
Year
Status
Illegal
Medical
Decriminalised

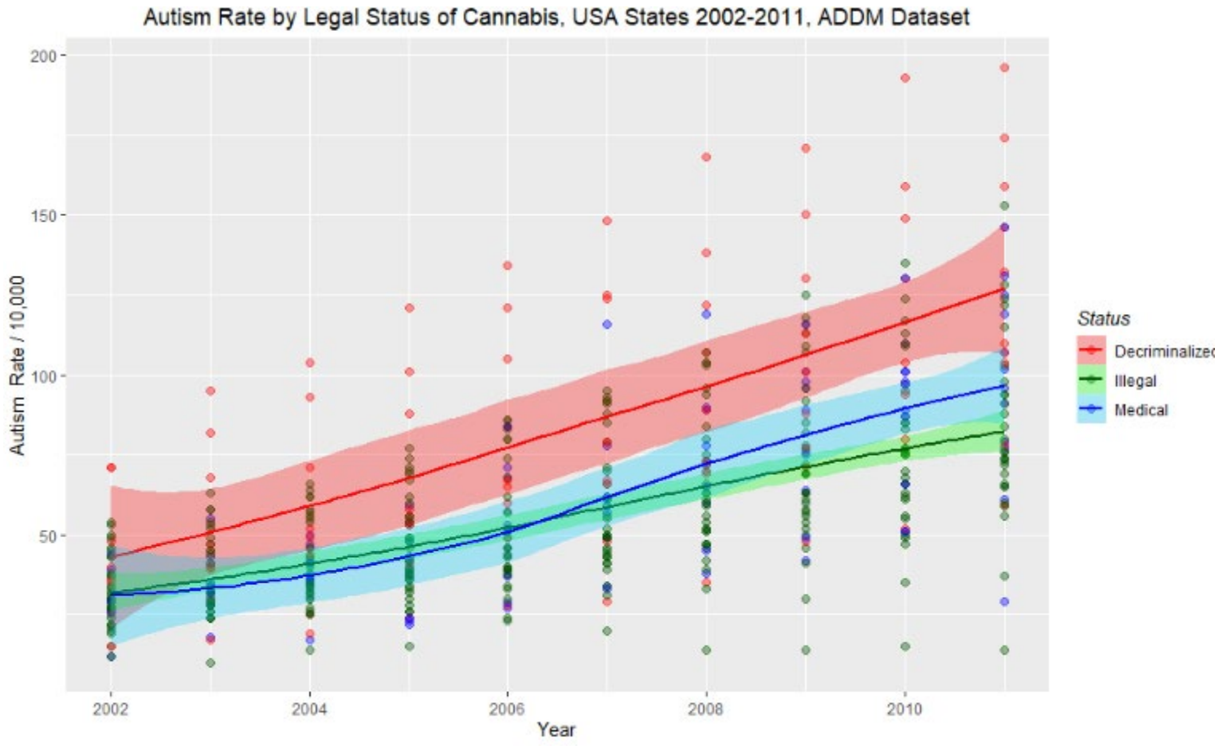
Autism Rate by Legal Status of Cannabis, USA States 2002-2011, ADDM Dataset
Autism Rate / 10,000
200
150
100
50
2002
2004
2006
2008
2010
Year
Status
Decriminalized
Illegal
Medical

F30 - Change 1995-2011 by Legal Status